WELDING Journal

SEPTEMBER 2020

AWS

Welding Gases and Consumables

Laser Welding

PUBLISHED BY THE AMERICAN WELDING SOCIETY TO ADVANCE THE SCIENCE, TECHNOLOGY, AND APPLICATION OF WELDING AND ALLIED JOINING AND CUTTING PROCESSES WORLDWIDE, INCLUDING BRAZING, SOLDERING, AND THERMAL SPRAYING

Gold Series X-FLO
Gold Series X-FLO

September 2020 • Volume 99 • Number 9

CONTENTS

FEATURES

WELDING RESEARCH SUPPLEMENT

At the American Welding Society (AWS), we are actively following the Novel Coronavirus (COVID-19) outbreak. The welding and fabrication industries have been determined to be an essential business, especially as it relates to repair and maintenance of key infrastructure. The content of the September 2020 issue of the Welding Journal *is intended to be accurate when published, but we recognize that we are in a rapidly changing situation. For AWS's official statement on COVID-19, as well as the latest updates and frequently asked questions, please visit* aws.org.

DEPARTMENTS

On the cover: TRUMPF's FusionLine enables users to add wire to their weld joint and bridge an opening up to 1 mm. (Source: TRUMPF Group.)

WELDING JOURNAL

Publisher/Editor *Annette Alonso*

Editorial
Managing Editor *Kristin Campbell*
Sr. Editor *Cindy Weihl*
Associate Editor *Katie Pacheco*
Associate Editor *Alexandra Quiñones*
Education Editor *Roline Pascal*
Special Contributor *Kathy Sinnes*
Peer Review Coord. *Brenda Flores*
Publisher Emeritus *Jeff Weber*

Design and Production
Managing Editor, Digital and Design *Carlos Guzman*
Production Manager *Zaida Chavez*
Assistant Production Manager *Brenda Flores*

Advertising
Senior Sales Executive, Corp. *Sandra Jorgensen*
Manager, Sales Operations *Lea Owen*

Subscriptions
Subscriptions Representative *Sonia Aleman*
saleman@aws.org

aws.org
8669 NW 36 St., # 130, Miami, FL 33166-6672
(305) 443-9353 or (800) 443-9353

AWS Promotes Diversity

AWS values diversity, advocates equitable and inclusive practices, and engages its members and stakeholders in establishing a culture in the welding community that welcomes, learns from, and celebrates differences among people. AWS recognizes that a commitment to diversity, equity, and inclusion is essential to achieving excellence for the Association, its members, and employees.

Welding Journal (ISSN 0043-2296 Print) (ISSN 2689-0445 Online) is published monthly by the American Welding Society for $120.00 per year in the United States and possessions, $160 per year in foreign countries: $7.50 per single issue for domestic AWS members and $10.00 per single issue for non-members and $14.00 single issue for international. Not available for resale in either print or electronic form. American Welding Society is located at 8669 NW 36 St., # 130, Miami, FL 33166-6672; telephone (305) 443-9353. Periodicals postage paid in Miami, Fla., and additional mailing offices. **POSTMASTER:** Send address changes to Welding Journal, 8669 NW 36 St., # 130, Miami, FL 33166-6672. **Canada Post:** Publications Mail Agreement #40612608 Canada Returns to be sent to Bleuchip International, P.O. Box 25542, London, ON N6C 6B2, Canada.

GAWDA Celebrates 75th Anniversary

Abydee Butler Moore
President, GAWDA,
and President/COO,
Butler Gas Products
Co.

"It is my honor to wish GAWDA a happy 75th anniversary and to thank our members and sister associations for their continued collaboration."

This year, the Gases and Welding Distributors Association (GAWDA) — a network of more than 500 suppliers and distributors with industrial and medical gas industry involvement in the United States — marks its 75th anniversary.

As I said in our commemorative reel at *gawda.org/75video*, once this gas and welding business is in your blood, you don't leave the industry. Members echoed similar sentiments in the same video, telling stories from the past and reminiscing about memories from former conventions.

One of the things that makes GAWDA special is the heavy saturation of family-owned or closely held businesses. We also reflect changes in the industry from innovations to more participation from women.

The next 75 years look even brighter for this organization.

Historical Highlights

GAWDA, based in Hollywood, Fla., exists to promote the safe operation and economic vitality of the gases and welding industry.

Founded in 1945 as the National Welding Supply Association, the association was formed to promote the value of distribution in the supply chain. Industry forefathers believed that distributors benefited the supply chain, both downstream to customers helping buyers buy and upstream to suppliers helping sellers sell.

Throughout the years, GAWDA has built upon this inaugural mission by creating a robust network of resources for independent distributors.

Additional Acknowledgments

In honor of its 75th birthday, here's why the independent distributor needs GAWDA:

- 24 h a day/7 days a week/365 days a year access to consultants
- Annual convention gathers more than 800 industry leaders
- Educational programs through the Association Education Alliance
- American Welding Society (AWS)/WEMCO relationship supports our manufacturers
- Access to Compressed Gas Association (CGA) training modules
- Build consumer safety awareness through provided posters and public service announcement videos
- COVID-19 Risk Mitigation Roundtables
- Cross-industry compensation report for benchmarking
- Department of Transportation recordkeeping checklists to always be audit ready
- More than 90% of GAWDA distributors are family businesses and share succession planning opportunities and challenges
- Read and share news in the GAWDA Connection e-newsletters
- Geographic and revenue membership diversity across North and Central America
- The Government Affairs Committee advises on regulatory issues and directs advocacy efforts
- Hazardous materials training resources
- Industry Partnering Committee provides a forum for suppliers and distributors
- Industry personal protective equipment checklists
- Learn from more than 200 suppliers
- Member Services Committee educates, enhances, recruits, and retains membership
- New employee orientation checklists
- Planning Committees develop the programs/meetings for members by members
- Regional meetings for local networking
- The Safety Committee liaises with CGA and AWS and promotes safe practices
- Sales training workshops
- Sample safety policies for drivers
- Scholarships program
- The sliding scale for dues fairly welcomes all members
- Spirit of volunteerism
- *Welding & Gases Today* magazine
- The Women of Gases and Welding Committee builds the network of women in the industry
- GAWDA's focus on young professionals provides young executives with educational programs and networking.

Closing the Curtain on 2020

It is my honor to wish GAWDA a happy 75th anniversary and to thank our members and sister associations for their continued collaboration.

The independent distributor needs GAWDA, because while we may not be able to fund or source these resources on our own, collectively we harvest and reap their benefits. Perhaps equally as important, GAWDA needs the independent distributor.

With independent distributors, multinational gas manufacturers, gas and welding equipment suppliers, and technology and service providers, GAWDA represents a symbiotic industry 75 years strong. WJ

FABTECH 2020 Canceled

FABTECH, scheduled for November 18–20 in Las Vegas, Nev., has been canceled due to the ongoing COVID-19 pandemic. The announcement was made by event partners SME, the Fabricators & Manufacturers Association, International, the American Welding Society (AWS), the Precision Metalforming Association, and Chemical Coaters Association International.

"FABTECH has long been a key element of AWS's efforts to support and advance the welding community," said Gary W. Konarska II, AWS executive director and CEO. "We look forward to continuing to work with our FABTECH event partners to identify new and enhanced ways – both online and physical – to connect the FABTECH community, share knowledge about the latest industry products and developments, and help companies move their business forward."

Sandra Bouckley, executive director and CEO of SME, added the decision to cancel the show was not taken lightly.

"We explored every option to find a way to produce this event in 2020. Unfortunately, COVID-19 has created an environment that makes it impossible to hold the event. Our top concern is always the safety of our exhibitors, attendees, speakers, sponsors, and employees, along with supplier partners and venue staff. While we didn't want to have to make this decision, we have found that we have no choice."

Frequently asked questions and answers about the canceled 2020 show can be found at *fabtechexpo.com/covid19*.

AWS Updates: *Welding Journal* Wins Awards; Virtual Conferences to Focus on Modern Pipe Welding and Aluminum; Podcast Launches

Several new awards for the *Welding Journal*, two virtual conferences, and a brand-new podcast series are making headlines at the American Welding Society (AWS).

• The ***Welding Journal*** earned six honors at the Florida Magazine Association's 2020 Charlie Awards.

Winners were announced virtually on July 24 via Facebook. In the trade/technical division, the magazine received two honors for best photography: photo essay/series, with a Charlie Award (1st place) for "Centennial Photo Contest Showcases the 'Art' of Welding" (September 2019) and silver award (2nd place) for "Putting the Extraordinary in Welding" (April 2019). Additionally, the publication received a Charlie Award for best special theme or show issue for "Celebrating AWS's Centennial" (April 2019) and silver award for best writing: feature headlines (on three different articles). *Welding Journal* covers earned two bronze awards (3rd place), best traditional illustration for the April 2019 cover, and best photography: cover, for the September 2019 issue.

For the best special theme or show issue win, the judge said the following: "This issue was a nice mixture of celebrating the rich past of the American Welding Society and looking forward to the future. It was packed with detailed, historical information, as well as interesting profiles..."

In addition, during the SIIA/Association Media & Publishing 40th annual EXCEL Awards, which was also held virtually, "AWS at 100 — Can a Woman Weld?" (March 2019) earned a bronze award in the magazine column category.

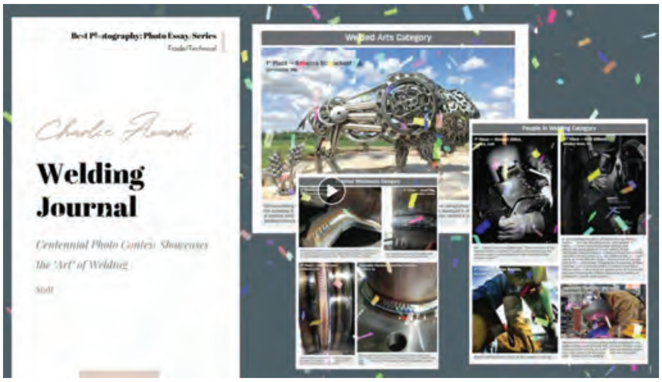

This screenshot from the 2020 Charlie Awards trade/technical division video celebrates a Welding Journal *win.*

• **Modern Pipe Welding Conference 2020.** This virtual event will take place September 29 and 30, and will cover all aspects of pipe welding. The cost is $300 for members and $400 for nonmembers. To register, visit *awo.aws.org/conferences/upcoming-conferences/pipe-welding-conference-2020/*.

• **Aluminum Virtual Conference – Back to Basics.** This virtual conference will be held October 20 and 21. It is designed to provide a basic understanding of aluminum welding and will include several topics. The cost is $300 for members and $400 for nonmembers. Go to *awo.aws.org/conferences/upcoming-conferences/aluminum-conference/*.

• AWS and Arc Junkies Podcast have launched the **"Weld Wednesday with AWS"** podcast series (*aws.org/podcasts*). The podcasts will serve as an avenue to inform the welding community about important innovations and trends in the industry. New podcasts will be released the first Wednesday of every month. The first episode aired on August 5.

"The goal of this partnership is to highlight how AWS supports the welding community with resources including standards, education, certification, and more," said Cassie Burrell, AWS senior vice president, strategy and membership development. "We're excited to collaborate with a podcast that has such a diverse and strong audience."

For the first podcast, Arc Junkies Host Jason Becker spoke with AWS District 5 Director Howard Record to discuss the advantages of AWS Section meetings and activities. Additional podcast topics will cover how codes and standards are developed, the how's and why's of welding procedure specifications, and much more.

Wayne State University Introduces Welding and Metallurgy Program

Beginning in the fall of 2020, students at Wayne State University, Detroit, Mich., will have the option of earning a bachelor of science in welding and metallurgical engineering technology from the College of Engineering. Wayne State's welding and metallurgical engineering technology program is an upper-level two-year curriculum for students who have completed their first two years in welding or a comparable program at another institution. Within the division of engineering technology, welding and metallurgy students will take courses on such topics as thermodynamics, design, automation and robotics, and structural analysis. WJ

AWS Foundation Awards Up to $25,000 to Welding Programs

The American Welding Society (AWS) Foundation has been dedicated to building the welding workforce through the Welder Workforce Grant. Established in 2017, the grant awards up to $25,000 to high schools, trade/technical schools, and community colleges seeking to enhance and improve their welding education programs, including making facility improvements or investing in capital items such as welding or metalworking equipment.

The following lists the 2020 spring grant recipients and details how the schools hope to enhance their welding programs with the funds received.

Funds Allow Growth

With $25,000 in grant funding, **Airport Community Schools**, Carleton, Mich., intend to expand students' metalworking capabilities by adding AWS advanced welder training and fabrication classes. Alongside the addition of key equipment, such as a larger bandsaw, CNC plasma table, and sheet metal brake press, students will be able to complete the SENSE Level II Advanced Welder Certificate Program and develop skills required by local industries.

"Through multiple community contacts, surveys, and state data, our district (Airport Community Schools) decided that we would like to offer our students the opportunity to learn the trade of welding," said Ryan Irwin, director of education, Airport Community Schools. "In 2018, our community supported a bond, and we decided to use a portion of the bond money to build a 5000-sq-ft facility . . . Now that we have a great space, we are working within our limit-

A welding student practices shielded metal arc welding in preparation for the 3G bend test. (Photo courtesy of Airport Community Schools.)

ed budget to outfit the lab with the best machines, tools, and technology that we can."

Chippewa Falls High School, Chippewa Falls, Wis., received $25,000 to increase and enhance the welding equipment and capacity of its laboratory space for full completion of the AWS SENSE Level I Certificate Program. The funds will be used to purchase 11 multiprocess machines, which allows all students a welding machine during their scheduled class period. The funds will also provide two hand plasma cutting machines, hose reels, and cutting stations. The remaining money will be used for upgrades for electrical and safety, including welding machine hookups and dedicated e-stop buttons, suspended welding/grinding curtains, and eight upgraded flexible welding/project stations.

"We want to establish and brand an updated welding program that promotes school-wide enrollment, provides industry credentialing and post-secondary education credits, and exposes and connects students to in-demand welding/welding-related employment and careers. Establishing a modern welding laboratory that provides relevant opportunities for all students will help accomplish this goal," said Jonathan Hiebl, technology education instructor at Chippewa Falls High School.

Chippewa Falls High School was awarded a $25,000 grant to increase and enhance the welding equipment and capacity of its laboratory space. (Photo courtesy of Chippewa Falls High School.)

Paso Robles High School, Paso Robles, Calif., will use its $25,000 fund to purchase a Miller Electric augmented arc reality system to break into hands-on welding and then continue to build upon that initial experience with virtual welding applications that culminate in small-project construction. Community outreach and instruction in hands-on welding skills via a mobile welding training trailer will help bring welding directly to students in minority populations.

"Our primary focus is to increase student involvement in the welding industry through community outreach. Specifically, we are targeting populations of students that are under-represented in the welding program at Paso Robles High School as young as fourth grade," said Justin Pickard, agriculture department chairman, Paso Robles High School. "Our goal is to bridge over stereotypes and preconceived notions that might otherwise prevent these students from taking classes in welding and ultimately not pursuing the welding industry as a career."

Hands-on instruction using gas metal arc welding. A Paso Robles High School student leader talks to students about operator factors for a successful fillet weld. (Photo courtesy of Paso Robles High School.)

To support a dual-credit partnership with the McCreary County School District, **Somerset Community College** (SCC), Somerset, Ky., will use its $24,995 grant to offer training to the district's students and provide a space with accommodations and resources. The equipment purchased through the grant will include five Miller XMT® 350 multiprocess welding machines with S-74 MPA plus wire feeders for gas metal arc, shielded metal arc, flux cored arc, and gas tungsten arc welding.

"With the addition of this equipment, a part-time program can potentially become a full-time high school pro-

Karl Watson, SCC welding instructor, gives instruction to McCreary Central High School dual-credit students. (Photo courtesy of Somerset Community College.)

gram during the day and grow into an evening program for adult students . . . The opportunity to be able to offer multiple welding processes in McCreary County will help meet the needs of the local industry and make welding education more accessible and affordable for these students and will help the community workforce," explained Elaine Kohrman, director of grants, SCC.

Ida High School, Ida, Mich., will apply its $15,000 AWS Detroit Section grant to purchase six new gas metal arc welding (GMAW) machines and add an additional welding booth to the lab. The purpose of this project is to improve the knowledge and skill set of the students in using GMAW and flux cored arc welding processes.

There's Still Time to Apply

The AWS Foundation is committed to securing the future of the welding industry by positively impacting welding education, and the Welder Workforce Grant is the latest effort to ensure a skilled workforce is ready when industry calls.

This year, the Foundation will award up to $325,000 in grant funding to programs across the country. The application cycle is currently open and schools may apply for the Welder Workforce Grant before the upcoming October 1 deadline.

To learn more, visit *aws.org/workforcegrant*, or contact John Douglass, associate director of the AWS Foundation, at *jdouglass@aws.org*. — *Roline Pascal, education editor*

Reassuring Signs Despite COVID-19: Trans Adriatic Pipeline Completes Offshore Section, Sciaky's EBAM® Continues Depositing High-Value Materials, and TRUMPF Hosts INTECH

As the pandemic continues, encouraging stories have emerged from Trans Adriatic Pipeline (TAP) AG, Baar, Switzerland; Sciaky Inc., Chicago, Ill.; and TRUMPF, Ditzingen, Germany.

• **TAP** has completed the 105-km-long offshore section of a pipeline across the Adriatic Sea. This milestone includes several deliverables, such as the offshore installation of

— *continued on page 55*

BY DAMIAN J. KOTECKI

Q: American Welding Society D1.6/D1.6M:2017, *Structural Welding Code — Stainless Steel,* contains two passages that are causing consternation in our organization. In Section 4, Design of Welded Connections, Clause 4.6 ends with the following sentence: "Details shall promote ductile behavior, minimize restraint, avoid undue concentration of welding, and afford ample access for depositing the weld metal." The informative Annex G, Nonprequalified Stainless Steels — Guidelines for WPS Qualification and Use, Clause G2 Nonprequalified Austenitic Stainless Steels (6) concludes with "Designing the weldment and the welding sequence to minimize restraint on the solidifying weld metal." We are concerned with the phrase "minimize restraint" in both of these sections. If we don't restrain the workpieces before welding, we generally do not end up with the finished weldment shape we want. Stainless steel weldments tend to distort more than carbon steel weldments of the same initial geometry. How are we to interpret "minimize restraint" and comply with the intent of the Code?

A: This cannot be considered as an official interpretation of the American Welding Society (AWS) D1.6/D1.6M, *Structural Welding Code — Stainless Steel*. Official interpretations can only be prepared by full action from the D1 Committee on Structural Welding. The following is only my opinion as an advisor to the D1K Subcommittee on Stainless Steel, which is responsible for D1.6/D1.6M.

The reason for minimizing restraint is to minimize the likelihood of cracking. I will consider that later in this column.

First, it is appropriate to decouple the two clauses according to their application. Clause 4.6 is mandatory and applies to all fabrication under the Code. Clause G2 is in an informative (nonmandatory) annex and applies specifically to fabrication of austenitic stainless steels that are expected to solidify entirely as austenite (no ferrite — steels such as 310, 320, and 330) and are therefore somewhat susceptible to solidification cracking.

Material provided in a nonmandatory annex, such as Annex G, consists essentially of suggestions. The engineer in charge of fabrication is expected to apply his or her engineering judgment as to whether or not a particular suggestion is appropriate for the given fabrication. The "minimize restraint" suggestion is just one of six in Clause G2. The others suggest using base metal and filler metal of low impurity content, using low heat input to produce convex beads, maintaining a low preheat and interpass temperature, using skip welding to avoid heat buildup in one area, and filling craters. Of these, the most effective method for preventing solidification cracks is the use of low heat input to produce convex beads and filling craters. Any time one is welding on fully austenitic stainless steels (such as 310, 320, or 330), I would strongly recommend following those two suggestions.

Clause 4.6 is concerned with design for welding and uses the mandatory wording "Details shall . . . minimize restraint." There is no objective criterion that describes how that shall be done. In effect, then, the engineer has to again apply his or her engineering judgment, this time as to what "minimize restraint" means and how that can be done in the context of the fabrication of interest.

Some restraint is unavoidable in welded fabrication. Because the weld metal shrinks as it cools, and that shrinkage is resisted by the surrounding cold base metal, residual stresses up to the yield point can be anticipated in and around all but very small welds. These stresses produce distortion. If distortion is not acceptable, some applied restraint (such as strongbacks) can be used to resist distortion, but that would appear to be counter to the instruction in Clause 4.6. One way to minimize the use of strongbacks and therefore restraint is to design for welding from two sides, whenever possible, instead of one side. In addition to minimizing restraint while countering distortion, a double-V or double-U joint preparation uses less filler metal than a single-V or single-U joint preparation. Therefore, a two-sided weld design, instead of a single-sided weld design, minimizes restraint.

Considering fillet welds, Clause 4.3.2.1 of D1.6/D1.6M:2017 states, "Stress on the effective area of fillet welds and of welds in skewed joints shall be considered as shear stress, regardless of the direction of application." Clause 4.4.2.1 adds, "The effective area shall be the effective weld length multiplied by the effective throat." Clause 4.4.2.2 asserts, "For fillet welds, the effective throat shall be

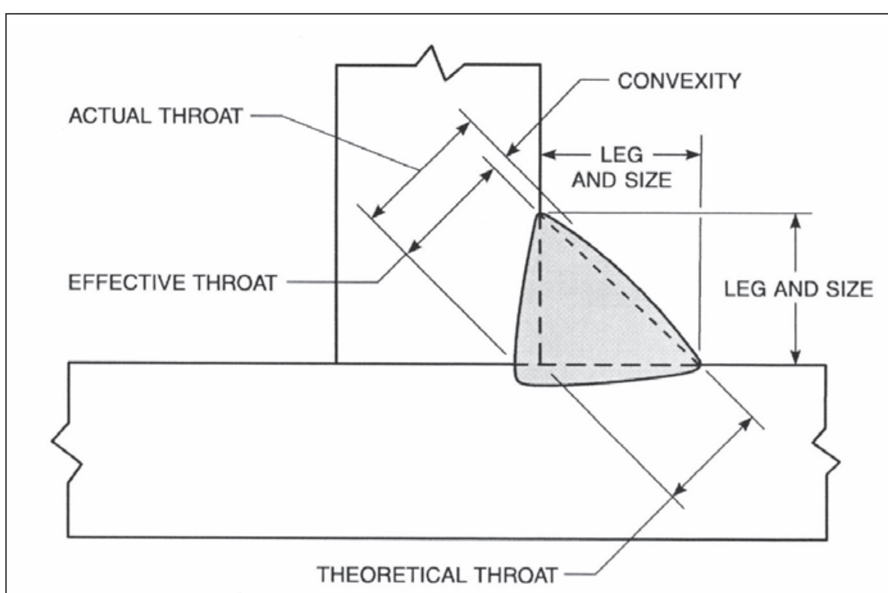

Fig. 1 — Fillet weld geometry (Credit: AWS A3.0M/A3.0:2020, Standard Welding Terms and Definitions, *Fig. B25 [A].)*

the shortest distance from the joint root to the weld face of the diagrammatic weld."

Two small fillet welds, one on each side of a lap or T-joint connection, can transmit the same amount of shear load as a single fillet weld twice as large on one side of the lap joint or T-joint connection, and the two small fillet welds will use less filler metal than the larger single fillet weld. This is because the shear-load-carrying capacity of a fillet weld is proportional to the throat dimension, but the volume of the weld metal is proportional to the square of the throat dimension — Fig. 1. Further, the two small fillet welds counter distortion more than the single larger fillet weld, and they distribute the load more evenly. The use of two fillet welds, instead of one larger fillet weld, is a design approach that minimizes restraint.

As seen in Fig. 1, the effective throat equals 0.707 × (leg length), and the effective area equals the effective throat times the effective length of the fillet weld. Suppose, for example, that the leg length is T and the effective length is L, then the effective area for design purposes is T × L. The volume of filler metal deposited is $\frac{1}{2}(T/0.707)^2 \times L = \frac{1}{4} \times T^2 \times L$, assuming no reinforcement.

If this fillet weld is replaced by two fillet welds, one on either side of the web, each with an effective throat = T/2, the effective area of the two fillet welds will be 2 × T/2 × L = T × L, same as the single larger fillet weld. But the volume of filler metal deposited to produce the two fillet welds is $2 \times \frac{1}{2}[(T/2)/0.707]^2 \times L = \frac{1}{8} \times T^2 \times L$, which is one half as much as required by the single larger fillet weld.

The resistance to cracking under restraint conditions depends upon the type of base metal and weld metal. Nominally austenitic stainless steel base metals and their matching filler metals (such as 304L, 308L, 309L 316L, and 347), which solidify as primary ferrite, are most resistant to cracking. They can generally be welded under conditions of severe restraint without likelihood of cracking. Almost as resistant are duplex ferritic-austenitic stainless steels and their approximately matching filler metals. Ferritic stainless steels and their matching filler metals are somewhat less resistant. Least resistant are martensitic stainless steels and fully austenitic stainless steels with matching weld metals. Therefore, the engineer has more latitude when designing a weldment in nominally austenitic or duplex stainless steel than in the other types of stainless steels. If the weldment does not experience cracking, I would say the design has sufficiently minimized restraint. WJ

DAMIAN J. KOTECKI is president, Damian Kotecki Welding Consultants, Inc. He is a past treasurer of the IIW and a member of the AWS A5D Subcommittee on Stainless Steel Filler Metals, D1K Subcommittee on Stainless Steel Structural Welding, and WRC Subcommittee on Welding Stainless Steels and Nickel-Base Alloys. He is a past chair of the A5 Committee on Filler Metals and Allied Materials and served as AWS president (2005–2006). Questions may be sent to Damian J. Kotecki c/o Welding Journal, *8669 NW 36 St., # 130, Miami, FL 33166-6672, or via email at* damian@damiankotecki.com.

BY ALLEN M. AGIN

Q: I weld nuts to hot-stamped parts and am having difficulty getting consistent results. This includes parts where the nuts appear welded to the part, but sometimes pop off in transit to our customer. We also get inconsistent push-out test results. How come? I have asked this question many times and have gotten many different answers.

A: This is a great question. It also raises additional questions and challenges to be considered when making consistently good fastener welds on stampings with an aluminum silicate (AlSi) coating.

First, we should touch on two different types of steel processing: mill processing and in-plant processing. Understanding these are different processes is the key to some of the major reasons for inconsistent weld results.

Mill processing is the processing done at the steel mill, prior to shipment to the supplier or end user. Many conventional metals are stamped and welded just as they come in from the mill, with no additional treatment. Mill-processed steel is malleable and can be shaped using conventional stamping presses and processes. Hot-stamped boron steel is not malleable and requires in-plant processing to stamp it.

In-plant processing is done at an

Fig. 1 — A, B — Showing color variations.

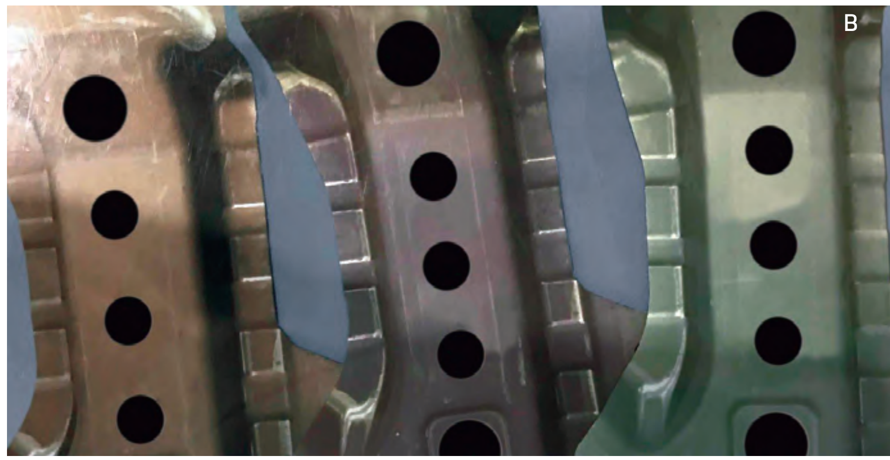

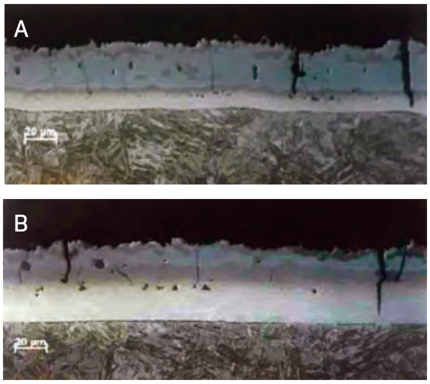

Fig. 2 — A — Thin surface microstructure; B — thick surface microstructure.

end-user plant, or sometimes at a supplier plant, where they have furnaces and stamping presses to form stampings after they come out of the oven. Hot-stamped or press-hardened materials must be formed using in-plant processing. During in-plant processing, the metal blanks are heated beyond 900°C prior to being formed in a press with water-cooled dies. The blanks are heated to increase the ductility of the steel, reducing springback during the stamping process. In-plant processing changes the metallurgical composition, multiplying the hardness from 50 kilopounds per square inch (ksi) to around 200 ksi. This new material develops an AlSi coating in the process. Welding fasteners to this material is much more difficult than to conventional steels. Think of it like pressing a ripe banana into tempered glass.

Why are my stampings different colors?

At first glance, this may seem like an unusual question until you look in your tote bin. Figure 1 shows an obvious difference in surface color (AlSi coating). This color inconsistency exists due to the variability of in-plant processing with normal everyday work schedules and adjustments. The color difference is caused by changes in the coating thickness due to deviations in line speed, furnace temperature, or die cooling from the ideal process parameters.

Does the color affect weldability?

Absolutely! Normally the steel used in production is processed at a mill, and

Fig. 3 — A — Weld measurements; B — graphed results.

what you get for production is generally consistent and the same color. However, during in-plant processing, color variations can occur, indicating a change in the thickness of the AlSi layers (see an example of the change in microstructure in Fig. 2). This changes the resistivity of the surface, which directly affects weld quality and repeatability.

What can I do to get consistent weld results?

The "best" textbook answer when using in-plant processing is to make sure there is no deviation from the recommended parameters of time, temperature, and die cooling for the stamping blanks. Even a slight change in the process can create a problem due to the AlSi coating.

The best real-world answer, however, is that holding a process like this to exact settings only seems to occur in laboratory conditions. Like an endangered species, it is almost never found in the real world. This brings us back to your original question.

What is the best way to weld nuts and studs to hot-stamped materials?

This question comes up quite often. The answer depends on a variety of factors, including the following: in-plant processing, thickness of material, AlSi coating, projection style, nut/stud size, and weld specifications. With variations of any of these, you can get different answers from different people.

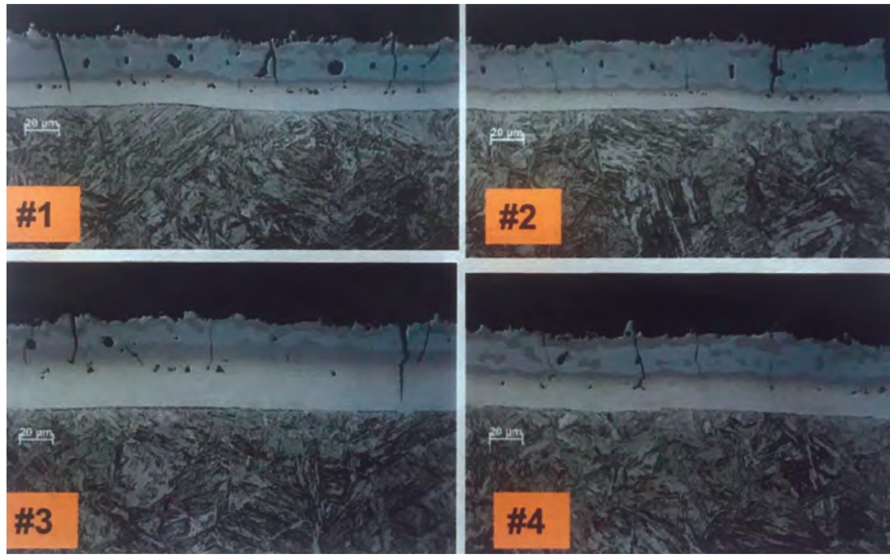

Fig. 4 — Four different microstructure surface thicknesses.

Today, the most common welding processes, when it comes to AlSi coated stampings, are capacitive discharge (CD) and medium-frequency direct current (MFDC).

Many years of lab testing and production have identified that a combination of short weld times, high current, high force, and fast follow up deliver the greatest consistency. An example of these parameters for welding

Fig. 5 — Overheated weld showing a large HAZ.

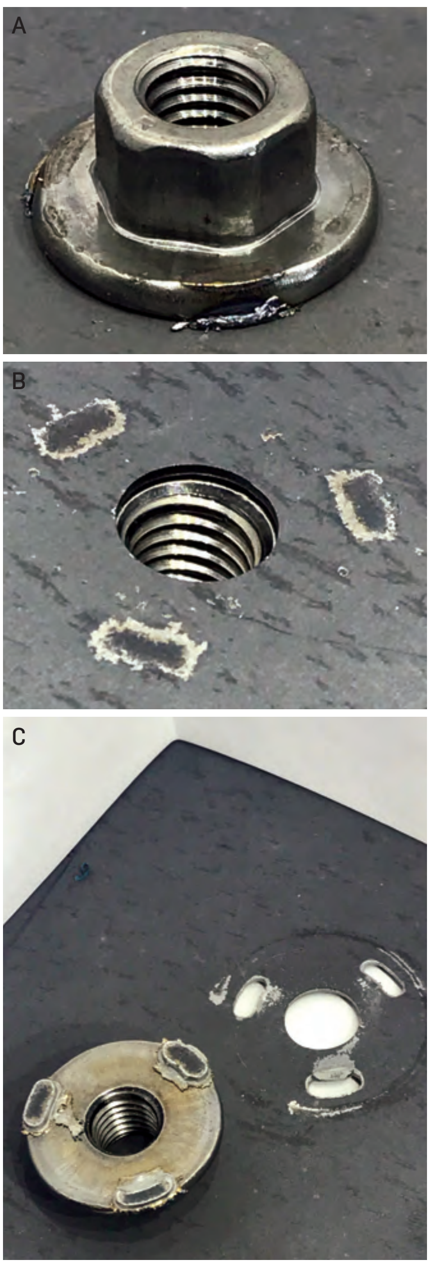

Fig. 6 — A — Showing almost no HAZ; B — showing bottom side again with almost no HAZ; C — showing nugget pull with almost no HAZ.

a M6 flange nut is shown in Fig. 3. Figure 3 shows the current output, time, and displacement when welding a M6 nut onto a 2-mm ALSi-coated material.

While a MFDC process can be ideal for the right application, it does require tight control of in-plant processing. A CD process allows for variations due to in-plant processing in real-world conditions, as described earlier. Figure 4 shows several examples of thickness differences in the multiple AlSi coating layers as slight process changes occurred due to variations in in-house processing control.

What other factors do I need to consider?

You may want to take the following factors into account:

- Primary power
- Water cooling

- Floor space/footprint
- Air filtration
- Electrode life
- Testing
- Rework
- Capital investment
- Weld quality
- Welder repurposing
- Life cycle cost
- In-plant processing

Expanding on a few of these factors, let's start with power supply. A MFDC system, including the latest "fast-rise time" type of transformer, can require up to 1000 ampere (A) of three-phase power and a 2200 A inverter. CD processes require a small fraction of that power. For example, one manufacturer's CD process only requires 30 A of single-phase 480 volts alternating current. Installation costs of the primary power supply, as well as power cost over the life cycle of the capital equipment, are substantial factors that should be considered.

Supplying chilled water can also be a significant cost to consider. For example, MFDC processes require significant water cooling for the weld control and transformer. A CD welding process that does not require water cooling for the control or transformer saves at least 8 gal per min (30 L per min). In high-duty-cycle CD applications, a small chiller might be recommended to cool the tooling. There are capital cost savings in buying a much smaller chiller, or not buying a chiller at all, not to mention the ongoing power savings from not running a large chiller.

Another often overlooked factor is floor space. Some capacitive storage banks are simply more space efficient. United States-built CD banks are typically much smaller than those sourced overseas. Recently, a large stamping company purchased CD welding machines based on price alone to keep the project cost down. The CD banks were three to five times the size of the domestic units they didn't purchase. The overall footprint of each machine was almost double what it could have been. Put together with the smaller chiller requirements mentioned earlier, the savings in facility investment would have been huge.

Rework is another major cost to consider. In another case, also due to upfront cost-saving measures, two automotive suppliers found themselves reworking lots of parts, and paying more than they had saved on the equipment purchase. They had chosen the MFDC process to weld stampings with AlSi coatings based on equipment price. They didn't recognize a variety of issues with their in-plant processing (some of which I've touched on above), so production welding yielded inconsistent results. Both companies were forced to implement "safety" gas metal arc welds (GMAW) to their fasteners, adding more weight to the vehicle and much greater production cost due to longer processing time, as well as additional personnel, welding gas, and consumables.

There are at least several other factors that I don't have the space to mention here. It is best to discuss all of these with a resistance welding machine builder who has a proven track record on hot-stamped materials. Designing your process for success should also include doing lab welding, testing, and performing a Design of Experiment (DoE) on your stampings before making a major investment.

I've been hearing about the heat-affected zone (HAZ). Why does this matter?

The HAZ is a very important, often critical, factor in all resistance welds. The ideal resistance weld utilizes the highest possible amount of heat for the shortest possible amount of time. Using a process that cannot deliver weld current in the shortest amount of time can end up heating an area far outside the weld zone. This may cause a change in hardness in the base material, which can lead to a material failure in the HAZ. Figure 5 shows what appears to be a good weld based on the number of weld nuggets, but with severe overheating leading to a weakened HAZ. In this case, the end user was using a MFDC power supply, and experiencing much lower push-out values than expected. Simply put, the metallurgy changed and the part was weakened due to excessive heating. Had the HAZ been much smaller, push-out values would have been much higher.

On the other hand, Fig. 6 shows examples of the desired HAZ and excellent push-out test results when using high currents and very short weld times. There is no visible HAZ around the projections, or around where they pulled.

As you can see, answering your original question is not simple. It raises many additional concerns that should be taken into account to create consistent and reliable welds.

In conclusion, one of the most important exercises you should consider is partnering with a reputable resistance welding machine builder who has the expertise, experience, and ability to demonstrate a variety of different processes when welding AlSi-coated stampings. While this demonstration can take place in the machine builder's welding lab, this demonstration should use your production parts and a range of their production welding equipment. This equipment should include both CD and MFDC welding machines with all necessary production features. Following this process will supply you with the absolute correct answers for your particular application, enabling you to consistently produce the strongest possible welds. WJ

Acknowledgments

I am very grateful for the assistance of the following people in answering your question in more depth: Bob Kollins, at Technical Sales and Solutions, for support with the measurements and waveforms shown in Fig. 3; and Min Kuo, PhD, at ArcelorMittal Global R&D, for the microstructure imaging on our parts shown in Figs. 2 and 4.

ALLEN M. AGIN is the Midwest regional sales manager and product manager for CD welding at Weld Systems Integrators Inc., Warrensville Heights, Ohio; a sustaining member of AWS; and an active member in RWMA and WEMCO. He has been involved in the applications, training, and sales of resistance welding since 1968. Agin is also an author and co-author of articles on the welding of fasteners to hot-stamped and press-hardened steels with AlSi coatings. He has presented to the American Institute of Steel Engineers, AWS Sheet Metal Welding Conferences, and most recently at the PMA Hot Stamping Experience & Tech Tour. Send your comments and questions to Allen Agin c/o Welding Journal*, 8669 NW 36 St., #130, Miami, FL 33166-6672, or via email at* allen@wsiweld.com.

Fiber Laser Facilitates Welding of Thin, Conductive Metals

The HighLight™ FL4000CSM-ARM fiber laser delivers a dual-beam output to enable the welding of thin, high-thermal conductivity metals. The dual beam, which consists of a center beam surrounded by a ring beam, offers a high brightness (nominal BPP 0.6) to allow for a smaller spot size and minimize heating of the material. The small spot size, coupled with the preheating effect from the ring beam, improves weld consistency, which is a challenge when welding thin, conductive materials. The fiber laser comes with an output power of 4 kW (a 1.5-kW center beam and a 2.5-kW ring beam that can be varied and modulated). It is also equipped with a 15-m length process fiber, making it easy to integrate in any production environment. The fiber laser meets welding requirements for e-mobility; energy storage; and general electrical interconnects consisting of dissimilar materials, such as copper and aluminum, and foil stacks that require precise control.

Coherent®
coherent.com
(800) 527-3786

SAW Wire Designed for Caster Roll Rebuilding

The Lincore® 420HC-S metal-cored, submerged arc welding (SAW) wire works for applications requiring higher hardness, such as caster roll rebuilding. It is used on work rolls and backup rolls when water spray causes pitting on tool steel deposits. The welding wire produces a high-carbon, 420-stainless steel deposit and can be used in the flat, horizontal, and circumferential welding positions. To offer

welders more options depending upon weld thickness, the welding wire comes in the following diameters and package sizes: 3/32 or 1/8 50-lb coil, and 3/32 or 1/8 600-lb Speed-Feed® drum. The coil is light enough for one person to lift and install on a wire feeder reel. The drum offers a larger, bulk package for high-production environments.

The Lincoln Electric Co.
lincolnelectric.com
(888) 935-3877

Consumables Cut Down on Piercing Time for Thick Steel

The QuickPierce 400-A consumables reduce piercing time by up to 40% on mild steel thicknesses ranging from 1.25 to 2.0 in. (30 to 50 mm). Faster piercing time reduces cycle time, especially for plates with a complex parts nest. The consumables also deliver arc-starting capabilities that increase part life, cut longer between consumable changes, and lower total cut cost. One such enhancement includes more shielding gas ports on the shield cap. By increasing gas pressure during arc start, pierce time is further reduced. The additional shielding gas ports also deflect molten metal away from the consumables.

Thermal Dynamics
thermal-dynamics.com
(866) 279-2628

Report Projects Growth for the Laser Welding Machine Market

Laser Welding Machine Market Research Report — Global Forecast to 2023 posits that this industry is projected to increase at a compound annual growth rate of 5%. The 111-page report attributes this growth to the thermal stability provided by laser welding machines, which helps in reducing scrap metal, as well as their inclusion in various end-user applications, such as medical, jewelry, automotive, and electronics. The report also forecasts that product innovations, advances in manufacturing processes, and technological improvements will continue to drive the demand for laser welding machines. The report concludes with an analysis on the impact of the COVID-19 pandemic on this industry. It covers the following topics: economic, supply chain (price variation of raw materials, production shutdown, cash flow constraints, and import/export), market demand (restrictions/lockdowns, consumer sentiments), and pricing.

Market Research Future®
marketresearchfuture.com
(628) 258-0071

Laser Welding System Offers a Large Work Area

The TruLaser Station 7000 3D laser welding system exhibits a beam with a laser power of up to 4 kW and a work

— *continued on page 57*

Take a Plunge into Underwater Welding and Cutting

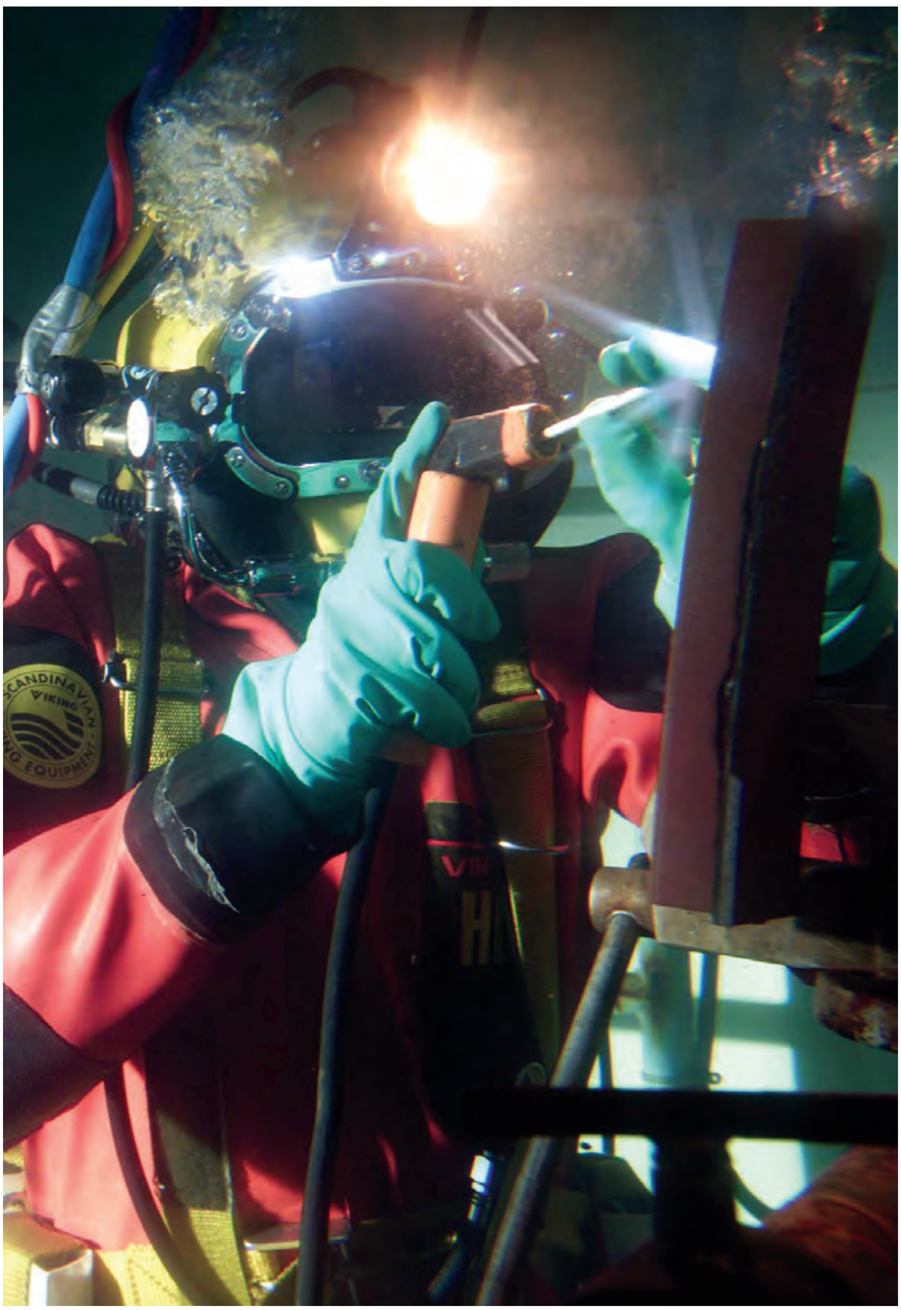

Fig. 1 — Welding for qualification test in tank with full diving gear. (Courtesy of the Royal Dutch Navy — Diving Group.)

A practical view of welding and cutting operations for marine and offshore applications

BY JAN HILKES AND JÜRGEN TUCHTFELD

A vast part of much marine and offshore construction, such as the supporting structures of platforms and wind towers as well as pipelines, manifolds, steel waterway and harbor construction, bulkhead panels, locks, ship hull repairs, and more, are to a great extent done under water. Hence, welding and cutting activities for maintenance and repair are bound to take place under water as well.

Shielded metal arc welding (SMAW) is a versatile, flexible, and practical welding process. For this reason, it is often used for underwater maintenance and repairs. For more than 80 years, this process has been applied for sealing leaking rivets in riveted ship hulls. A power source and a covered electrode as the consumable is almost all that is required for this type of SMAW operation. In this case, the power source has to be adapted and prepared for underwater welding to meet all safety requirements. The

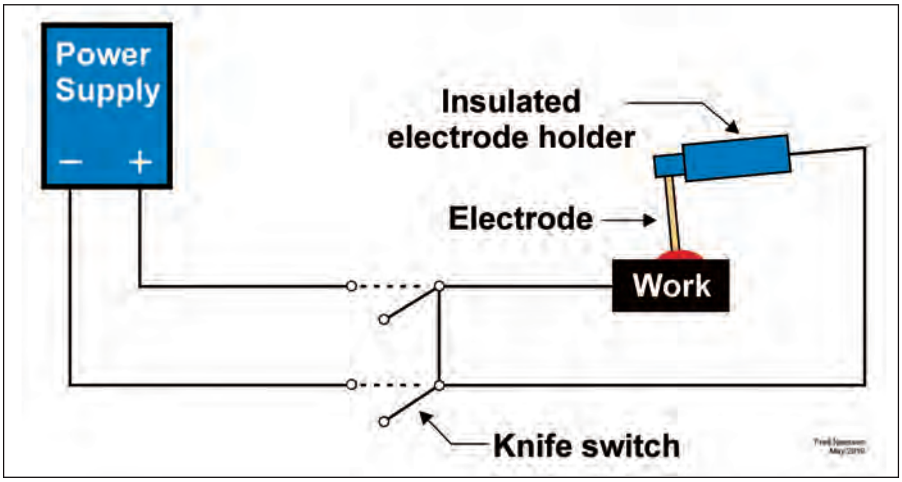

Fig. 2 — A basic electrical equipment setup for underwater welding with SMAW. (Courtesy of Fred Neessen.)

same setup can also be applicable for underwater cutting operations. Since safety is the first priority, many measures have to be taken into consideration to ensure the entire operation is safe (Ref. 1).

The underwater environment is always wet. It is also cold and dark, in Northern Europe, which makes working conditions for the welder/diver less than ideal. Serious diving training and welder qualification are required to prepare for such a demanding job. During training, the basics of diving and working in underwater circumstances will be highlighted and explained, as will how underwater conditions affect the welding behavior of the consumables applied. These variables present challenges in the execution of the welds and repairs.

This article covers the diving, welding, and metallurgical aspects of underwater wet welding and cutting using covered electrodes based on industrial examples and applications for joining and repair welding.

Diving In

When a diver submerges, their body experiences the pressure of the surrounding water. With every 10 m comes an additional bar in pressure. One bar of pressure equals a mass of 1 kg on a 1-cm^2 surface area. As a result of this dive, the pressure on the diver's body at 10 m is two bar, one from the ambient surface pressure plus one from the 10-m water column.

At 20 m, the pressure increases to three bar, and so on. For the chest and lungs not to be compressed or squeezed, the diver has to inhale breathing air that has the same pressure as the surrounding water pressure. The pressure inside the lungs has to be equal to the external water pressure on the body to prevent any damage.

The pressure of the breathing air is equalized by a regulator or demand valve with a mouthpiece, which the diver uses to breathe. The regulator connects with the first stage, which reduces the high initial pressure, to the air supply in the form of gas cylinders that contain compressed breathing air.

Working Under Pressure

Underwater wet welding takes place directly in the water with "wet" welder/divers, who dive with compressed air or an enriched air mixture, with restricted depth and residence time. The advantage of such wet welding operations is that they are very flexible and mobile, also ideal for short repairs and welding jobs in a larger area, in docks, waterways, floodgates, locks, anchor lines, etc. The setup is also relatively quick and practical, from either the shore or a boat. Obviously, the underwater work has to be properly scheduled and planned in detail.

Welding with coated electrodes is often applied for underwater welding but other welding processes, such as gas metal arc welding (GMAW), flux cored arc welding (FCAW), and gas tungsten arc welding (GTAW), can also be applied when using special welding guns with special nozzles. The weld quality with electrodes is acceptable and very suitable for maintenance and repair welding, and for multipass fillet welds. To optimize the diver's comfort, drysuits with wool jumpsuits underneath are mostly used. Also, full-face masks or helmets with communication systems included are used — Fig. 1.

Another option is "dry" hyperbaric welding with an underwater habitat, referred to as a cofferdam, built around the parts of the structure that needs to be welded or welded upon. In this situation, the water is pressed out with air to create a relatively "dry" environment. This means the humidity in the habitat is relatively high but there is no surrounding water to come in contact with the workpiece or the welding consumables and the electrical arc.

Wet Welding with Covered Electrodes

Because of its versatility and flexibility in application, SMAW with covered electrodes is often used for underwater maintenance and repairs, and is suitable for welding in all positions. A covered electrode as the consumable and a direct current (DC) power source are all that is necessary to be operational, and this process is suitable for welding in all positions. However, the DC power source has to be adapted and prepared for underwater welding to safeguard a welding operation under such conditions.

The DC power source can be a DC generator, transformer, or inverter, as long as the device is manufactured and approved for use in underwater welding operations. The modern welding machines can have additional options, such as hot start, arc force, and remote control functions, to make the welding easier to execute, and to provide better penetration and protection of the welding arc during welding. Many specialist welding power source producers focus their marketing efforts on underwater welding, since their product responds to the special demands of underwater welding companies.

Setting Up

When the suitable welding source has been determined, the connections of the workpiece and the electrode holder cable are as follows. From the welding machine, one cable connects to the electrode holder and another cable to the workpiece connector, as shown in Fig. 2 (Ref. 2). The electrode cable connects to the negative terminal (straight polarity). When connecting the electrode cable to the positive terminal, electrolysis can occur, which could potentially deteriorate the metallic parts in the electrode holder. Hence, the workpiece lead connects to the positive terminal. The electrodes can usually be welded with direct current electrode positive (DCEP) or direct current electrode negative (DCEN), and many procedures are welded DCEP as well, so when having a problem losing the electrode holder, DCEN could be a possible solution.

Precautions have to be taken to prevent mixing up the cables with positive and negative polarity when preparing the welding operation. A fully insulated electrode holder is used to prevent any current passing through the hand of the welder/diver, as current always follows the way of least resistance. To ensure the electrical safety of the operation, the welder has to be completely insulated from all electrical circuits; the welder should wear watertight rubber or rubberized canvas gloves, all the metallic parts inside the helmet shall be completely electrically insulated, and a dry suit should possibly be used to complete the overall electrical insulation. When lowering the electrode holder to the diver changing the electrodes, during any break and in any case of possible danger, the power shall be off with a zero open circuit voltage (OCV).

This safety switch is only to be operated to switch the welding current on or off, upon the specific and direct request from the welder/diver in the water below.

An overview of the basic setup for an underwater welding operation is illustrated in Fig. 3. The figure shows the support vessel with the required equipment; the DC welding power source, the workpiece leads, the bulk cylinder with compressed air or mixed gas for the welder to breathe, and the audio-video communication system to connect the welder with the dive master/operator on the vessel.

The video connections make it possible to follow the welding processes and work underwater, for guidance and/or for documentation of the actions. The knife switch connects the workpiece and lead with the welding machine above. Below the water surface, the welder wears a full drysuit and diving helmet, carries a safety cylinder with breathing air on his/her back, and has a fully insulated electrode holder in hand. The airhose, the communication and light cables, and the depth tube all have a different color and combine to form a so-called "umbilical" that connects the diver with the equipment on board the vessel.

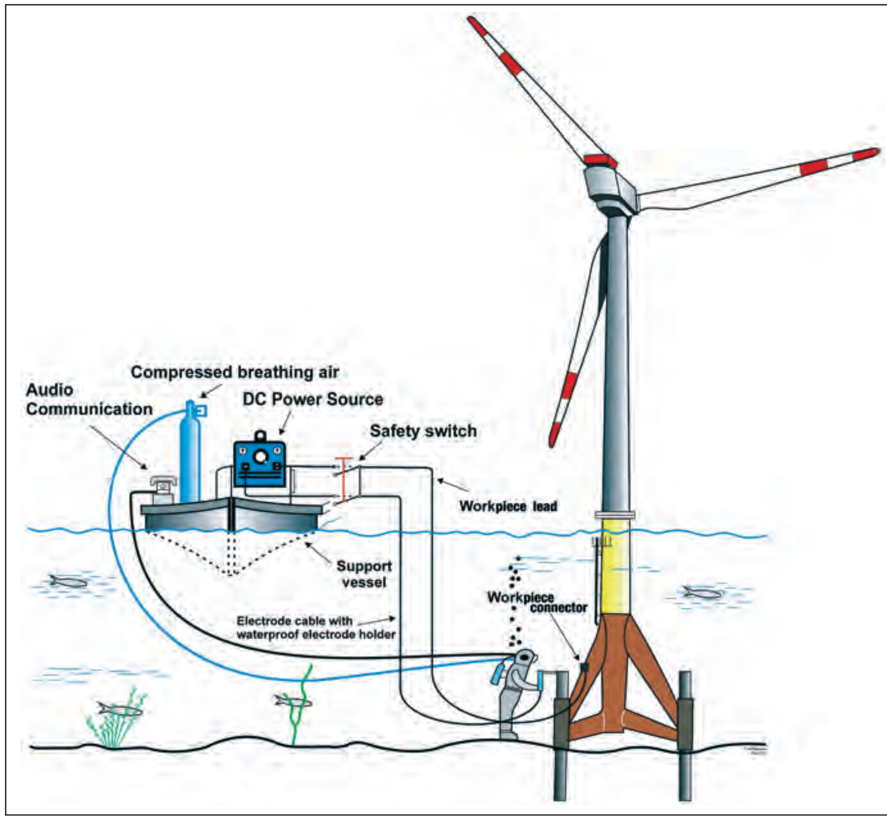

Fig. 3 — Overview of an underwater welding operation setup with equipment and support vessel. (Courtesy of Fred Neessen.)

Although the breathing air for the welder is supplied from the bulk unit or directly from the compressor on the vessel, referred to as surface supplied equipment (SSE), the diver also needs to carry a small bottle on their back as a safety precaution in case the supply from the SSE may encounter a problem and fail to supply breathing air. As previously mentioned, the support vessel can also carry a recompression tank for safety and for carrying out complex and deep diving operations. The full organization of such an operation can become complex, since everything has to come together in one smooth and safe combination of events and in a team of individuals with different responsibilities.

Staying in Touch

The communication between the welder/diver in the water and the dive master/welding operator on the surface has to be seamless since lives are at stake. A great deal of training, learning, experience, and trust has to be intrinsic for cooperation within the whole team. The welder/diver has to be a highly competent professional and commercial diver, as opposed to a sport diver, knowing all the ins and outs of safe diving and also be an expert welder to execute welds under extreme, often dark and cold, circumstances. When welding underwater with electrodes, due to the gas that develops in the arc and the heat that makes the water boil, the welder cannot really see the actual weld pool and slag as he would under dry circumstances. These conditions require the welder to have an elevated skill level and competence to produce a suitable and solid weld. The welding training therefore requires significant practice and qualification welding with subsequent maintenance of the qualifications by repeating the performance regularly.

Many national and international underwater welding and training facilities have been established to provide organized training and practice as well as for qualification of welder/divers and welding procedures under international standards. Some standards used for such qualifications include AWS D3.6M:2017, *Underwater Welding*

Fig. 4 — Essentials for the dive: electrodes in hermetically sealed metal cans to protect the electrodes before the welding operation, and a Kirby Morgan diving helmet. (Courtesy of Jan Hilkes.)

Code; ISO 15618-1:2016, *Qualification testing of welders for underwater welding — Part 1: Hyperbaric wet welding*; and ISO 15618-2:2002, *Qualification testing of welders for underwater welding — Part 2: Diver-welders and welding operators for hyperbaric dry welding*.

Metallurgy and Electrode Coating Development

Being underwater, electrodes are exposed to both a wet or very high humidity environment, the water/seawater, and an increased pressure caused by the water pressure, whereas every 10 m of water depth equals one bar of pressure. This means that consumables need to be specially developed and designed to meet the necessary welding, chemical, and mechanical requirements under these extreme circumstances.

When developing electrodes for underwater welding (Ref. 3), three main phenomena have to be taken into account and play an eminent role in the chemical composition and the mechanical properties of the resulting weld:

1) The surrounding water dissociates in the electrical arc, hence, the hydrogen and oxygen content in the arc and weld metal increase to relatively high levels. The amount of dissociated water is proportional to the water depth, hence, also the amount of hydrogen and oxygen in the arc and subsequently in the weld metal.

2) The water pressure influences the metallurgical processes in the electrical arc and results in a change in chemical composition, caused and enhanced by the higher oxygen content.

3) The surrounding water increases the cooling rate, resulting in a three-dimensional and shorter t8/5 time. While preheating is usually not easy or practical to carry out, the hardness of the weld metal and adjacent base material increases.

Waterproofing the Electrodes

When the coated electrode is ready, it subsequently has to be protected against the underwater environment, which is the water itself, and the water pressure from the depth. This means applying protective waterproofing that meets certain requirements such as being nonconducting, nonhygroscopic, impervious, not water solvable, clear, can melt or burn away gradually during welding, and seal-tight to the electrode coating to prevent water coming in between the sealing and the electrode coating. It should also not have a negative influence on the welding behavior and be strong enough and resistant to impact or damage by the water pressure. For example, a type of alkyd resin varnish is used to provide an extremely tight waterproof coating that meets these requirements.

After the protective coating is applied, the electrodes should be properly packed in hermetically sealed metal cans or vacuum packaging to guarantee the optimal condition after transport and storage, before the electrodes are used on the job — Fig. 4.

Underwater Applications

Applications for underwater wet welding and cutting are numerous considering how much steel is used in and around water. Just as naval or commercial ships and submarine hulls need welding patches or repairs, many other situations require welding: platforms or wind towers in the sea with corrosion-preventing anodes welded upon them; corrugated bulkhead pan-

Fig. 5 — Two welder/divers in a practice tank for training and qualification. (Courtesy of the Royal Dutch Navy — Diving Group.)

els (sheet pile walls) in waterways sealed with welds to make them watertight; and steel harbor constructions such as water locks and sluice gates.

What all the welds in these applications have in common is that the majority are fillet welds and welded at water depths down to about 20 m. In the case of ships, it makes a huge difference when a welding repair is carried out while in the water as opposed to a very expensive dry dock solution. For all these applications, wet welding with electrodes is very suitable. Also, electrodes are much more economical than complicated underwater oxygen arc cutting for underwater cutting of small parts or forming a hole.

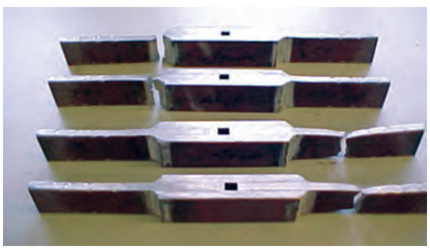

Fig. 6 — Double welded lap joints, partly made in the shop and partly made underwater for the welding procedure qualification. (Courtesy of the Royal Dutch Navy — Diving Group.)

Fig. 7 — A three-pass fillet weld appearance after welding and cleaning. (Courtesy of the Royal Dutch Navy — Diving Group.)

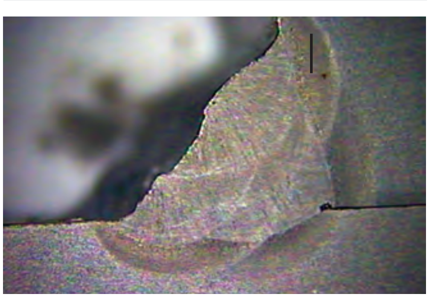

Fig. 8 — The cross section of the three-pass fillet weld, perfect profile, and penetration. (Courtesy of the Royal Dutch Navy — Diving Group.)

Fig. 9 — A fully equipped welder/diver preparing to go under for underwater welding and cutting. (Courtesy of Jan Hilkes.)

Since all these applications fall under certain regulations and approvals, such as those governed by the American Bureau of Shipping (ABS), DNV-GL, or Lloyd's Register (LR), the welding procedure qualifications and the welder performance qualifications have to be carried out in accordance and under the supervision of these approval agencies per their regulations.

Putting it to the Test

The Dutch Navy qualified using UTP Nautica 20 electrodes under LR for welding patches or lap joints onto naval ship hulls, in case the material thickness has reduced due to corrosion or other damage (Ref. 4). To qualify the wet welding procedures and the welders, fillet welds were executed in plates of 10 mm thickness. This took place in an indoor diving tank filled with 3% saltwater to simulate marine seawater conditions, as shown in Fig. 5.

Part of the qualification welds were fillet welds that were produced in double lap joints, prepared on one side with full fillet welds made in the workshop. The other side was welded in the tank with a 3.2-mm electrode at about 150 A in the downhill position. The test weld was a smaller size in order to test if the specimen would break in the weld or in the base material that was to be tested.

Figure 6 shows the double lap joints with one side welded in the shop (left) and the other side welded under water (right) showing the specimen broke in the base material or on the side of the workshop welds. The result of the multipass fillet weld in downhill position is shown in Fig. 7. The bead appearance was very good, especially considering the lack of visibility of the welder. The cross section of this weld in Fig. 8 shows joint penetration, which is one of the qualification requirements, proven by a break test that shows the amount of penetration per length of weld.

Practice Makes Perfect

Open-water training sessions are organized for the entire underwater diving and welding team of the Dutch Navy. Figure 9 shows the welder/diver with insulating rubber gloves and getting ready to plunge, standing behind an underwater workbench with a clamping device on a platform that can be lowered into the water for practicing purposes. These welders have also performed underwater cutting with the same electrodes.

Using 240 A, a 10-mm plate could easily be cut into many parts. The cutting length is up to 200 mm with one electrode. The electrode is 3.2 mm in diameter and 450 mm long. The electrode length of 450 mm made it possible to distinguish them from the repair electrodes used, which were 350 mm. The welder can easily carry both types to be prepared for all applications under water. WJ

Acknowledgments

The authors thank Gerrit Weerstand and his colleagues of the Royal Dutch Navy — Diving Group for their valuable contributions and practical insight on underwater welding as discussed in this paper. Thanks also go to Fred Neessen, an international welding engineering consultant, for the expressive graphics (Figs. 2 and 3).

References

1. Szelagowski, P. 2015. *Unterwateterwasser-Schweißtechnik, Grundlagen - Forschung - Anwendung*. DVS Media, Düsseldorf, Germany.

2. Keats, D. J. 1990. *Professional Diver's Manual on wet-welding*. Abington Publishing, Cambridge, England.

3. Hilkes, J., and Tuchtfeld, J. 2019. *Unterwasserschweißen mit umhüllten Stabelektroden für Schiffbau- und Offshore-Anwendungen*, DVS - Große Schweißtechnische Tagung, 16/17 September, DVS Reports, Vol. 355, p. 385-397. DVS Media, Düsseldorf, Germany.

4. Bos, R. 2001. De kwaliteit van een onderwatergelaste verbinding met beklede electrode. NIL Lastechniek, Oktober 2001: 4-8.

JAN HILKES (jan.hilkes@voestalpine.com) is managing director and JÜRGEN TUCHTFELD is manager, global application engineering, at voestalpine Böhler Welding UTP Maintenance GmbH, Bad Krozingen, Germany.

Understanding Shielding Gas Flow in GTAW

BY ANDREW PFALLER

The combination of gas lens and proper gas flow rate in GTAW applications improves quality, efficiency, and throughput.

Using the right shielding gas and following best practices can help you save money

Using shielding gas flow rates that are too high for gas tungsten arc welding (GTAW) applications can double gas costs, resulting in upwards of $3300 in added annual costs per welder. Many operations may not realize there is huge potential for immediate payback and reduced costs by using a better gas consumable.

Improper shielding gas flow can drive up costs through wasted gas and added rework. When there is a lack of knowledge about shielding gas best practices, operations might also use temporary solutions that don't address the root issue and simply push these hidden costs higher.

This article will help you learn the importance of using the right shielding gas consumables and how following best practices can reduce operational costs.

Standard Collet Bodies for GTAW

Many operations use GTAW in high-profile applications where the greatest weld aesthetics, quality, and integrity are required — Fig. 1. The GTAW process requires an inert atmosphere to protect the tungsten (where the arc is generated) and, more importantly, the molten pool of the metal being welded — Fig. 2. One consumable used for this in many GTAW applications is a collet body, which provides shielding gas coverage over the part being welded.

Companies often choose collet bodies because they are a less expensive method of delivering the shielding gas compared to other options. However, collet bodies can be the source of problems that end up costing time and money — much more than the initial small amount saved up front.

When using a standard collet body in GTAW, a considerable amount of turbulence and atmospheric contamination are introduced into the stream. This can cause issues such as porosity, base metal oxidation (also called sugaring on stainless steel), poor welding performance, and arc flutter — problems that are unacceptable in applications that require high quality.

The turbulence in the shielding gas flow also limits how far the tungsten can be extended past the end of the nozzle, which may restrict the operator's ability to complete the weld.

Adjusting the Shielding Gas Rate

To overcome these quality or access issues, operations may take the common step of increasing the shielding gas. However, this only exacerbates problems because increasing the flow rate increases the instability in the gas column. Increasing the flow rate also causes more shielding gas to be consumed than before — a point that is often overlooked.

This can drive up costs in the following three ways:

- **Expenses associated with the consumable shielding gas.** A 300-ft^3 tank costs on average $35, or $0.11 per ft^3. If an operation uses one tank per welder per week, that's $1750 per year spent on shielding gas. Some operations studied have used as much as 60 ft^3/h of gas in a high duty cycle application, with approximately 50% arc-on time. This would mean shielding gas costs are about $6600 per welder shift per year. If that company had 25

Fig. 1 — The GTAW process is often used in high-profile applications that prioritize weld aesthetics, quality, and integrity.

Fig. 2 — The GTAW process requires an inert atmosphere to protect the tungsten and the molten pool.

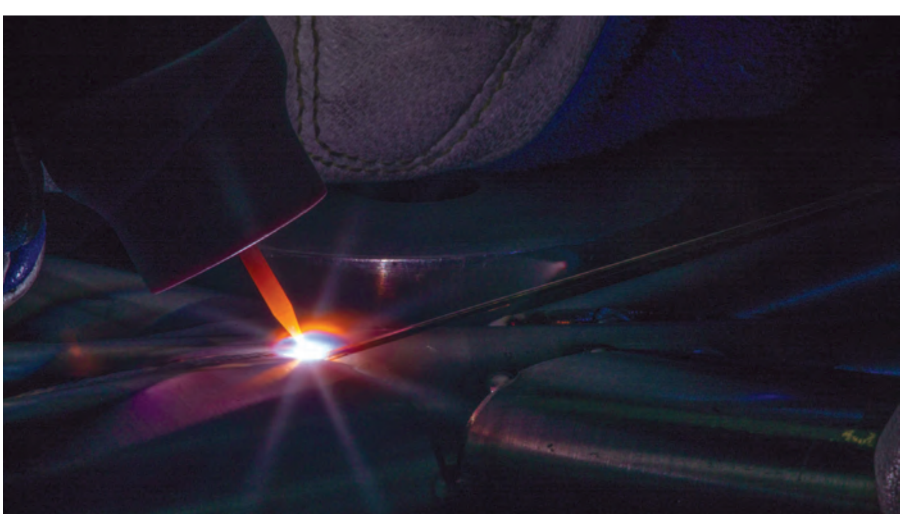

Fig. 3 — Swapping your collet body for a gas lens consumable can give you better results, including improved gas flow.

welders on two shifts, that's about $330,000 per year spent on shielding gas alone.

• **Time and materials lost to rework.** Greater instability in the gas column can result in problems like porosity, poor welding performance, or arc flutter. In high-purity applications, this often means rework, which can take three to seven times longer to complete compared to a weld where no rework is required.

• **Downtime to change gas cylinders.** If the operation is using shielding gas cylinders, going through the gas at a faster rate results in more downtime for changing out the gas cylinders.

Moderate shielding gas rates such as 10 to 20 ft^3/h are the most common, and higher flow rates greater than 40 ft^3/h are not generally recommended.

Most welding procedures specify a proper cup or nozzle size and gas flow rate. If an operation changes the cup size without also adjusting the gas flow rate, it has a drastic impact on the stability of the gas flow. Therefore, it's important to make any changes in concert with each other, rather than simply changing gas flow rate or cup size alone.

Options to Improve Shielding Gas Coverage

If increasing shielding gas flow isn't the answer, what can operations do to improve shielding gas coverage and results in GTAW?

Switching from a collet body to a gas lens consumable can offer better results provided by improved gas flow, which will help reduce secondary costs — Fig. 3. Gas lenses often do have a higher upfront cost, typically a few dollars more per consumable compared to collet bodies, but operations shouldn't be deterred by this. The small added cost of a gas lens can deliver appropriate gas coverage that significantly helps reduce costs elsewhere.

Results of a Gas Lens Study

Past real-world applications have shown that gas lenses do provide better results. However, there were still knowledge gaps about how exactly the better results occurred, and what best practices could be used to help optimize results.

Miller Electric Mfg. LLC recently completed a study to better understand shielding gas flow and the differences in gas lenses. To capture imagery, the study used Schlieren photography, which is essentially a scientific method of developing the shadows that result from light refracting differently as it passes through varying densities of gas. Using this method, the goal was to see the flow pattern as shielding gas exits the front of the GTAW torch. The gas flowing out of the torch creates friction with the stationary atmosphere, and this friction causes the two gases to mix in a wavelike form. These waves initially start small but continue to grow until the flow is fully turbulent.

This is known as the Kelvin-Helmholtz (K-H) Instability, which occurs when a gas has a different density and/or velocity than the surrounding gas. K-H Instability begins as a wavelike motion at the outer edge of the shielding gas column and ultimately grows until the flow becomes completely turbulent. That turbulence introduces atmosphere into the shielding gas, which reduces coverage effectiveness.

The study proved that using a gas lens vs. a collet body makes a substantial difference in the flow pattern, with gas lenses producing a longer laminar, or stable, shielding gas column and, therefore, having a lower K-H Instability.

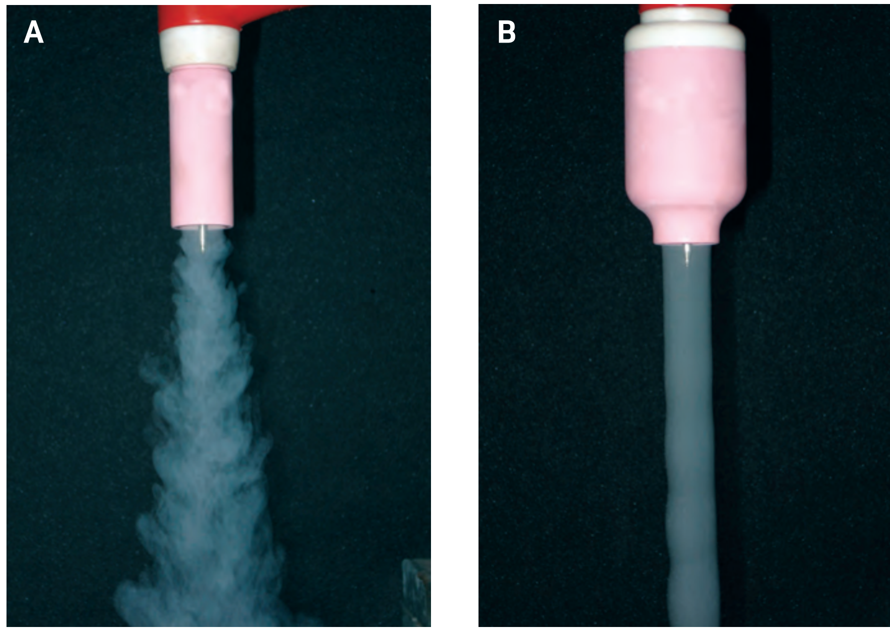

Fig. 4 — A gas lens increases shielding gas coverage and reduces turbulence compared to a collet body: A — Collet body in use; B — gas lens in use.

Other Important Factors

Keep in mind there isn't one accessory or consumable that will be the perfect solution for every application because there are several variables involved. However, the study showed that the following factors and best practices can help optimize shielding gas coverage:

- **Gas flow rate.** As previously mentioned, a gas flow rate that is too high causes more instability. But be aware that too low of a flow rate can make the gas more susceptible to interference from outside forces, such as wind or fans. Moderate rates, such as 10 to 20 ft^3/h, are recommended. Lower flow rates with a gas lens can save 50% or more in consumable shielding gas spend, which could eliminate more than $3000 annually per welder at 20% duty cycle at 60 ft^3/h. Going back to the earlier example of an operation with 25 welders, this is more than $75,000 in annual savings.
- **Nozzle diameter.** The study validated that larger-diameter, converging-type nozzles provided a longer laminar shielding gas column. This is because larger nozzles produce lower gas velocities, resulting in lower K-H Instabilities. Many companies will use the smallest consumable possible to get into tighter spaces. However, in actuality, a larger nozzle can improve access by allowing the welder to stick the tungsten out more, thus increasing visibility and access to hard-to-reach areas.
- **Nozzle shape and lens design.** Larger converging lenses provide longer laminar flow, but that doesn't mean any lens with a large opening is a good choice. Nozzle shape and lens design are very important to performance. The ultimate goal is to guide the shielding gas to the weld zone and provide a gentle blanket over the weldment. Regarding nozzle shape, a converging style gives coverage over the entire orifice and helps transition the plug flow into a developed flow, which reduces K-H Instabilities or makes a stable column. A diverging or "champagne-style" nozzle gives a false sense of security due to the lack of shielding in the outer portion of the cup, like putting a funnel on the end of a garden hose. The gas will continue to flow out in a straight path, causing a false perception of gas coverage that could compromise the weld material. The plenum/screen design also is important. Look for a lens with multiple screens that vary in mesh count to achieve optimal flow profile.
- **Nozzle length.** Another important factor is nozzle length. A longer nozzle helps further transition the plug flow into a fully developed flow, which describes a slower flow on the outer portions of the stream and higher flows in the middle. With plug flow, K-H Instabilities are decreased, and the stable laminar region of the shielding gas column is longer. Similar to the larger lens diameter, a longer converging-type nozzle also provides a longer laminar shielding gas column.

Improving GTAW with Proper Gas Delivery

A gas lens increases shielding gas coverage and reduces turbulence compared to using a collet body — Fig. 4. Gas lenses also allow the tungsten to extend farther for more accessibility to weld complex joints. While a gas lens has a slightly higher upfront cost than a collet body, operations will quickly see return on that investment through significant reductions in gas and rework costs. The combination of gas lens and proper gas flow rate in high-profile GTAW applications can help reduce or eliminate rework, cut costs, and improve process efficiencies and throughput. WJ

ANDREW PFALLER (andrew.pfaller@millerwelds.com) *is an American Welding Society Certified Welding Inspector and segment manager at Miller Electric Mfg. LLC, Appleton, Wis.*


When the world is counting on you, you can count on us.
Being essential means the world is depending on you to keep moving forward, even when everything else is standing still. While the rest of the world is depending on you, you can depend on us.
Turn to the Pros
HARRIS
A LINCOLN ELECTRIC COMPANY
©2020 Harris Products Group. All Rights Reserved.

Shielding Gas: Lower Your Costs by Eliminating Inefficiencies

BY DAVID GAILEY

Shielding gas is typically one of the largest expenditures that companies incur to support their welding operations.

Learn how gas-saving devices, on-site blending, and continuous supply support operations

In an industry where every penny counts, finding ways to reduce costs is essential. One of the areas with the most opportunities involves the use of shielding gas, which is typically one of the largest expenditures that companies make to support their welding operations. Fortunately, there are low-cost solutions through equipment that maximizes the value these companies get out of their gas purchases.

While it may seem counterintuitive on the surface, a small investment into the proper gas equipment can easily provide significant gas savings. The following article presents simple upgrades to consider, if gas savings could benefit your organization.

Where Do the Inefficiencies Occur?

As a first step, take an analytical look at each specific welding process and determine benchmarks. Determine the precise amount of gas needed to provide an adequate weld. This is crucial to determining where gas is wasted in your operations, and many will be surprised to find out that they are wasting an enormous amount of gas in their shielding flow rates.

When searching for ways to save costs, those who have set benchmarks in gas usage will most likely discover that their processes are extremely wasteful when it comes to shielding gas. Then, after determining there is waste within the process, the next step is pinpointing where this waste is so it can be eliminated.

Finding Savings in the Surge

Reducing gas surge can lead to significant cost savings.

These surges occur every time the solenoid is activated, more precisely, at every trigger pull on the welding torch. Most flow control equipment used with shielding gas, whether from a cylinder or a pipeline, is designed to operate at pressures of about 20 to 30 pounds per square inch gauge (psig), while applications using pure carbon dioxide may operate at pressures up to 50 psig. This means every time a welder squeezes the torch trigger, the upstream pressure of 20 to 30 or even 50 psig exits the welding nozzle, wasting a large amount of gas when the trigger is pulled.

Different Gas-Saving Devices

What can welders do to keep from using higher flows than necessary or that exceed the recommended rates?

There are many gas-saving devices on the market that can greatly reduce the amount of gas surge associated with every trigger pull. These devices include, but are not limited to, gas guard regulators, point-of-use orifices, lower pressure flowmeters, and even surge reducing hoses — Figs. 1, 2. These flow-control accessories set a limit so excessive flow rates that make the gas turbulent, drawing oxides and nitrides into the weld, cannot be used. While these devices have been around for more than two decades, they rarely receive sufficient attention until market conditions create the need for companies to seek out cost-saving measures. Therefore, there is a great deal of misunderstanding surrounding these products.

Some of the more popular devices that can be added to the wire feeder to control gas surge include gas-saving regulators and point of use orifice fittings. Welding professionals should be wary of in-line restricted orifices as shielding gas savers, as these devices, if not installed at the correct point in the gas stream, will not have any effect in eliminating gas surge. The most effective way to eliminate shielding gas surge is to introduce a pressure-regulating device into the gas system.

Point-of-use orifice fittings can work well and are generally a low-cost solution. However, to work properly, the orifice fittings must be installed precisely in front of the solenoid valve. Anywhere else in the gas stream, like back at the regulator or the flow meter, will not work and the surge problem will remain.

In contrast, an inert gas guard can be placed anywhere in the stream and work effectively, taking that high upstream pressure and regulating it down to eliminate the surge. When the solenoid valve opens, there will not be the usual high pressure upstream, so instead of 50 psig there is only roughly 10 psig. That type of change can easily result in significant annual gas savings when added to a welding machine.

This is an issue because welding equipment is typically designed to operate at relatively high line pressures, such as 20, 30, or 50 lb/in.^{2}, and that creates the high surge at the welding nozzle. Also, the typical welding lead that has been in use for a while may be twisted, have a kink, or the gas diffuser can become partially clogged due to a build-up of spatter. This results in flow restrictions at the welding tip, which can only be overcome with more shielding gas pressure. And the older they get, the more imperfect these welding leads become. This need to clear out any imperfections or potential clogs that would restrict flow is why many welding flow meters are designed to deliver 20, 30, or 50 psig of pressure to the solenoid valve to be released when the valve opens.

There are other types of shielding gas flowmeters offered in the industry that are calibrated at atmospheric pressure or zero psig. These are typically called "zero-comp" flowmeters, as they release the flow of shielding gas at atmospheric pressure with no back pressure whatsoever. So when the solenoid opens, there is no wasteful back pressure to create the surge.

These lower pressure compensated devices work better with newer welding leads rather than older leads. Older leads may have imperfections and kinks due to wear. This may require a higher back pressure. However, a new installation or an application, like a technical trade school with many welding booths and students, would be an ideal choice for a lower pressure compensated device. Other applications,

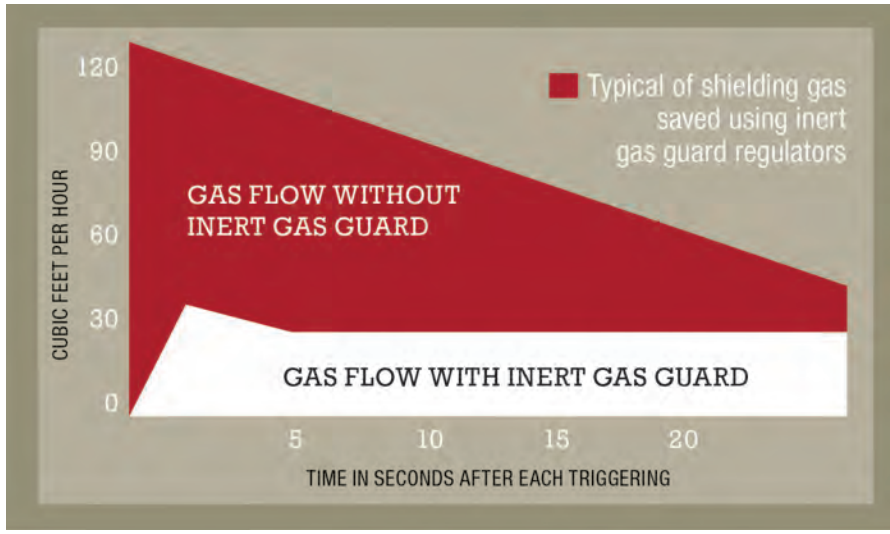

Fig. 1 — Inert gas guard regulators reduce gas surge when a gas metal arc gun or gas tungsten arc torch is activated.

such as in a construction site, fab shop, or where equipment could be handled roughly and not well maintained, a lower pressure compensated device may not be ideal and will cause other issues.

In addition to reducing costs through waste-optimized shielding gas systems, another option to consider is blending gases on-site.

Add Flexibility and Customization by Blending Gases On-Site

Traditionally, gas metal arc welding is done with pure argon or with a mixture of argon and CO_2. Whatever combination a company used, they would usually order the mixture to be delivered preblended in a cylinder. As welding has evolved, the techniques used in different applications have become more and more specialized, with specific blends of argon and CO_2.

Keeping in mind that many applications may require a different blend every time they start a new job, many welders seek the flexibility to change their mixture on the fly to best suit different applications, projects, and materials.

But because gas blenders can cost anywhere from $1000 up to $10,000, a company should consider how much gas it uses to determine the return on investment (ROI) of buying a gas blender. For just a handful of stations, a minimal investment of around $1200 would likely suit their blending needs. However, for 28 welding stations, then the blender investment would be closer to $7000. Consider the cost benefit not only to the streamlined supply chain, but also the reduction of downtime switching between jobs.

Using a gas blender, gas mixtures can be changed easily. Because this will prevent companies from having to purchase many different cylinders with preblended mixtures, they can minimize their costs and streamline their gas purchasing.

Fig. 2 — A typical flowmeter regulator is a fixed pressure/variable orifice device. Pressure is set at the factory to a compensated or calibrated pressure, depending on the flow range desired and the gases being used.

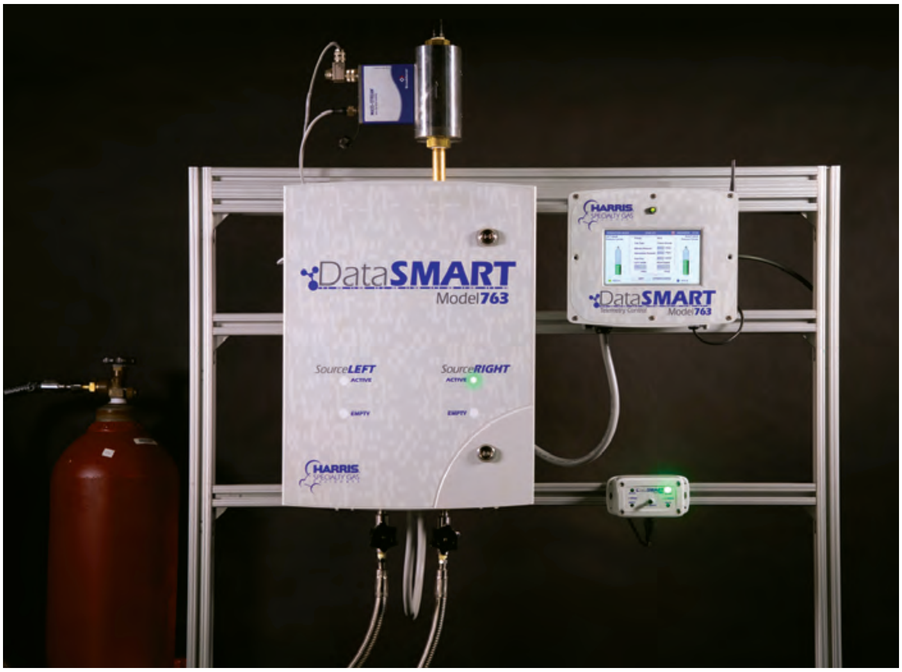

Fig. 3 — Automatic switchover manifolds ensure a continuous supply of gas. Some systems, such as DataSMART, provide detailed data on usage and other information to help users better manage gas consumption.

Going back to our welding school example, in a situation where every welding booth will likely be using, for instance, a 75/25 blend, an expensive gas blender might not be a good investment. In cases like these, it may actually be beneficial to continue using packaged gas in premixed cylinders.

There is no hard and fast rule, but it would be beneficial for many companies to examine their processes, workflow, and supply chain to determine whether a gas blender may be a potential opportunity to increase productivity while reducing costs.

Continuous Gas Supply: Reducing Downtime and Increasing Productivity

It is estimated that more than 50% of the welding market uses packaged gas; either liquid dewars or high-pressured cylinders. In that case, those companies should ask themselves whether it would be advantageous to invest in a system that provides continuous gas and never shut down. These companies are not making money when they cannot weld. And with large-production companies, every minute of downtime is extremely costly.

In bulk gas systems, they come equipped with an alarm that goes off when the gas supply hits a certain, predetermined level. That alerts the gas supplier to send out a truck to refill the bulk system. But if you are using packaged gases, changing cylinders is an in-house job. And even more than the responsibility, your revenue stream ceases during the time it takes to change the cylinder. So when a cylinder runs out, how long does it take to change it out? And how much money does that cost? Over time, it can add up.

However, this downtime can be removed from the equation by putting in a system with a continuous gas supply. These automatic changeover manifold systems have a gas supply on both the left and right side, with one as the primary supply and the other as the reserve. When the primary cylinder reaches a predetermined level of depletion, it seamlessly switches over to the reserve source, leaving plenty of time to replace the empty cylinder(s). The former "reserve" side now becomes the new "primary" side, and the system will switch back and repeat the process when the new primary side goes empty.

In addition, fully automatic changeover manifolds are becoming popular and have been proven to be an ideal solution for high-pressure cylinders, liquid dewars, and even bulk systems requiring a packaged gas backup. This manifold could be attached so the bulk system is always the primary, but with a six- or 12- pack of high-pressure cylinders in reserve in case they were unable to get a delivery of gas before their bulk system was depleted. For high-end, high-production companies, this would provide the security of avoiding downtime.

New technology is enhancing the capabilities of these automatic changeover manifold systems. With new systems in development, like DataSMART(TM) from Harris Products Group, these will be interconnected with data that can provide in-depth efficiency and usage analysis, as well as providing alerts at preset levels both internally and externally, so replenishment becomes automatic — Fig. 3.

Additionally, systems that plug into the Internet of Things could prevent waste by not only monitoring a cylinder or cylinder bank to determine whether it needs to change over to the reserve cylinder, but users could also easily program and adjust the changeover pressure settings on either side for further optimization. This would maximize gas usage and avoid sending cylinders back to the supplier with as much as 25% of the gas still left in them. DataSMART will feature a mass flow meter, too, that will measure molecules of gas consumed in the process to determine gas usage.

Find the Best Fit to Reduce Your Gas Waste

If you want to control your welding process and shielding gas system, then you really need to understand how eliminating inefficiencies in your system can result in a significant cost reduction and ROI. By analyzing the data, you may be surprised to learn how much you are wasting on shielding gas annually. If you do not have sufficient gas-saving protocols in place, an investment based on your unique needs could be a potential windfall for you. There are many options out there, so take advantage of the data that you have to find a solution that maximizes your efficiency and output. WJ

DAVID GAILEY (David_Gailey@lincolnelectric.com) is product manager of specialty gas products for the Harris Products Group, a Lincoln Electric Co., Mason, Ohio.

Adaptive Remote Laser Welding Ushers in Innovative Manufacturing

This welding process determines part location and beam position to meet weld quality standards

BY JASON WOOLLEY

Remote laser welding was made popular at the turn of the century. The ability to direct a beam of light to the workpiece and join materials without contact promised to dramatically reduce cycle time and lower manufacturing costs. However, the technology was not widely adopted. Due to the inherently narrow laser welds, and the large part-to-part tolerance of the workpiece, products not only had to be designed specifically for the remote laser welding process, but fixturing prices increased to better locate parts. Ultimately, this increase in both part and system cost limited the financial benefit of decreased cycle time to only high-volume applications. In other words, if you were making hundreds of thousands of the same exact part per year, the financial justification could be made.

The challenge of broader industrial adoption of remote laser welding did not stop there. The bigger problem was the beam positioning process. The typical scanner optic is programmed to position the laser beam based on a software coordinate system or computer-aided design model. The weld locations are loaded into the computer-controlled coordinate system, which in turn adjusts the scanner mirror to position the beam, according to the model. However, the real problem is that parts are rarely placed in the same exact position. This inaccuracy of the parts resulted in the use of lap welds, which placed several millimeters of additional material to the edge of the part to ensure the weld did not miss the upper sheet. This larger flange subsequently increases the part weight and cost.

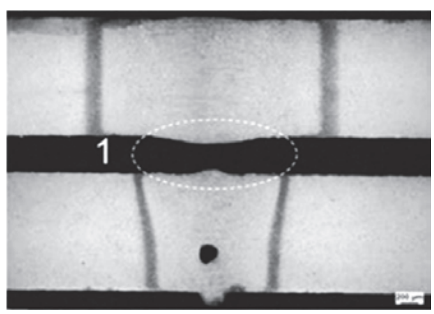

Fig. 1 — False friend — cross section shows no weld between the upper and lower sheets.

The next problem with the process is related to weld quality. With a lap weld, an inspector can see the weld on the top sheet. In the case of a complete joint penetration weld, the inspector can also see the weld on the bottom of the lower sheet. What they cannot be sure of is if the two sheets are joined in the middle. This weld quality problem is often referred to as false friend — Fig. 1. To overcome this problem, the part designer would design the part with more welds than it actually needed to statistically prevent part failure if a few false friends were present. Again, this process leads to excessive part weight, additional cycle time, and increased part cost.

What if there were a way to no longer worry about part location, and position the laser beam exactly on the edge of the part? This would change traditional lap welds to edge fillet welds. With edge fillet welds, flanges can be reduced, part weight is lowered, part cost is reduced, and inspectors can see the top, bottom, and middle of the weld. What if we no longer needed robust, over-designed fixtures to push parts into exact locations and remove small gaps* to prevent false friends? Both of these things are now possible through utilization of an approach referred to as adaptive remote laser welding.

Adaptive remote laser welding technology provides a direct look at the workpiece; determines the location of the edge that needs to be joined, if a gap is present between the two sheets; makes on-the-fly adjustments to the process parameters; and positions the

*Note: The terms *gap* and *gap bridging* are typically referred to as *sheet separation*. The American Welding Society (AWS) A3.0M/A3.0:2020, *Standard Welding Terms and Definitions*, defines sheet separation as "The distance between faying surfaces adjacent to the weld once a spot, seam, or projection weld has been produced."

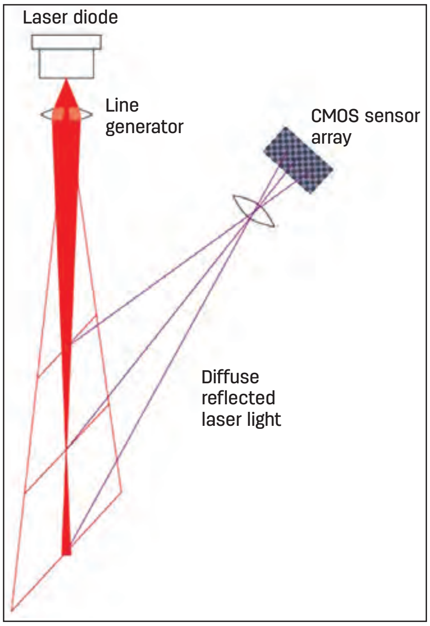

Fig. 2 — Laser triangulation for optical seam tracking.

beam in the exact location required to meet weld quality standards. This adaptive process is possible by seam tracking to position the beam via laser triangulation sensors or shape recognition cameras.

Laser Triangulation Seam Tracking

With optical seam tracking sensors, a laser beam is emitted from a diode integrated either into the unit or as part of a line generator package — Fig. 2. This beam is converted by an optical line generator into one or multiple (i.e., three) lines depending on the make of the sensor. The laser line hits the measurement object and is diffusely reflected at an angle such that it hits a cloud of individual, more or less bright points of light, onto the camera chip. The individual pixels are filtered and summarized in an application-specific integrated circuit chip. Filters, both software and hardware related, will remove the reflections and other light influences. The data is then calculated by the seam tracking controller, and the position of the points of light on the chip are converted to positional information as it relates to the process. A profile of the joint is assembled and the results are linearized and compared with those of the customer's chosen seam profile. Other supporting parameters are calculated with respect to the profile and are then compared with the defined values of the parameters set within the motion-control side of the process. Offset data is determined and then output to the machine control, resulting in a modified motion path according to the offsets found during the tracking process.

The information output from the sensor package will include information such as Y position, Z position, gap, mismatch, and angles about the sensor datum. Analysis of the data provided through software algorithms can use the data to not only track the seam but also adjust process parameters such as laser power, spot size, Y-offset, amplitudes, and oscillation frequencies of the beam. When combining the control of all of these process parameters, a true adaptive weld process is created to accommodate the variation in the parts — Fig. 3.

Shape Recognition Cameras

Shape recognition technology is a comparative process that looks for a shape on the workpiece that matches a predefined shape stored in the software. The shape is located by the image processing camera using a technology called dark field illumination. This process uses external lights that flood the part's surface. When an image is captured, the top surface appears light gray while features below the surface, (such as holes, part edges, and slots) appear to be darker. This dark image is then compared with the stored shape, and a positive shape recognition is determined.

Once the shape is recognized, the location of the shape on the image can be determined based on the pixel location. These parameters are then sent to the scanning mirrors, which direct the laser beam to the correct location of the actual part being processed — Fig. 4.

Both technologies, laser triangulation seam tracking and shape recognition, are made possible by ultra-fast 1 GHz on-board communication and high-powered scanner mirrors capable of 1000 Hz. This combination allows process speeds of 1 m/s, which is necessary to make the highly dynamic reorientation movements needed to adapt to real-time tracking requirements.

When the two technologies are combined into one tool, a new manufacturing reality becomes possible: the replacement of resistance spot welding. Resistance spot welding has been the go-to method for joining stampings in many industries, especially the

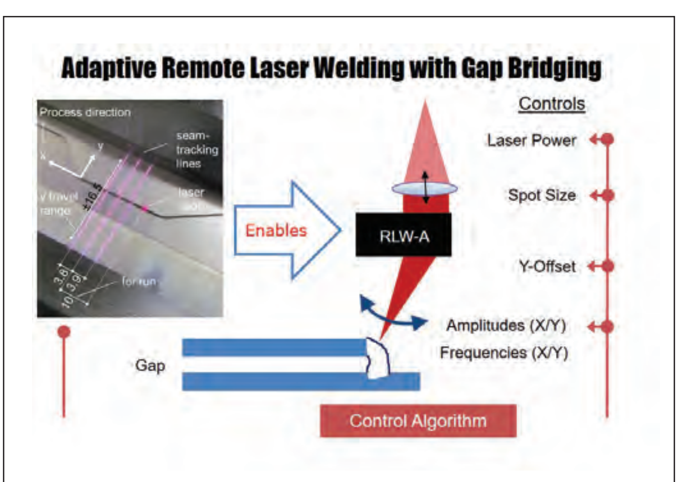

Fig. 3 — Adaptive remote laser welding with gap bridging.*

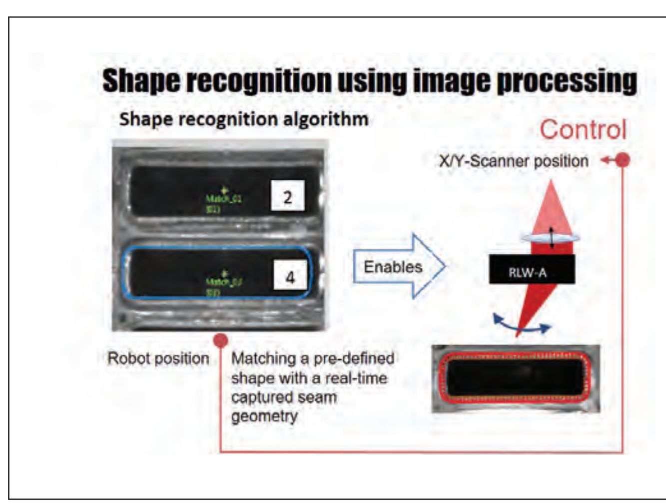

Fig. 4 — Adaptive shape recognition.

automotive industry. The process requires access to both the top and bottom of the final part. The heat created in the process leaves visible deformations in the material, and electrodes must be continuously replaced. The spot welding guns themselves are big and heavy, requiring robots to manipulate either the part or the gun, and the process requires about 3 s per spot weld. All of these limitations add up to additional subassemblies, heavier parts, increased cycle time, greater manufacturing floor space, and higher product costs. Remote laser processing can improve these adverse factors through a process called shaped fillet welding.

Shaped fillet welding, often referred to as plug welding, allows the design of the part to change because access to both the top and bottom sheets are no longer required. By adding a hole in the top sheet and using shape recognition and laser triangulation technology to locate this hole, the laser can weld the edge of the top sheet directly to the bottom — Fig. 5. The entire process, including shape recognition, adaptive location, and weld completion, is approximately 0.5 s per weld, six times faster than traditional resistance spot welding. The increased speed is not only a cycle time advantage, but also a manufacturing floor space advantage. Being able to process faster allows more welds to take place in the same manufacturing cell, while remaining under the manufacturing line's required takt time. Toyota Motor Co. conducted a study that shows a 40% decrease in floor space requirements and a 50% reduction of CO_2 could be achieved if this technology is implemented as compared with today's body shop (Ref. 1). In addition to cost savings realized with less equipment and floor space, there are less consumables required. Finally, the weld process parameters can be controlled so that complete joint penetration through the bottom sheet is avoided, thus allowing joining on visible surfaces in many cases.

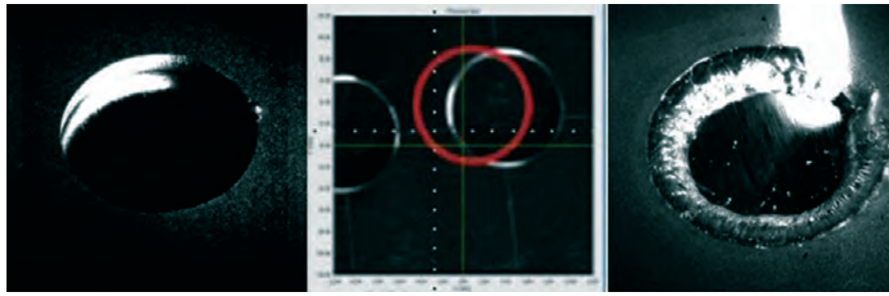

Fig. 5 — Laser plug welding process.

Conclusion

Adaptive remote laser welding is changing modern manufacturing processes. With the advent of laser triangulation seam tracking, shape recognition imaging, and fast processing speeds, we are finally able to realize true adaptive joining methods. These methods will allow us to overcome part variation and assembly fit-up issues as well as pave the way to a lighter, less costly production, all within a smaller manufacturing facility. WJ

Reference

1. Pittman, Kagan. 2015. What engineers need to know about laser screw welding (LSW). *engineering.com*

JASON WOOLLEY (jwoolley@abicorusa.com) *is key accounts laser group manager, Abicor Binzel, Frederick, Md.*

Note: The 2020 schedules for all certifications are posted online at *awo.aws.org/instructor-led-seminars/seminar-exam-schedule/*.

Certified Welding Inspector (CWI)

Seminar covers Parts A, B, and C of the CWI exam. Only Part B of the exam is taken following the conclusion of the seminar. Parts A and C are given at Prometric testing centers.

Location	Seminar Dates	Part B Exam Date
Miami, FL	Sept. 13–18	Sept. 19
Houston, TX	Sept. 13–18	Sept. 19
Seattle, WA	Sept. 13–18	Sept. 19
Benicia, CA	Sept. 20–25	Sept. 26
Louisville, KY	Sept. 20–25	Sept. 26
Minneapolis, MN	Sept. 20–25	Sept. 26
New Orleans, LA	Sept. 27–Oct. 2	Oct. 3
Boston, MA	Sept. 27–Oct. 2	Oct. 3
Nashville, TN	Sept. 27–Oct. 2	Oct. 3
San Antonio, TX	Sept. 27–Oct. 2	Oct. 3
Miami, FL	Oct. 4–9	Oct. 10
Long Beach, CA	Oct. 11–16	Oct. 17
Detroit, MI	Oct. 11–16	Oct. 17
Tulsa, OK	Oct. 11–16	Oct. 17
Atlanta, GA	Oct. 18–23	Oct. 24
Las Vegas, NV	Oct. 18–23	Oct. 24
Houston, TX	Oct. 18–23	Oct. 24
Kansas City, MO	Oct. 25–30	Oct. 31
Pittsburgh, PA	Oct. 25–30	Oct. 31
Orlando, FL	Nov. 1–6	Nov. 7
Indianapolis, IN	Nov. 1–6	Nov. 7
Reno, NV	Nov. 1–6	Nov. 7
Dallas, TX	Nov. 1–6	Nov. 7
Sacramento, CA	Nov. 8–13	Nov. 14
Miami, FL	Nov. 8–13	Nov. 14
Syracuse, NY	Nov. 8–13	Nov. 14
Cleveland, OH	Nov. 8–13	Nov. 14
Waco, TX	Nov. 15–20	Nov. 21
Norfolk, VA	Nov. 15–20	Nov. 21
San Diego, CA	Dec. 6–11	Dec. 12
Miami, FL	Dec. 6–11	Dec. 12
St. Louis, MO	Dec. 6–11	Dec. 12

Certified Welding Inspector (CWI) Part B

Course covers only Part B of the CWI exam. The Part B exam follows the conclusion of the three-day course.

Location	Seminar Dates	Part B Exam Date
Minneapolis, MN	Oct. 21–23	Oct. 24
Louisville, KY	Dec. 9–11	Dec. 12

9-Year Recertification Seminar for CWI/SCWI

For current CWIs and SCWIs needing to meet education requirements without taking the exam.

Location	Seminar Dates
Orlando, FL	Sept. 13–18
Sacramento, CA	Oct. 4–9
Dallas, TX	Oct. 11–16
Denver, CO	Oct. 25–30
St. Louis, MO	Nov. 1–6
New Orleans, LA	Nov. 8–13
Miami, FL	Dec. 6–11
Phoenix, AZ	Dec. 6–11

Certified Welding Educator (CWE)

Seminar and exam are given at all sites listed under Certified Welding Inspector. Seminar attendees will not attend the Code Clinic portion of the seminar (usually the first two days).

Certified Welding Sales Representative (CWSR)

CWSR exams are given at Prometric testing centers. More information at *aws.org/certification/detail/certified-welding-sales-representative*.

Certified Resistance Welding Technician (CRWT)

A comprehensive two-day seminar to arm attendees with the knowledge needed to take the exam with confidence. More information at *awo.aws.org/crwt/*.

Location	Seminar Dates
Nashville, TN	Oct. 27–28

Certified Welding Supervisor (CWS)

CWS exams are given at Prometric testing centers. More information at *aws.org/certification/detail/certified-welding-supervisor.*

Location	Seminar Dates
Atlanta, GA	Dec. 6–11

Certified Radiographic Interpreter (CRI)

The CRI certification can be a stand-alone credential or can exempt you from your next 9-Year Recertification. More information at *aws.org/certification/detail/certified-radiographic-interpreter*.

Location	Seminar Dates	Exam Date
Houston, TX	Oct. 5–9	Oct. 10

Certified Robotic Arc Welding (CRAW)

OTC Daihen Inc., Tipp City, OH; (937) 667-0800, ext. 218
Lincoln Electric Co., Cleveland, OH; (216) 383-4723
Wolf Robotics, Fort Collins, CO; (970) 225-7667
Milwaukee Area Technical College, Milwaukee, WI; (414) 456-5454
College of the Canyons, Santa Clarita, CA; (661) 259-7800, ext. 3062
Ogden-Weber Applied Technology College, Ogden, UT; (801) 627-8448
Genesis Systems IPG Photonics Co., Davenport, IA; (563) 445-5688

IMPORTANT: This schedule is subject to change without notice. Please verify your event dates with the Certification Dept. to confirm your course status before making travel plans. Applications are to be received at least six weeks prior to the seminar/exam or exam. Applications received after that time will be assessed a $395 Fast Track fee. Please verify application deadline dates by visiting our website at *aws.org/certification/docs/schedules.html.* For information on AWS seminars and certification programs, or to register online, visit *aws.org/certification* or call (800/305) 443-9353, ext. 273 for Certification; or ext. 455 for Seminars.

Laser Beam Delivery and Focusing Optics

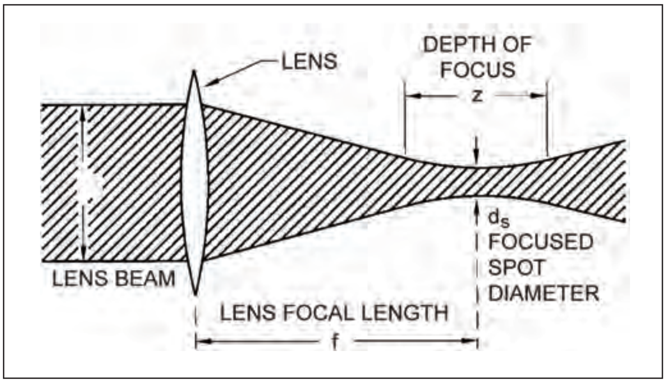

Fig. 1 — A Gaussian laser beam focused with a simple lens.

Laser beams must be focused to a small diameter to produce the high power density required for welding. Focusing is accomplished with transmitting lenses (Fig. 1) or reflective mirrors (Fig. 2). The spot size can be varied by the design of the optics and the choice of focal length. For a given laser beam, the final focused spot size is directly proportional to the focal length. The resultant power density is inversely proportional to the square of the focal length, while the depth of focus attained varies directly with focal length. Therefore, laser beams focused with short focal-length lenses require greater precision in maintaining the lens-to-workpiece distance than when longer focal-length lenses are used.

The shortest practical focal length used for CO_2 laser beam welding is about 125 mm (5 in.) because of the adverse effects on focusing that result from the spatter and vapor produced during welding. Since the spot size at the focal plane varies inversely with the diameter of the laser beam incident on the focusing optic element, a laser beam expander, i.e., an optical system used to increase the diameter of the beam, may be used prior to focusing. This allows longer focal lengths to be used without loss of power density. Figure 1 illustrates the ratio of the focal length of a lens to the diameter of a laser beam passing through the lens, in which the diameter (f/d_o) is referred to as the F-number. The spot size of the focused laser beam, i.e., the focused beam spot diameter (d_s), varies directly in proportion to the wavelength (λ) of the laser beam and the F-number of the focusing system. This is expressed in the following equation:

$$d_s = K(\text{F-number})\lambda = K(f/d_o)\lambda$$

where d_s is the focused beam spot diameter; K is the quality measure specifying the ability to focus the laser beam; F-number is the ratio of the focal length of the lens to the diameter of the beam passing through the lens; f/d_o is the diameter of optic (F-number); and λ is the wavelength of the laser beam.

The power density of the laser beam at the focus spot is inversely proportional to the laser beam diameter, squared.

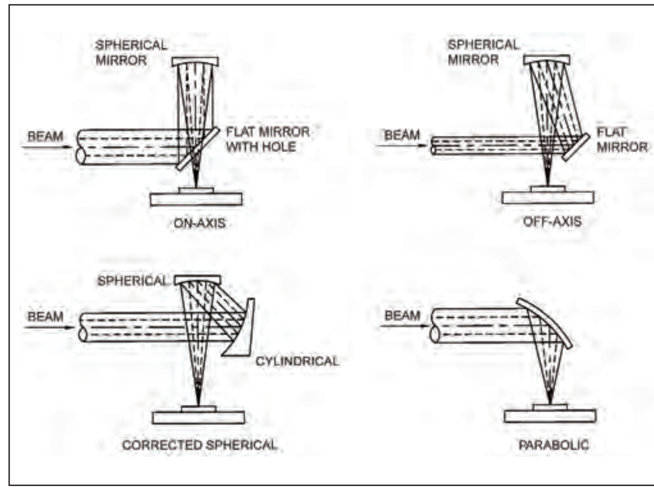

Fig. 2 — Laser beam focusing heads.

As the F-number used for a particular system decreases, so does the focused spot diameter, resulting in greater power density.

Fiber optic delivery is possible for Nd:YAG wavelengths and may provide additional flexibility in laser beam delivery systems. Up to 6 kW of Nd:YAG wavelength energy can be delivered through a single quartz fiber as small as 300 µm (0.012 in.). A small percentage of energy is lost with the fiber, but transmission losses are negligible in distances of 100 m (328 ft) or less. During transmission within a fiber, the beam path is fully enclosed and impervious to dust and contamination. Optical switching mechanisms can divert all or part of the laser beam energy to multiple fibers serving multiple processing locations.

Focusing Systems

The transmissive and reflective optics used in laser beam systems are lenses and mirrors. Solid-state laser systems, as well as lamp-pumped, diode-pumped, or direct-diode systems, generally use a lens to focus the laser beam on the workpiece. The type of lens ranges from a simple plano-convex lens with an anti-reflective coating to a compound lens, cylindrical lens, or lens with a graded index of refraction.

Gas lasers generally employ mirrors as reflective optics. The mirrors are usually made of highly polished metal and are water-cooled to withstand high-incident power. The mirrors may be either bare or coated to enhance reflectivity. Compared to transmissive lenses, these mirrors are less sensitive to damage from spatter and fumes, and are easier to maintain in production welding. Highly polished copper or molybdenum mirrors are common, but gold-coated mirrors provide the highest reflectivity, and thus the least amount of laser beam attenuation. However, they are expensive and susceptible to surface damage because gold is relatively soft. WJ

Excerpted from the Welding Handbook, *Ninth Edition, Volume 3, Welding Processes, Part 2.*

American Welding Society®
MEMBERSHIP

SPARKING CONNECTIONS – 2020 AWS MEMBERSHIP CHALLENGE

■ *What it is:*

Be the spark that ignites the people you know to become AWS members, and get rewards.

■ *How it works:*

Build up points throughout the year for each AWS Member you recruit: 5 Points per Individual Membership and 1 Point per Student Membership.

■ *What you get:*

Grand Prize Winner:	$200 gift card
2nd Place:	$100 gift card
3rd Place:	$100 gift card
4th Place:	$100 gift card

All other participants earning 10 or more points will get AWS branded merchandise based on points accrued throughout 2020.

__The Fine Print:__ All AWS members in good standing may participate and are eligible to receive rewards based on points accrued January 1 – December 31, 2020. Participant eligibility is determined at the sole discretion of AWS program administrators. AWS staff members and administrators of commercial / corporate or educational packages that include AWS memberships in the pricing structure are not eligible to participate. For more information, visit aws.org/be-the-spark

American Welding Society®
MEMBERSHIP

8669 NW 36 ST. #130 | Miami, FL 33166-6672
T: 800.443.9353 | F: 305.443.5647 | *aws.org*

Application for Membership

PRIMARY CONTACT INFORMATION (Please Print)

☐ Mr. ☐ Ms. ☐ Mrs. ☐ Dr.

Last Name: ______________ First Name: ______________ M.I: ________ Birthdate: ________

E-Mail: ______________ Mobile Phone: (   ) ________ Secondary Phone: (   ) ________ ☐ Home ☐ Work

Company/School (if applicable): ______________________________

Mailing Address: ______________________________

City: ______________ State/Province: ________ Zip/Postal Code: ________ Country: ________

☐ Check here if you would prefer to not receive email updates on AWS programs, Member benefits, savings opportunities and events.

Technical Interests (Circle All That Apply)

A Ferrous Metals
B Aluminum
C Nonferrous Metals Except Aluminum
D Advanced Materials/Intermetallics
E Ceramics
F High Energy Beam Processes
G Arc Welding
H Brazing and Soldering
I Resistance Welding
J Thermal Spray
K Cutting
L NDT
M Safety and Health
N Bending and Shearing
O Roll Forming
P Stamping and Punching
Q Aerospace
R Automotive
S Machinery
T Marine
U Piping and Tubing
V Pressure Vessels and Tanks
W Sheet Metal
X Structures
Y Other
Z Automation
1 Robotics
2 Computerization of Welding

STUDENT MEMBERSHIP

☐ New ☐ Renewal, Member #:

☐ 1 Year-Digital *Welding Journal* $15
☐ 1 Year-Print and Digital *Welding Journal* (US, Canada, and Mexico) $35
☐ 1 Year-Print and Digital *Welding Journal*.......... $85 (outside of US, Canada, and Mexico)

$ ________

INDIVIDUAL MEMBERSHIP

☐ New ☐ Renewal, Member #:

Were you referred to AWS by an AWS Member? ☐ Yes ☐ No

Member's Name: ______________ Member's # (if known) ______________

DOMESTIC (INCLUDES US, CANADA, AND MEXICO)

New Member

☐ Initiation Fee $12
☐ 1 Year - Print and Digital *Welding Journal* $88
☐ 2 Year - Print and Digital *Welding Journal* $151

$ ________

Renewing Member

☐ 1 Year - Print and Digital *Welding Journal* $88
☐ 2 Year - Print and Digital *Welding Journal* $171

$ ________

INTERNATIONAL (OUTSIDE OF US, CANADA, OR MEXICO)

New Member

☐ Initiation Fee $12
☐ 1 Year - Digital *Welding Journal* $88
☐ 1 Year - Print and Digital *Welding Journal* $138
☐ 2 Year - Digital *Welding Journal* $151
☐ 2 Year - Print and Digital *Welding Journal* $251

$ ________

Renewing Member

☐ 1 Year - Digital *Welding Journal* $88
☐ 1 Year - Print and Digital *Welding Journal* $138
☐ 2 Year - Digital *Welding Journal* $171
☐ 2 Year - Print and Digital *Welding Journal* $271

$ ________

NEW MEMBER OPTIONAL BOOK SELECTION (Not available to renewals. Choose ONE option ONLY. Includes shipping & handling.) Visit *aws.org/memberships/page/new-member-book-offer* to view selections and write your choice here:

☐ Domestic $35
☐ International $85

$ ________

TOTAL $ ________

Business (Circle ONE Letter Only)

A Contract Construction
B Chemicals & Allied Products
C Petroleum & Coal Industries
D Primary Metal Industries
E Fabricated Metal Products
F Machinery Except Electric (Incl. Gas Welding)
G Electrical Equipment, Supplies, Electrodes
H Transport Equip. – Air, Aerospace
I Transport Equip. — Automotive
J Transport Equip. — Boats, Ships
K Transport Equip. — Railroad
L Utilities
M Welding Distributors & Retail Trade
N Misc. Repair Services (Including Welding Shops)
O Educational Services (Univ., Libraries, Schools)
P Engineering & Architectural Services (Including Assns.)
Q Misc. Business Services (Including Commercial Labs)
R Government (Federal, State, Local)
S Other

Job Classification (Circle ONE Letter Only)

01 President, Owner, Partner, Officer
02 Manager, Director, Superintendent (Or Assistant)
03 Sales
04 Purchasing
05 Engineer — Welding
20 Engineer — Design
21 Engineer — Manufacturing
06 Engineer — Other
10 Architect Designer
12 Metallurgist
13 Research & Development
22 Quality Control
07 Inspector, Tester
08 Supervisor, Foreman
14 Technician
09 Welder, Welding or Cutting Operator
11 Consultant
15 Educator
17 Librarian
16 Student
18 Customer Service
19 Other

PAYMENT INFORMATION

Payment can be made (in U.S. dollars) by check or money order (international), payable to the American Welding Society.

☐ Check ☐ Money Order

☐ AMEX ☐ Diners Club ☐ MasterCard ☐ Visa ☐ Discover ☐ Other Application Date: ________

Name on Card: ______________ CC#: ____ / ____ / ____ / ____

Expiration Date (mm/yy): ____ / ____ CVV: ________ Applicant Signature: ________

OFFICE USE ONLY Source Code: **WJ** Account #: ________ Check #: ________ Amount: ________

Date: ________ AWS Staff: ________

AWS A5.36 Specification Withdrawn from Publication

By Teresa A. Melfi

American Welding Society (AWS) A5.36/A5.36M, *Specification for Carbon and Low-Alloy Steel Flux Cored Electrodes for Flux Cored Arc Welding and Metal Cored Electrodes for Gas Metal Arc Welding*, has been withdrawn as an AWS specification. It has also been withdrawn as a national specification under the American National Standards Institute (ANSI). A withdrawn standard is one that has been officially removed from publication. It will not be revised and will not be cited in new AWS standards or publications. This decision, which was not taken lightly by the A5 committees or the AWS Technical Activities Committee, was done in response to a clear direction from the welding community.

AWS A5.36 was a classification standard for flux cored arc welding and metal-cored arc welding electrodes. The specification was broad in scope and covered the following:

• All flux-cored electrodes classified to AWS A5.20/A5.20M, *Specification for Carbon Steel Electrodes for Flux Cored Arc Welding* (E71T-1C, E71T-8, E71T-1M, etc.)

• All flux-cored electrodes classified to AWS A5.29/A5.29M, *Specification for Low-Alloy Steel Electrodes for Flux Cored Arc Welding* (E80T1-Ni1M, E70T8-Ni2, E91T1-K2C, etc.)

• All metal-cored electrodes classified to AWS A5.18/A5.18M, *Specification for Carbon Steel Electrodes and Rods for Gas Shielded Arc Welding* (E70C-6M, E70C-3C, etc.)

• All metal-cored electrodes classified to AWS A5.28/A5.28M, *Specification for Low-Alloy Steel Electrodes and Rods for Gas Shielded Arc Welding* (E120C-K4, E80C-Ni1, etc.)

Why A5.36 was Withdrawn

AWS A5.36 was first published in 2012 with the thought that welding consumable manufacturers and users would gravitate to this specification, and AWS A5.20 and A5.29 could be withdrawn. However, that was not the case. The reception from users was that the specification itself, and the classification designations in particular, were too complex. A5.36 provided a lot of flexibility in how electrodes were classified — in the as-welded or postweld heat-treated condition, with various shielding gases, various strength levels, and various impact test temperatures. To accommodate that flexibility, the classifications were quite complex and did not exactly "roll off the tongue." The A5.36 designation system is shown below.

Open Classification System for AWS A5.36/A5.36M

$EX_1X_2TX_3 – X_4X_5X_6 – X_7$

- E designates an electrode
- X_1 is the Tensile Strength designator
- X_2 is the Position Designator
- TX_3 is the Electrode Usability Designator
- X_4 is the Shielding gas Designator
- X_5 designates the condition of heat treatment
- X_6 is the Impact Designator
- X_7 is the Weld Composition Designator

- Plus, three optional supplemental designators

Because of the lack of acceptance by much of the industry, filler metal manufacturers continued to classify electrodes to A5.20, A5.29, A5.18, and A5.28, in addition to A5.36. One product often had multiple classifications, which complicated the documentation on qualification and welding procedure records and led to confusion about which classification to use as an essential variable. Certificates of conformance could be many pages long, and the print on the product labels became very small.

How to Transition from A5.36 Back to A5.18, A5.20, A5.28, or A5.29

AWS A5.36 was incorporated into the following documents: AWS D1.1/D1.1M, *Structural Welding Code — Steel*, in 2015; American Society of Mechanical Engineers, Boiler & Pressure Vessel Code, Section II, Part C, in 2013; and CSA W48, *Filler metals and allied materials for metal arc welding*, in 2014.

It is recognized that there will be an impact on the welding community as a result of the decision to withdraw A5.36, but the clear message was to move back to the previous specifications as quickly as possible. To aid users in this transition, three different options are listed below. The most appropriate one may be selected based on the consumable, the application, and the code or contract.

1) The most widely used cored wire classifications from A5.18 and A5.20 have always been included in A5.36. These E70T- and E71T- classifications still account for the vast majority of flux-cored and metal-cored electrodes used today. In these cases, no changes to existing documentation should be necessary. The classifications will remain the same as in the existing specifications, with metal-cored electrodes classified in A5.18 and flux-cored electrodes classified in A5.20. These classifications are listed below. In these cases, the only change that might be necessary is to reference A5.18 or A5.20, rather than A5.36.

Carbon Steel Classifications in A5.36

E70T-1C	E71T1C	E70T-1M	E71T-1M
AAE70T-5C	E71T-5C	E70T-5M	E71T-5M
E70T-9C	E71T-9C	E70T-9M	E71T-9M
E70T-12C	E71T-12C	E70T-12M	E71T-12M
E70T-6	E71T-6		
E70T-8	E71T-8		
E70T-11	E71T-11		
E70T-4	E71T-4		
E70T-7	E71T-7		
E70T-14	E71T-14		
E70T-GS	E71T-GS		
E70C-6C	E70C-6M	← A5.18	

2) For electrodes other than these, mainly those electrodes used for welding low-alloy steels, the most efficient method is to record the A5.18, A5.20, A5.28, or A5.29 designations on records. Qualification and welding procedure records from before 2012 will already carry only these references. Records from after 2012 might carry both the A5.36 electrode classification and the classification from

A5.18, A5.20, A5.28, or A5.29, since these designations were retained on most product and certification documents by the electrode manufacturers.

3) For records created since 2012 that carry only an A5.36 classification designation, a bit more detail is necessary. Tables B.1, B.2, and B.3 from A5.36 show equivalents from A5.36 and the corresponding A5.18, A5.20, A5.28, and A5.29 classifications. If the A5.36 classification recorded on the qualification or welding procedure is not listed there, the electrode manufacturer should be consulted to determine the appropriate designation.

Additional Consumable and Weld Metal Properties

A5.36 contained provisions to classify electrodes under a wide variety of welding and testing conditions. Sometimes information is needed about an electrode or its weld metal properties, such as impact testing at low temperatures or the properties of weld metal deposited with a specific shielding gas. In these cases AWS A5.01, *Procurement Guidelines for Consumables — Welding and Allied Processes — Flux and Gas Shielded Electrical Welding Processes*, can be used to specify the details of testing, the acceptance criteria, and whether the testing be done on a specific heat or lot of electrode. Terms like "heat," "lot," and "certified material test report" are defined so there is no confusion regarding the level of testing, the lot classification, or the documentation that will be supplied. A5.01 is a valuable tool for procurement of any consumables with nonstandard testing or reporting requirements and can be used to fill any gaps in information that may come about from the withdrawal of A5.36. WJ

TERESA A. MELFI (teresa_melfi@lincolnelectric.com) *is a Technical Fellow at The Lincoln Electric Co., Cleveland, Ohio, and chair of the AWS A5 Committee on Filler Metals and Allied Materials.*

AWS Celebrates Its Life Members with Exclusive Offers

Experience and involvement should be celebrated, and the American Welding Society (AWS) honors those who have shared a significant portion of their lives with AWS. Any individual who has served as president of the Society or has reached 35 years of paid membership is eligible to become an AWS Life Member.

AWS Life Members are exempt from further payment of dues and continue to receive all benefits of the AWS Individual Membership, including the *Welding Journal*; access to discounts on publications, education, and certification; and free registration to the AWS Professional Program.

To learn more about AWS Life Membership, and to check your status, contact Darrill A. Gaschler, AWS senior manager of Sections and Student Chapters, at *dgaschler@aws.org* or (800) 443-9353, ext. 260.

Candidates Sought to Receive the MIT Masubuchi Award

The Prof. Koichi Masubuchi award, with a $5000 honorarium, is presented to one person, 40 years old or younger, who has made significant contributions to the advancement of materials joining through research and development.

Send a list of your candidate's experience, publications, honors, awards, and at least three letters of recommendation from fellow researchers to Prof. Todd Palmer, *tap103@psu.edu*. This award is sponsored annually by the Massachusetts Institute of Technology, Dept. of Ocean Engineering.

Nominate AWS Members to be Profiled

The *Welding Journal* is celebrating the diversity of its membership by profiling AWS members each month in its Society News section. Brian Keeton is profiled on page 48.

To nominate an AWS member, submit a short statement about what makes the nominee a noteworthy member, along with the nominee's contact information, to Katie Pacheco, *kpacheco@aws.org*.

To see member profiles from previous issues, visit *aws.org/about/page/diversity-inclusion*.

TECH TOPICS

Opportunities to Contribute to AWS Technical Committees

The following committees welcome new members. Some committees are recruiting members with specific interests in regard to the committee's scope, as marked below: Producers (P), General Interest (G), Educators (E), Consultants (C), and Users (U). For more information, contact the staff member listed or visit *aws.org/library/doclib/Technical-Committee-Application.pdf*.

S. Borrero, *sborrero@aws.org*, ext. 334. **Definitions and symbols**, A2 Committee (E). **Titanium and zirconium filler metals**, A5K Subcommittee. **Piping and tubing**, D10 Committee (C, E, U). **Welding practices and procedures for austenitic steels**, D10C Subcommittee. **Aluminum piping**, D10H Subcommittee. **Chromium molybdenum steel piping**, D10I Subcommittee. **Welding of titanium piping**, D10K Subcommittee. **Purging and root pass welding**, D10S Subcommittee. **Low-carbon steel pipe**, D10T Subcommittee. **Orbital pipe welding**, D10U Subcommittee. **Duplex pipe welding**, D10Y Subcommittee. **Joining metals and alloys**, G2 Committee (E, G, U). **Reactive alloys**, G2D Subcommittee (G).

R. Gupta, *gupta@aws.org*, ext. 301. **Filler metals and allied materials**, A5 Committee (E). **Magnesium alloy filler metals**, A5L Subcommittee.

P. Portela, *pportela@aws.org*, ext. 311. **Additive manufacturing**, D20 Committee (C, E, G). The D1N Subcommittee on Titanium Structures is recruiting all interest groups.

J. Molin, *jmolin@aws.org*, ext. 304. **Structural welding**, D1 Committee (E). **Sheet metal welding**, D9 Committee (C, G). The D1 Committee is recruiting educators. The D9 Committee is recruiting producers, consultants, and general interest members.

K. Bulger, *kbulger@aws.org*, ext. 306. **Methods of weld inspection**, B1 Committee (C, E). **Brazing and soldering**, C3 Committee (C, E, G). **Welding in marine construction**, D3 Committee (C, E, G, U). **High energy beam welding and cutting**, C7 Committee (C, E, G). **Hybrid welding**, C7D Subcommittee (G). **Welding of machinery and equipment**, D14 Committee (C, E, G, U).

M. Diaz, *mdiaz@aws.org*, ext. 310. **Resistance welding**, C1 Committee (C, E, G, U). **Friction welding**, C6 Committee (C, E). **Automotive welding**, D8 Committee (C, E, G, U). **Resistance welding equipment**, J1 Committee (C, E, G, U). **Welding in the aircraft and aerospace industry**, D17 Subcommittee (C, E, G).

S. Hedrick, *steveh@aws.org*, ext. 305. **Metric practice**, A1 Committee (C, E). **Mechanical testing of welds**, B4 Committee (E, G, P). **Joining of plastics and composites**, G1 Committee (C, E, G). **Safety and health committee**, SHC Committee (E, G). **Welding in sanitary applications**, D18 Committee.

J. Rosario, *jrosario@aws.org*, ext. 308. **Procedure and performance qualification**, B2 Committee (E, G). **Thermal spraying**, C2 Committee (C, E, G, U). **Oxyfuel gas welding and cutting**, C4 Committee (C, E, G). **Welding iron castings**, D11 (C, E, G, P, U). **Railroad welding**, D15 (C, E, G, U). **Robotic and automatic welding**, D16 Committee (C, E).

Technical Committee Meetings

All AWS technical committee meetings are open to the public. Contact the staff members listed or call (800/305) 443-9353 for information.

The Fall 2020 D1 Committee and Subcommittees on Structural Welding meetings will occur via teleconferences at the discretion of the D1 Task Groups, D1 Subcommittees, and D1 Main Committee Chairs. Contact: J. Molin, *jmolin@aws.org*, ext. 304.

Standards for Public Review

AWS was approved as an accredited standards-preparing organization by the American National Standards Institute (ANSI) in 1979. AWS rules, as approved by ANSI, require that all standards be open to public review for comment during the approval process. This column also advises of ANSI approval of documents.

A5.29/A5.29M:20XX, *Specification for Low-Alloy Steel Electrodes for Flux Cored Arc Welding*. Revised Standard. $36.00. ANSI public review expired 8/31/2020. Contact: R. Gupta, ext. 301, *gupta@aws.org*.

D17.3/D17.3M:20XX, *Specification for Friction Stir Welding of Aluminum Alloys for Aerospace Applications*. Revised Standard. $38.00. ANSI public review expired 8/24/2020. Contact: M. Diaz, *mdiaz@aws.org*, ext. 310.

J1.3/J1.3M:20XX-AMD1, *Specification for Materials Used in Resistance Welding Electrodes and Tooling*. Addenda. $27.00. ANSI public review expired 8/17/2020. Contact: M. Diaz, ext. 310, *mdiaz@aws.org*.

New Standards Approved by ANSI

C3.9M/C3.9:2020, *Specification for Resistance Brazing*. Approval Date: 7/9/2020.

Revised Standard Approved by ANSI

A5.28/A5.28M:2020, *Specification for Low-Alloy Steel Electrodes and Rods for Gas Shielded Arc Welding*. Approval Date: 6/30/2020.

A5.34/A5.34M:2020, *Specification for Nickel-Alloy Flux Cored and Metal Cored Welding Electrodes*. Approval Date: 6/30/2020.

C3.8M/C3.8:2020, *Specification for the Ultrasonic Pulse-Echo Examination of Brazed Joints*. Approval Date: 7/9/2020.

Amendment Standard Approved by ANSI

D1.4/D1.4M:2020-AMD1, *Structural Welding Code — Steel Reinforcing Bars*. Approval Date: 7/14/2020.

MEMBERSHIP ACTIVITIES

AWS Member Counts
August 1, 2020

Sustaining	*584*
Supporting	*358*
Educational	*829*
Affiliate	*610*
Welding Distributor	*62*
Total Corporate	***2443***
Individual	*57,090*
Student + Transitional	*9,937*
Total Members	***67,654***

2020 Membership Challenge

Listed here are the members who participated in the 2020 Membership Challenge — point standings as of July 16. The campaign runs from Jan. 1 to Dec. 31, 2020. Members receive 5 points for each Individual Member and 1 point for every Student Member they recruit.

For more information, please see page 41 of this *Welding Journal* or call the AWS Membership Dept. at (800) 443-9353, ext. 480.

J. W. Fregia, Houston — 95
A. D. Dillon, Detroit — 38
S. A. Milner, San Francisco — 36
B. J. Cain, Los Angeles/Inland Empire — 34
J. P. Theberge, Boston — 31
J. C. Durbin, Tri-River — 30
D. L. Galiher, Detroit — 29
T. A. Uff, Lehigh Valley — 29
D. P. Thompson, SW Virginia — 29
A. P. Duris, NW Ohio — 26
R. Young, Iowa — 24
T. Edwards, Tulsa — 20
H. J. Merrill II, Louisville — 20
W. H. Wilson, New Orleans — 17
B. A. Cheatham, Columbia — 17
O. Ortiz, Los Angeles/Inland Empire — 16
G. J. Smith, Lehigh Valley — 15
C. W. Gilbertson, Northern Plains — 14
C. Consentino, Pittsburgh — 13
V. O. Harthun, Northern Plains — 13
T. A. Harris, Johnstown-Altoona — 13
S. Silverstein, Milwaukee — 12
M. D Stein, Detroit — 11

New AWS Supporters

Sustaining Members

AOES LLC
13507 Gulf Blvd.
Madeira Beach, FL 33708

Elite Welding & Industrial Services LLC
279 Kefauver Rd.
Millwood, KY 42762

IQS Inspection LLC
1718 Engineers Rd., Ste. A
Belle Chasse, LA 70037

KS Engineers P.C.
494 Broad St., 4th Floor
Newark, NJ 07102

PTT Exploration and Production Public Co.
Energy Complex Building A
6th and 19–36th Floor
555/1 Vibhavadi-Rangsit Rd.
Bangkok, Thailand

Qube-MRS LLC
1625 Candler Rd.
Gainesville, GA 30507

State Fabricators
30550 W. 8 Mile Rd.
Farmington Hill, MI 48336

Vigor Works LLC
9700 SE Lawnfield Rd.
Clackmas, OR 97015

Educational Institution Members

Caddo Kiowa Technology Center
1415 N. 7 St.
Fort Cobb, OK 73038

Clark State Community College
570 East Leffel Lane
Springfield, OH 45501

Detroit Lakes Public Schools — Detroit Lakes High School
702 Lake Ave.
Detroit Lakes, MN 56501

Great Bay Community College
5 Milton Rd., Ste. 32
Rochester, NH 03867

Hartman Welding & Fabrication LLC
3719 E. Hwy. 90
Brookshire, TX 77423

Hoek Iron Ltd.
8119 101 Ave.
Fort St. John, BC V1J2A2 Canada

Lowell Senior High School — Tri-Creek School Corp.
2051 E. Commercial Ave.
Lowell, IN 46356

Viswam Institute of Maritime Studies
762 E. Second Main Rd.
KTC Nagar Palayam Kottai, Tirunelveli
Tamil Nadu 627011 India

Supporting Company Members

Bar H Welding LLC
P.O. Box 2766
Kilgore, TX 75663

Depue Mechanical
P.O. Box 857
113 S. Ridge Rd.
Minooka, IL 60447

New England Small Tube Corp.
480 Charles Bancroft Hwy.
Litchfield, NH 03052

Affiliate Corporate Members

Abbott Properties
1523 Oak St.
Kansas City, MO 64108

Apex Mechanical
248 Miles Hill Rd.
Cecilia, KY 42724

Factory Direct Supply WPB
1733 Hill Ave.
Mangonia Park, FL 33407

Lowder Steel Inc.
2450 Coltrane Mill Rd.
Archdale, NC 27263

Richards Industries
4 Fairfield Crescent
West Caldwell, NJ 07006

RWP Inspections Ltd.
3995 Hi Mount Dr.
Victoria, BC
V9C 3X9 Canada

Scenic Ridge Co.
2550 Steelton Rd.
Lancaster, PA 17601

Solid Form Fabrication Inc.
P.O. Box 119
2706 NE Rivergate St.
McMinnville, OR 97128

Change of Address? Moving?

Make sure delivery of your *Welding Journal* is not interrupted. Contact Kim Hugley in the Membership Department with your new address information — (800) 443-9353, ext. 204; *khugley@aws.org*.

AWS District 17 Conference Held in Texas

American Welding Society's District 17 held its annual conference on June 5–6 at the Hampton Inn & Suites in Tyler, Tex. Conference attendees included District 17 Director J Jones, Bryan Baker, Andy Stormer, Paul Wittenbach, Jim Bridwell, Paul Stanglin, and Donnie Williams. Pictured are conference attendees and their wives.

AWS District 17 Director J Jones (right) presented Paul Wittenbach with the District CWI of the Year Award.

(From left) Debra and Paul Stanglin of the AWS North Texas Section presented AWS District 17 Director J Jones with a metal-crafted yellow rose of Texas in appreciation of his service.

AWS Member Profile

Brian Keeton

"The most rewarding thing about being a welding instructor is having a student come back after graduation and tell me I changed their life."

Brian Keeton's journey with welding began in his high school agriculture (AG) class, where he learned shielded metal arc welding (SMAW) using old, well-worn equipment.

"We had only AC [alternating current] machines and had to hold our hood up with one hand and weld with another," he recollected. "I learned the basics of SMAW in the flat, horizontal, and vertical positions."

Drawn more to welding than to academic subjects, Keeton took AG all four years of high school, even signing up for the class for three periods in his senior year.

"I hated learning from a book but have always been pretty good at watching someone do something and then doing it myself," he recalled.

The welding skills learned in high school allowed Keeton to excel in the U.S. Army, where he worked as a Bradley Fighting Vehicle mechanic. The job required him to regularly perform welding and cutting operations.

"My welding skills were significantly better than the others. I ended up doing most of the welding," he said. "I guess learning the basics with old, worn-out equipment made it easier to make myself look good when given the opportunity to weld with good rods and equipment."

After serving in the military for six years, Keeton began working at Walmart's meat market, where he was promoted to manager. Although he enjoyed it, after six years, he felt ready to return to welding.

In the years ensuing, Keeton took on various welding jobs. He ran a welding business out of a local garage, performed welding repairs on equipment for the logging industry, joined the Tennessee National Guard as a mechanic/welder, and worked for the Sheet Metal Workers Local 48. He also returned to college, earning an associate's degree in welding from Northwest-Shoals Community College (NW-SCC) in Alabama.

"I decided to take welding in college so I could obtain industry-recognized credentials to help me get a better job," he said. "I learned a lot at Northwest-Shoals. Before I attended, I could melt two pieces of metal together and make them hold, but there I learned the proper way of doing things and the theory behind it. I discovered there is more to welding than dropping a hood and making sparks."

Leaving a lasting impression on the school's instructors, Keeton was offered a job as an instructor's assistant. After nine months, he was promoted to welding instructor and took over the dual-enrollment welding classes for Russellville City School District and the Franklin County Career Technical Center. He then established the welding program in NW-SCC's Phil Campbell campus, where he currently works.

Additionally, Keeton went on to earn a bachelor's in career technical education and a master's in education. He also became an American Welding Society (AWS) Certified Welding Inspector (CWI) and Certified Welding Educator (CWE).

"I feel the more knowledge I have, the more I can pass on to my students," Keeton explained. "I became a CWI/CWE for the benefit of my students. I am the only welding instructor on the Phil Campbell campus of Northwest-Shoals, and I think my CWI/CWE credentials make them feel like they are getting trained from a subject-matter expert who gives them confidence when they get to a job site."

After more than ten years as NW-SCC's welding instructor, Keeton still enjoys his job.

"The most rewarding thing about being a welding instructor is having a student come back after graduation and tell me I changed their life," he affirmed. "Most students you never hear from until they need you, but it is a great feeling when someone just stops by to say, 'thanks for what you taught me.'"

He teaches SMAW; gas tungsten, gas metal, and flux cored arc welding; plasma and carbon arc cutting; and oxyfuel cutting.

"As much as the trade of welding, I think we teach life's lessons," he said. "Many of our students just need direction or a little nudge in the right direction, and that, along with a skilled trade, can completely change their lives."

A long-time AWS member, Keeton became involved with the AWS Greater Huntsville Section in 2016. He helps the Section organize its local SkillsUSA high school welding competitions. When asked why he volunteers his time with the Section, he identified networking with other educators, as well as industry members, as a major benefit.

"Most of my AWS Section is made up of educators or retired educators, so they feel my pain. I think the AWS Section is a great way to network with others who have the same student issues, and we can discuss what they have done to overcome the issues. We are all in this business to train the workforce of the future, and we want to see results of the pride and craftsmanship we are trying to instill in the future generation," he explained. "Our members who are not educators are involved in the welding industry. I consider the AWS Section an extension of my local advisory committee. It gives me an idea of what I can change in my welding program to help students obtain jobs in a larger geographic area."

District 1

Douglas A. Desrochers, director
(508) 763-8011
dadaws@comcast.net

CONNECTICUT

June 4
Location: Barkhamsted, Conn.
Presenters: Douglas A. Desrochers, District 1 director; and John Jones, Section chair
Summary: Desrochers traveled to Barkhamsted to assist Jones in recording a video presentation in honor of the Connecticut Section Named Scholarship Award, changing its name to the Walter Chojnacki and Albert J. Moore Jr. Connecticut Section Scholarship. The video was played during the virtual District 1 Conference on June 13.

District 2

Harland Thompson, director
(631) 546-2903
harland.w.thompson@ul.com

District 3

Sean Moran, director
(717) 885-5039
sean.moran@ahydro.com

READING

June 20
Location: Womelsdorf, Pa.
Presenter: Lisa Davis, Section scholarship chair
Summary: The Reading Section 100 Millennium Scholarship was presented to Jack C. Yengo, a student at Pennsylvania College of Technology pursuing a bachelor's of science degree in welding and fabrication engineering technology. Yengo is a member of both his school's AWS student chapter and the AWS Reading Section. The scholarship is for $2000.

District 4

Mr. Lynn Showalter, director
(757) 848-8029
lynneshowalter@gmail.com

District 5

Howard Record, director
(352) 816-0835
howard@rtdtools.com

District 6

Ronald Stahura, director
(716) 207-7869
rstahura@esab.com

District 7

Roger E. Hilty, director
(740) 317-9073
rhilty@comcast.net

District 8

James Thompson, director
(256) 347-6481
jim.thompson@wallacestate.edu

District 9

Michael Skiles, director
(337) 501-0304
michaelskiles@cox.net

NEW ORLEANS

March 13
Location: Kenner, La.
Summary: Section Vice Chair Bruce Hallila arranged for Delgado Community College welding students to take a plant tour of Pellerin Milnor Corp., a manufacturer of commercial laundry equipment. Students witnessed robotic gas metal arc welding (GMAW) of a large carbon steel frame, mechanized GMAW seam welding of thin-gauge stainless steel shells, and flux cored arc welding of thick stainless steel press cans. Students also learned how welding in the flat position increases speed and productivity.

District 10

Mike Sherman, director
(216) 570-9348
mike@shermanswelding.com

CONNECTICUT — Seen are the crystal awards for the newly named Walter Chojnacki and Albert J. Moore Jr. Connecticut Section Scholarship.

READING — *Section Scholarship Chair Lisa Davis (left) presented Student Jack C. Yengo with a $2000 Section Scholarship.*

NEW ORLEANS — *Delgado Community College welding students toured Pellerin Milnor Corp.*

District 11

Phillip Temple, director
(734) 546-4298
nwcllc_ptemple@att.net

District 12

Dale Lange, director
(715) 732-3645
dale.lange@nwtc.edu

District 13

Ronald Ashelford, director
(815) 218-8766
r.ashelford@rockvalleycollege.edu

District 14

Tony Brosio, director
(765) 215-7506
tbrosio@yahoo.com

District 15

Michael Hanson, director
(763) 221-5951
mikhan318@comcast.com

District 16

Karl Fogleman, director
(402) 677-2490
fogleman3@cox.net

District 17

J Jones, director
(832) 506-5986

District 18

Thomas Holt, director
(409) 721-5777
tholt@techcorr.com

District 19

Shawn McDaniel, director
(509) 793-5182
shawnm@bigbend.edu

District 20

Denis Clark, director
(208) 357-6626
denis.clark.51@gmail.com

COLORADO

June 1

Location: Ruby Hill Park, Denver, Colo.

Summary: The Section presented Certified Welding Inspector Awards to Norma Escobedo, welding lead at Liberty Home Products; and Chad Jackson, Colorado Department of Transportation. A Section Instructor Award was presented to Jessica Lanka.

District 21

Sam Lindsey, director
(858) 740-1917
slindsey@sandiego.gov

District 22

Robert Purvis, director
(916) 599-5561
purviswelds@gmail.com

CENTRAL VALLEY

February 26

Location: College of the Sequoias, Tulare, Calif.

Summary: College of the Sequoias hosted a Section meeting focused on exposing local students, educators, and industry partners to various methods and techniques used in the nondestructive examination of welds. Representatives from Krazan & Associates Inc. gave in-depth presentations and Kip Williamson presented on weld discontinuities, followed by demonstrations of magnetic particle inspection and ultrasonic testing performed by Jose Acosta and Casey Mathis. The meeting was attended by more than 40 individuals and concluded with Section Chair Randy Emery's presentation of the Section Educator Award to Ricardo Gonzalez, welding instructor at Farmersville High School.

CENTRAL VALLEY — *Section Chair Randy Emery (left) presented the Section Educator Award to Ricardo Gonzalez.*

COLORADO — *Section Chair Jeremy Mowry (far left) and AWS Past President Bob Teuscher (far right) presented awards to Section members (from left) Norma Escobedo, Chad Jackson, and Jessica Lanka.*

CENTRAL VALLEY — *Section meeting attendees gather for a group photo.*

GUIDE TO AWS SERVICES

American Welding Society®
8669 NW 36 St., #130
Miami, FL 33166-6672
(800/305) 443-9353
Phone extensions are in parentheses.

AWS PRESIDENT
Robert W. Roth..*rroth@romanmfg.com*
President and CEO, RoMan Manufacturing Inc.

SENIOR LEADERSHIP TEAM
Executive Director/Chief Executive Officer
Gary Konarska II.. *gkonarska@aws.org* . . . . .(207)

Chief Financial Officer/ Chief Administrative Officer
Gesana Villegas.. *gvillegas@aws.org* . . . .(252)

Senior Vice Presidents
Cassie Burrell.. *cburrell@aws.org* . . . .(253)
Research, Strategy, and Membership

John Gayler.. *gayler@aws.org* . . . .(472)
Welding & Technology

EXECUTIVE OFFICE
Associate Director
Chelsea Steel.. *csteel@aws.org* . . . .(294)

Program Administrator, National Awards
Malisa Mercado.. *mmercado@aws.org* . . . . . .(293)

HUMAN RESOURCES
Director
Alex Diaz.. *adiaz@aws.org* . . . .(209)

GOVERNMENT LIAISON SERVICES
Hugh Webster.. *hwebster@wc-b.com*
Webster, Chamberlain & Bean, Washington, D.C. (202) 785-9500; Fax: (202) 835-0243
Monitors federal issues of importance to the industry.

CERTIFICATION SERVICES
Dept. information . . . .(273)

Managing Director
Denny Smith.. *dsmith@aws.org* . . . .(263)

ACCREDITATION
Senior Manager
Emil Pagoaga.. *epagoaga@aws.org* . . . .(448)

CONFERENCES & EVENTS
Dept. information . . . .(213)

CUSTOMER SERVICE & SUPPORT
Customer Service.. *customerservice@aws.org*(280)

SALES & CUSTOMER SERVICE

Senior Sales Executive, Corporate
Sandra Jorgensen.. *sjorgensen@aws.org* . . . .(254)

CONVENTION AND EXPOSITIONS
Director, Expositions
Matthew Rubin.. *mrubin@aws.org* . . . .(239)

Senior Sales Executive, Expositions
Sarah Dickson.. *sdickson@aws.org* . . . .(297)

EDUCATION & TRAINING
Director
Alicia Garcia.. *agarcia@aws.org* . . . .(229)

INFORMATION SYSTEMS
Managing Director
John Perry.. *jperry@aws.org* . . . .(247)

ITSA — INTERNATIONAL THERMAL SPRAY ASSOCIATION
Program Manager
Alfred Nieves.. *anieves@aws.org* . . . .(467)

RWMA — RESISTANCE WELDING MANUFACTURING ALLIANCE and WEMCO — ASSOCIATION OF WELDING MANUFACTURERS
Program Manager
Adrian Bustillo.. *abustillo@aws.org* . . . .(295)

MEMBER SERVICES
Dept. information . . . .(480)

Director, Membership
Nici Banks.. *nbanks@aws.org* . . . .(270)
Serves as a liaison between members and AWS headquarters.

Senior Manager, Sections and Student Chapters
Darrill Gaschler.. *dgaschler@aws.org* . . . .(260)

PUBLISHING & EDITORIAL
Dept. information . . . .(275)

Welding Journal
Publisher/Editor
Annette Alonso.. *aalonso@aws.org* . . . .(299)

Managing Editor
Kristin Campbell.. *kcampbell@aws.org* . . . . .(257)

Society News Editor
Katie Pacheco.. *kpacheco@aws.org* . . . .(275)

Section News Editor
Cindy Weihl.. *cweihl@aws.org* . . . .(256)

***Inspection Trends* Editor**
Carlos Guzman.. *cguzman@aws.org* . . . .(348)

STANDARDS DEVELOPMENT
Dept. information . . . .(340)

Director — Standards Development
Peter Portela.. *pportela@aws.org* . . . .(311)
Technical Committee Activities, Additive Manufacturing, Structural Subcommittee on Titanium

Director — International Activities
Andrew Davis.. *adavis@aws.org* . . . .(466)
International Standards Activities, American Council of the International Institute of Welding

Program Managers

Stephen Hedrick.. *steveh@aws.org* . . . .(305)
Metric Practice, Safety and Health, Joining of Plastics and Composites, Personnel and Facilities Qualification, Mechanical Testing of Welds, Welding in Sanitary Applications

Stephen Borrero.. *sborrero@aws.org* . . . .(334)
Definitions and Symbols, Structural Subcommittees on Bridge Welding, Reinforcing Steel and Stainless Steel, Joining of Metals and Alloys, Piping and Tubing

Rakesh Gupta.. *gupta@aws.org* . . . .(301)
Filler Metals and Allied Materials, International Filler Metals, UNS Numbers Assignment, Computational Weld Mechanics

Jennifer Molin.. *jmolin@aws.org* . . . .(304)
Structural Welding, Sheet Metal Welding

Mario Diaz.. *mdiaz@aws.org* . . . .(310)
Automotive, Resistance Welding, Resistance Welding Equipment, Welding and Brazing in Aerospace, Friction Welding

Kevin Bulger.. *kbulger@aws.org* . . . .(306)
Brazing and Soldering, Methods of Weld Inspection, High-Energy Beam Welding, Welding in Marine Construction, Welding of Machinery and Equipment

Jennifer Rosario.. *jrosario@aws.org* . . . .(308)
Oxyfuel Gas Welding and Cutting, Railroad Welding, Robotics Welding, Thermal Spraying, Welding Iron Castings, Welding Qualification

***Welding Handbook* Editor**
Kathy Sinnes.. *ksinnes@aws.org* . . . .(255)

AWS FOUNDATION INC.
aws.org/w/a/foundation
General Information
(800/305) 443-9353, ext. 212, *jdouglass@aws.org*

Chairman, Board of Trustees
William A. Rice.. *brice@oki-bering.com*

Executive Director, Foundation
Monica Pfarr.. *mpfarr@aws.org* . . . .(461)

Associate Director, Foundation Services
John Douglass.. *jdouglass@aws.org* . . . .(212)

The AWS Foundation is a not-for-profit 501(c)(3) charitable organization established to provide support for the educational and scientific endeavors of the American Welding Society. Promote the Foundation's work with your financial support.

AWS American Welding Society

Lockheed Martin Appoints President and CEO

James D. Taiclet has been promoted to president and CEO of Lockheed Martin Corp., Bethesda, Md., a global security and aerospace company. He succeeds Marillyn A. Hewson, who has served as chair, president, and CEO since 2014. Taiclet will continue to serve as a member of the corporation's board, which he joined in 2018. Prior to joining the company, Taiclet was with American Tower Corp. since 2001. He became CEO in 2003, followed by chair and president in 2004. He guided the company's transformation from a primarily U.S. business to a global player in its industry. Additionally, from 1999 to 2001 he was president of Honeywell Aerospace Services, a unit of Honeywell International, and vice

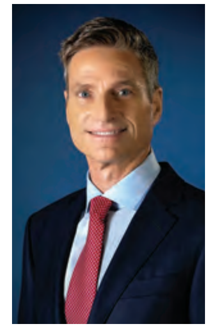

J. D. Taiclet

president of engine services at Pratt & Whitney from 1996 to 1999. He was also previously a consultant at McKinsey & Co. Taiclet began his career as a U.S. Air Force officer and pilot and served a tour of duty in the Gulf War. He holds a master's degree in public affairs from Princeton University, where he was awarded a fellowship at the Woodrow Wilson School, and is a distinguished graduate of the United States Air Force Academy with degrees in engineering and international relations.

General Motors Promotes Executive Vice President and President

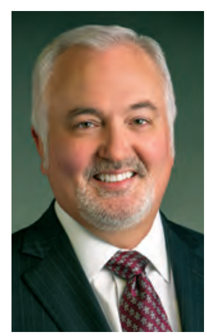

S. Carlisle

General Motors (GM), Detroit, Mich., the multinational automaker and distributor, has appointed Steve Carlisle as executive vice president and president, North America. He had served as senior vice president and president, Cadillac, since April 2018. With Carlisle's promotion, GM will have one sales, service, and marketing leader across its portfolio of automotive and connected services brands in North America, including Chevrolet, Buick, GMC, Cadillac, OnStar, ACDelco, and GM Genuine Parts. He will report to GM President Mark Reuss. Before joining Cadillac, he was president and managing director, GM Canada, since November 2014. He began his GM career in 1982 as an industrial engineering co-op student at the Oshawa Truck Assembly Plant. Over the course of his career with the automaker, he has held senior leadership positions, including vice president, global product planning and program management, 2010–2014; vice president, U.S. sales operations, 2010; and president and managing director, Southeast Asia operations, 2007–2010.

Meridian Adhesives Group Adds Global Sales Director

N. Schwarz

Meridian Adhesives Group, a manufacturer of adhesives and sealant technologies, has hired Nicolas Schwarz as global sales director of its electronics division. He joins the company after a long tenure with John P. Kummer (JPK) GmbH, where he held the position of managing director. Prior to his appointment with JPK, he worked as director of R&D at Hartmann Group in Heidenheim, Germany, where he was tasked with developing medical devices, commodities, and cosmetics for the global consumer market. His experience also includes corporate management, business development, sales, and project management.

Industrial Scientific Welcomes Vice President of Engineering

S. Antony

Saldy Antony has joined Industrial Scientific, Pittsburgh, Pa., a provider in gas detection and connected safety, as vice president of engineering. He will be responsible for leading the company's engineering team while also developing and executing the company's global technology strategy. Antony most recently served as vice president of engineering and product at Petcube, where he led a multinational and multifunctional engineering team in the design and development of a complex IoT-enabled product. Prior to Petcube, he held various leadership positions within Dolby, Amazon, and Netflix. He also holds several patents across a variety of Silicon Valley technology companies.

Huntington Ingalls Announces Leadership Changes

J. Jones

G. Fuller

Huntington Ingalls Industries, Newport News, Va., a military shipbuilding company, has made changes to its leadership team at its Newport

News Shipbuilding division. Julia Jones was promoted to vice president of manufacturing and facilities, where she will be responsible for all manufacturing and facilities operations. Jones has more than 22 years of shipbuilding experience, including positions of responsibility in operations, planning, manufacturing, nuclear support, and corporate strategic planning. She has served as trades director for surface preparation and treatment, and most recently served as director of operations integration where she led transformation efforts to improve overall efficiency and effectiveness at the shipyard. Gary Fuller was promoted to vice president of fleet support programs. He brings 38 years of experience in construction and overhaul, as well as nuclear and radiological areas. Prior to this role, Fuller served as director of test engineering in the Nuclear Propulsion division. He has also served as chief test engineer, nuclear superintendent, overhaul control engineer, trades director, and nuclear construction director, most recently on the *USS Gerald R. Ford* (CVN 78) during its post-shakedown availability.

Obituary

John "Jack" Miaskowski

J. Miaskowski

John "Jack" Miaskowski, of Strongsville, Ohio, passed away on May 29. He was 82. Miaskowski was in advertising/sales for more than 50 years. Highly regarded in the welding industry, he was a prominent fixture at every welding show and GAWDA event. His career began at Penton Publishing, from 1973 to 1997, where he served as the Northeast regional advertising sales manager for the publishing house's two welding magazines, *Welding Design & Fabrication* and *The Welding Distribution*. He went on to become the publisher of those titles. After 24 years, he moved on to open his own advertising/sales company named Miaskowski Enterprises, which he ran for 14 years. At the same time, he was an independent contractor at *Cryogas International* (now *Gasworld*) from 1998 to 2014, where he worked as an advertising sales manager. Afterward, he worked as an independent sales representative at Label Solutions, a provider in the industrial gas industry, until his passing. Additionally, he was an active community member. He was a member of the American Welding Society from 1974 to 1998. He also served as past president and honorary District Governor of Rotary. Miaskowski is survived by his wife of 55 years, Kathleen; daughters, Kathy, Lisa, and Maureen; and grandchildren, Michael, Patrick, Brian, Carter, Callie, Max, Joe, Sam, and Jake. WJ

— continued from page 11

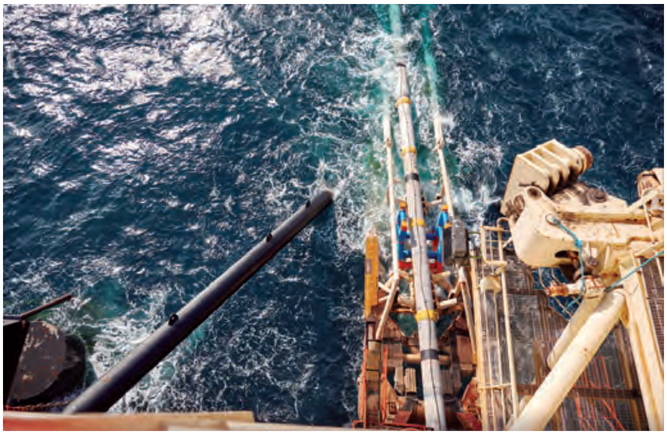

Castoro Sei pipelay activity during shore pull operations.

36-in. pipes by Castoro Sei — Saipem's semisubmersible pipelaying vessel, the above water tie-in with the onshore infrastructure in Albanian waters, as well as hydrotesting.

Activities to connect the Italian and Albanian coasts began in mid-January 2020, with pipes welded and tested on board Castoro Sei, and then laid onto the bottom of the Adriatic Sea in a continuous stretch, starting from the Italian shores toward Albania. Considering the COVID-19 pandemic, the company and its contractor Saipem implemented a range of stringent measures to protect health and safety.

"These are unprecedented times for all of us, and the energy industry is engaged in a delicate balancing act: handling operations on the ground with extreme care while continuing to provide the energy needed for our homes and businesses," said John Haynes, the company's project director. "The TAP project is now more than 95% complete, and we look forward to crossing the finish line by the end of this year."

• **Sciaky** has announced a rise in demand for its Electron Beam Additive Manufacturing (EBAM) and electron beam welding solutions, despite the global COVID-19 pandemic. The company has reported a dozen new projects, from high-level research and development to production of prototype and production parts, mostly tied to the aerospace industry.

Many of the EBAM metal 3D printing projects involve a variety of high-value materials, such as titanium, Inconel, niobium, copper-nickel, and stainless steel. The company's EBAM metal 3D printing solution is a wire-based direct energy deposition process.

• **TRUMPF** recently held its in-house trade show, INTECH, digitally for the first time. Around 1600 visitors from 56 countries took part in the virtual trade show. "With a digital INTECH, we were able to optimally meet the requirements of our international customers in these Coronavirus times," said Reinhold Gross, managing director sales and services of TRUMPF Werkzeugmaschinen GmbH + Co. KG.

The company set up an online platform for the show. During topic dialogs, experts presented new machines and technologies. In advance, visitors could register for program items; during the event, they were able to address questions live to experts. Videos for the new TruLaser Tube 3000 fiber laser tube cutting machine and the TruPrint 2000 3D print-

For the digital INTECH, TRUMPF made video topic dialogs on the machines and technologies in advance. (Photo: TRUMPF)

er received the most feedback. Talks on the topics of electromobility and the smart factory were also popular.

Crozier Welding Grows in Ohio to Support Nearby Oil and Gas Industry

A JobsOhio Grant will help Crozier Welding LLC, Coshocton, Ohio, to expand and improve logistical efficiencies. The company plans to invest $2.5 million and create 15–25 jobs. It will also relocate to a larger facility to improve logistical efficiencies and allow for company expansion.

Crozier has grown from high-pressure pipeline welding and fabrication into being a key equipment supplier to some of the country's largest oil and gas producers.

"We continually strive to make a positive impact in the industry as well as our community. This investment positions Crozier Welding for future growth and increased productivity," said Owner Bob Crozier.

Ohio's energy industry has attracted many shale investments, as the state sits atop the Utica and Marcellus shale formations.

ANDRITZ to Supply Laser Welding Systems for Tailor-Welded Blanks to Toyota

International technology group ANDRITZ, Graz, Austria, has received a package order from Toyota Motor North

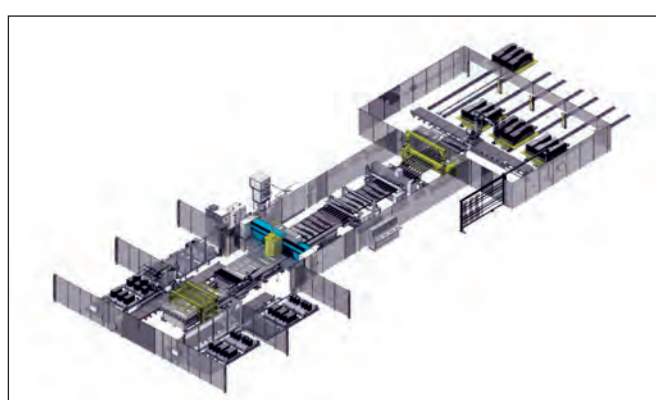

A SOUTRAC II tailored blank laser welding system for curved seams is shown. (© ANDRITZ)

America (TMNA), Plano, Tex., for the supply of three jointly developed SOUTRAC II tailor-welded blank (TWB) laser welding systems to be installed in its North American manufacturing plants.

The TWB laser welding systems are suitable for curved applications. The processing head it contains has been exclusively developed for TMNA. The TWB applications implemented will support Toyota's New Global Architecture. The fully automated production system will also be capable of integrating automatic guided vehicles that will connect plant logistics systems with warehouse/production equipment.

The new core piece incorporates 15 axes in combination with a welding shuttle concept and will be implemented in the new generation of the SOUTRAC II welding system.

ESAB Introduces GCE Specialty Gas and Valve Product Lines in North America, Opens Texas Configuration Center

Recently, ESAB announced North American distributors and end-users have full access to the GCE Druva specialty gas equipment and GCE Valves product lines.

Since completing the acquisition of Gas Control Equipment (GCE) in October 2018, ESAB Welding & Cutting Products, Annapolis Junction, Md., has focused on aligning its global product offerings and innovations into four areas: cutting and welding, healthcare, specialty gas equipment, and cylinder valves. Furthering the global integration, the company has announced North American distributors and end-users have full access to the GCE Druva® specialty gas equipment and GCE Valves product lines.

In addition, to support the move, ESAB revealed the completion of a dedicated Configuration Center at its Denton, Tex., facility. The center, which serves both the GCE and Victor® brands, is isolated from the manufacturing areas for Victor industrial products, which are also part of the company portfolio.

"The Configuration Center provides build-to-order services for specialty gas equipment products in a specially designed clean-room environment," said Curt Rocha, global product and business director gas equipment, ESAB. "We have also added GCE-dedicated engineering, applications, assembly, and sales support teams to ensure 'best-in-class' equipment solutions and quick turnaround."

Industry Notes

• **Lamar Institute of Technology**, Beaumont, Tex., was named one of 15 Best Trade Schools in Texas by the **World Scholarship Forum**. Ranked number eight, the institute was chosen, according to the selection criteria, because "these programs are focused on benefits offered and career outlook. We also considered the quality of education, average earnings of graduates, accreditation, and several other relevant factors." Among its offerings is a welding degree.

• **Keen Compressed Gas Co.**, Wilmington, Del., recently announced its receipt of ISO 17025:2017 accreditation from **Perry Johnson Laboratory Accreditation Inc.** In 2018, the company began construction on a new, automated $6 million fill plant; completed in the fall of 2019, it's now backed by the ISO accreditation.

• **United Performance Metals** has installed a new, 8-kW fiber laser in the company's Cincinnati, Ohio, headquarters. United now operates four laser cutting machines in its Ohio laser center: two fiber lasers and two CO_2 lasers.

• In San Diego, Calif., a fundraising effort by **GovX**, the online shopping site exclusively for current/former military and first responders, has raised more than $7000 for **Workshops for Warriors**, a school providing hands-on training, STEM educational programs, and opportunities to earn third-party credentials that enable veterans/transitioning service members to be placed into careers at no additional cost.

• In 2019, **Postle Industries and Hardface Technologies**, Cleveland, Ohio, celebrated its 50th anniversary and in honor of the milestone, has given its company logo an upgraded, new look. In business since 1969 with its Postalloy® Hardfacing and Hardbanding Products, a range of welding alloys to protect equipment and components from wear caused by abrasion, impact, metal-to-metal friction, and more are offered.

• **Bug-O Systems**, Canonsburg, Pa., is launching a communication system accessed at *bugo.com*. Its Live Support Program has three areas of focus — distributor/dealer product support, send and show application solutions, and field fix user assistance. Webinars will also allow offering customers timely guidance for all cutting and welding products. WJ

AWS American Welding Society

Do You Have Some News to Tell Us?

If you have a news item that might interest *Welding Journal* readers, send it to the following address:

Welding Journal Dept., Attn: Kristin Campbell
8669 NW 36 St., #130
Miami, FL 33166
Items can also be sent by email to *kcampbell@aws.org.*

PRODUCT & PRINT SPOTLIGHT

— continued from page 21

area 150% larger than its predecessors. This combination allows users to weld larger parts, form deeper weld seams, and achieve higher feed rates, allowing parts to be produced faster. The laser system also features an intelligent image-processing system that automatically corrects the laser beam if the part to be welded is out of alignment. This makes the process more reliable and reduces scrap. The laser system is suitable for complex medical devices, such as endoscopes. It also works with common metals, including mild steel, stainless steel, copper, aluminum, and titanium.

TRUMPF
trumpf.com
+49 7156 3030

Website Displays Nearly 500 Weld Camera Videos

The website offers a library of nearly 500 videos on weld processes that have not been enhanced. Taken with the company's weld cameras, the library shows videos of gas metal arc, gas tungsten arc, shielded metal arc, laser, electron beam, and plasma welding applications on various substrate materials in both monochrome and color. The new website also features a more intuitive process to help visitors decide which camera system best fits their needs, including blog posts and other content describing how the company's products are used across various industries. Other highlights of the website include a direct link to the company's customer support center, an enhanced blog resource page, and a detailed listing of the company's global partners.

Xiris Automation Inc.
xiris.com
(905) 331-6660

Flux Cored Welding Wire Boosts Crack Resistance

The Cryo-Shield Ni9, a Ni-Cr-Mo alloy flux cored welding wire, enhances crack resistance to enable all-position welding of 9% Ni steel storage tanks with 100% CO_2 shielding gas. This modified 625-type welding wire features mechanical properties similar to Hastelloy® ENiMo-13 flux cored wires, but at a lower purchase price because of its modified formula. Its typical as-welded mechanical properties are a yield strength of 440 MPa, a tensile strength of 730 MPa, an elongation of 44%, and a Charpy impact value of 65 J at –196°C. The welding wire also lowers operating cost through its use of 100% CO_2 shielding gas instead of an argon blend. The welding wire carries approvals from the following classification societies: American Bureau of Shipping, Bureau Veritas, DNV GL, Korean Register, Lloyd's Register, and China Classification Society. It comes in 1.2 mm diameter on 300-mm wire baskets or plastic spools and is delivered in vacuum-seal foil packaging that provides moisture absorption.

ESAB Welding & Cutting Products
esab.com
(800) 372-2123

Laser Cutting Machine Works with a Variety of Metals

The FiberPro comes equipped with the Flashcut Pro Controller software to efficiently cut materials like brass, copper, stainless steel, mild steel, and aluminum. For precise and consistent cuts, the machine comes standard with a Precitec cutting head, as well as a direct-drive helical rack and pinion. Boasting a Class 1 safety rating, it also contains a viewing glass to provide the operator with optimal protection while he or she is watching the machine during cutting. Additionally, it

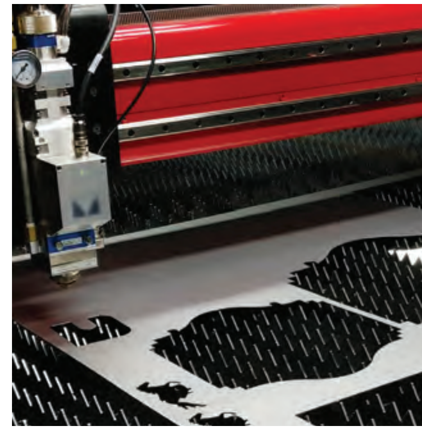

features ISO 230-2 machinery standard specifications and the option of a 2- or 4-kW laser. The machine is easy to set up and requires minimal maintenance. It comes with a two-year warranty and free phone support for life.

Koike Aronson Ransome
koike.com
(800) 252-5232

Report Analyzes the Global Shielding Gas Market

Global Welding Gas/Shielding Gas Market estimates this industry will reach $2214.6 million by 2026, from 2139.8 million in 2020, at a compound annual growth rate of 3.2%. The 110-page report includes the production, revenue, price, market share, and growth rate of each type of welding/shielding gas according to the following categories: argon, carbon dioxide, oxygen, hydrogen, and others. It focuses on the status and outlook for major applications/end users, consumption (sales), market share, and growth rate for metal manufacturing, construction, energy, and aerospace applications. The report also looks at the major players in this industry, including Air Products and Chemicals Inc., The Linde Group, Praxair Inc., Taiyo Nippon Sanso Corp., and Air Liquide SA. It concludes with information on the present and future effects of COVID-19 on the shielding gas market.

Industry Research
industryresearch.biz
(424) 253-0807

FOR SALE OR RENT

ADVERTISER INDEX

SUPPLEMENT TO THE *WELDING JOURNAL,* SEPTEMBER 2020
Sponsored by the American Welding Society

Deep Learning-Based Detection of Penetration from Weld Pool Reflection Images

An innovative approach was achived to identify the weld penetration state using a convolutional neural network

BY C. LI, Q. WANG, W. JIAO, M. JOHNSON, AND Y. M. ZHANG

ABSTRACT

An innovative method was proposed to determine weld joint penetration using machine learning techniques. In our approach, the dot-structured laser images reflected from an oscillating weld pool surface were captured. Experienced welders typically evaluate the weld penetration status based on this reflected laser pattern. To overcome the challenges in identifying features and accurately processing the images using conventional machine vision algorithms, we proposed the use the raw images without any processing as the input to a convolutional neural network (CNN). The labels needed to train the CNN were the measured weld penetration states, obtained from the images on the backside of the workpiece as a set of discrete weld penetration categories. The raw data, images, and penetration state were generated from extensive experiments using an automated robotic gas tungsten arc welding process. Data augmentation was performed to enhance the robustness of the trained network, which led to 270,000 training examples, 45,000 validation examples, and 45,000 test examples. A six-layer convolutional neural network trained with a modified mini-batch gradient descent method led to a final testing accuracy of 90.7%. A voting mechanism based on three continuous images increased the classification accuracy to 97.6%.

KEYWORDS

• Weld Pool • Pool Oscillation • Machine Learning
• Deep Learning • Penetration •Machine Vision
• Gas Tungsten Arc Welding (GTAW) • Image

Introduction

Gas tungsten arc welding (GTAW) is one of the most widely used welding processes in industrial manufacturing, especially for critical applications, such as pressure vessels and aerospace. Benefits of GTAW include its stability and high-quality weld joints. In these critical applications, weld joint penetration is an important criterion to judge weld joint integrity, which affects mechanical properties especially fatigue and service life of the welded structure. Therefore, it is important to estimate the weld joint penetration in real time as an intermediate step to controlling the penetration in a desired state. The penetration state is determined by the depth and bottom surface of the weld pool, which are hidden from view and cannot be monitored directly in practical applications. Therefore, researchers have been trying to detect weld joint penetration using available characteristic information from the welding process.

The abrupt transition of the weld pool's natural oscillation frequency from incomplete joint penetration to complete joint penetration has been applied to monitor and control the weld joint penetration by Xiao and Ouden (Refs. 1, 2). Chen et al. found the depth of joint penetration was related to the infrared thermal images of the weld pool captured by infrared cameras, which were used for characterizing the surface temperature distribution of the weld pool (Refs. 3–5). Reflected ultrasonic waves have also been used to determine and control weld joint penetration in real time (Refs. 6, 7).

Recently, convolutional neural networks (CNNs) have become the prevalent method for solving computer vision problems. As a specialized kind of neural networks to process grid-like topology data, CNNs are inspired by the study of a monkey's visual cortex (Refs. 20, 21). LeCun et al. proposed the architecture of modern CNNs (Ref. 22) and developed a five-layer CNN (LeCun-5), including two convolutional layers, two pooling layers, and one fully connected layer, which will be trained by the back propagation optimization algorithm (Ref. 23).

In this modern CNN architecture, convolutional layers are used to process raw pixels and extract features automatically; and fully connected layers are used to do high-level reasoning based on the features extracted. Inspired by the successful application of LeNet-5 in classifying handwritten digits, deeper and more ingenious CNNs have been developed to deal with more complex computer vision tasks. In 2012, AlexNet won the Large Scale Visual Recognition Challenge with a top five test error rate of 15.3%, compared to 26.2% achieved by the second-best entry using non-CNNs (Ref. 24). After the success of AlexNet, additional work has been done to improve the performance of CNNs for image classification, object detection,

https://doi.org/10.29391/2020.99.022

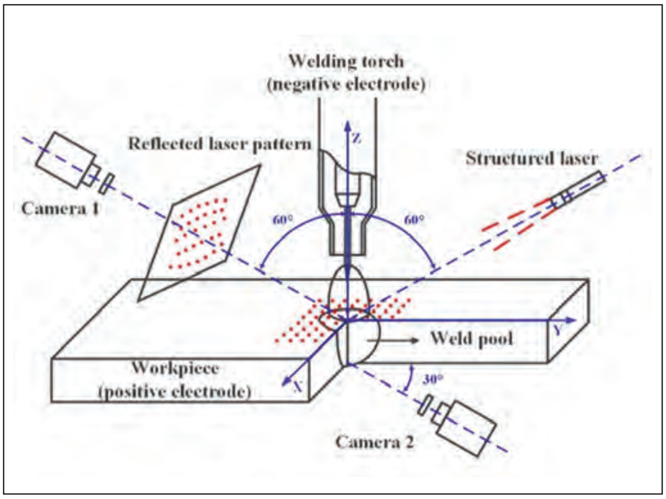

Fig. 1 — Experimental setup of the weld pool and weld joint penetration system.

and tracking, such as R-CNN (Refs. 25–27), *ZFNet (Ref. 28), VGGNet (Ref. 29), GAN (Ref. 30), GoogLeNet (Ref. 31), and ResNet (Ref. 32). In addition, CNNs have also been successfully applied in other areas such as speech processing (Refs. 33, 34) and natural language processing (Refs. 35, 36).The analysis suggests that the ability of CNNs to directly process raw images avoids the problems of manual selection and extraction of features from the images.

This paper presents an effective CNN-based method to detect weld joint penetration from the raw reflected dot-structured laser pattern of a weld pool. A weld pool sensing system was designed and built to capture reflected dot-structured laser patterns and corresponding backside images of the joints simultaneously. Data augmentation was then performed to expand the size of the raw dataset, generating the following three independent datasets: training data, validation data, and test data. A six-layer convolution neural network, including two convolutional layers, two pooling layers, one fully connected layer, and one regression layer, was trained taking the raw reflected laser patterns as data and weld penetration states as labels and using the revised mini-batch gradient descent method. The final test showed the prediction accuracy of a neural network is 90.7%.

This paper is organized as follows: Section I introduces the principles of CNNs; Section II describes the dataset building process; Section III presents the network architecture, hyper parameters, training process of the proposed model, testing results, and discussion; and Section IV summarizes this paper and draws conclusions.

I. Principle of Proposed Method

The basic components and framework of CNNs are similar across domain applications. Typically, the convolution operation is used in place of matrix multiplication in at least one of the network layers (Ref. 37). The network structure typically includes convolutional layers, pooling layers, and fully connected layers (Ref. 38). In convolutional layers, small-sized kernels flow across previous layers and operate via a dot product with the previous layer by

Table 1 — Weld Joint Penetration Label

Area (px)	Label
650–950	0
950–1350	1
1350–1650	2
1650–1950	3
1950–2250	4
2250–2500	5

$$S^l(i, j, k) = \Sigma_{m,n} I^{l-1}(i+m, j+n)K_k^l(m, n) \quad (1)$$

where S^l is the calculated value after convolutional layers; i, j indicates the position; I^l is lth layer; and K_k^l is the kth kernel used in lth layer.

A non-linear activation function will take in the convoluted value to produce the next layer to extract the non-linear feature:

$$I^l(i, j, k) = a(S^l(i, j, k)) \quad (2)$$

where a is the activation function.

Typical activation functions are sigmoid, tanh, and ReLU (Refs. 39, 40). To decrease complexity and increase robustness of CNNs, pooling layers follow the convolutional layers. In pooling layers, a region of data from the last layer is compressed into one value using predefined pooling methods such as average pooling (Ref. 22), max pooling (Ref. 41), L_p pooling (Ref. 42), and stochastic pooling (Ref. 43):

$$I^l(i, j, k) = pool(I^{l-1}(m, n, k)), \forall (m, n) \in R_{ij} \quad (3)$$

where R_{ij} is the local neighborhood around location (i, j).

After convolutional and pooling layers, traditional fully connected layers are applied. In the fully connected layers, grid-like topology data in the previous layer is reshaped into a column vector, which is premultiplied by a weight matrix W^l and added with a bias term B^l:

$$I^l = W^l \cdot I^{l-1} + B^l \quad (4)$$

The classified labels are calculated using forward-propagation-based architecture and the parameters include kernels, weights, and biases that are denoted by θ in CNNs. The average loss L is defined based on the difference between classified and true labels:

$$L = \frac{1}{N}\sum_{n=1}^{N} l\left(\theta;\ y^{(n)},\ o^{(n)}\right) \quad (5)$$

where $y^{(n)}$ is the the true label and $o^{(n)}$ is the predicted label.

Typical loss functions ℓ include squared error, Hinge loss (Ref. 44), and cross-entropy loss (Ref. 37). The CNNs are

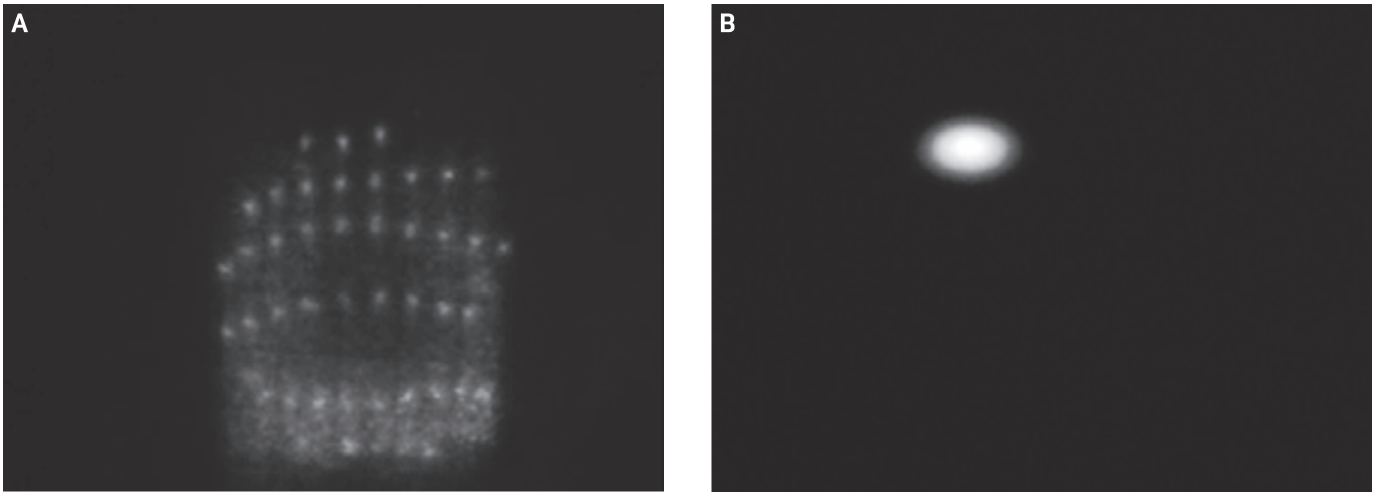

Fig. 2 — Typical images in experiments: A — From camera 1; B — from camera 2.

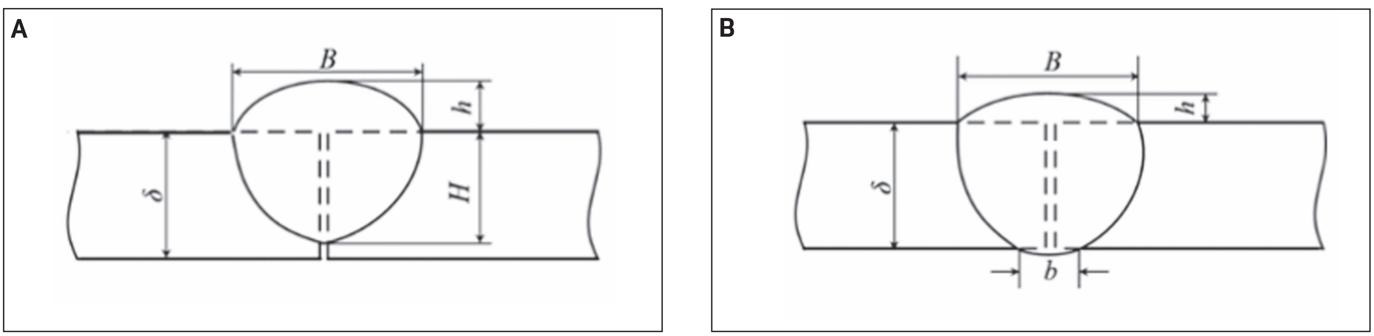

Fig. 3 — Weld joint penetration: A — Incomplete joint penetration; B — complete joint penetration.

trained using the stochastic gradient descent optimization technique. In our approach, the parameter updating rule was mini-batch stochastic gradient descent (mini-batch SGD), as shown in Equation 6:

$$\theta_{t+1} = \theta_t - \eta_t \nabla_\theta L(\theta_t; y^{(i:i+n)}, o^{(i:i+n)}) \quad (6)$$

where η_t is the learning rate and n is the mini-batch size. The method used to determine how the parameters are changed, from θ_t to θ_{t+1} toward the ones that can minimize Equation 5, in neural networks is called optimizer. When using Equation 6 to change the parameters, the optimizer is to adaptively adjust the learning rate η_t based on the computed gradient to accelerate the training processes or achieve better prediction performance. Widely used optimizers include momentum (Ref. 45), Adagrad (Ref. 46), Adadelta (Ref. 47), and Adam (Ref. 48) that have been developed and became the benchmark works in training neural networks.

II. System Setup and Dataset Building

Weld Pool and Weld Joint Penetration Sensing System

In our experiments, autogenous, pulsed GTAW spot welds were conducted on a 0.125-in.-thick 304 stainless steel. In each pulsing period, the peak current was applied at 60 A for 47 ms and followed by a 20-A base current for 3 ms. The weld pool oscillated and an image was captured, one image per pulsing cycle, at 2 ms of the base current to ensure that the arc had become darker. A weld pool sensing system had been designed and established based on the experiment platform proposed in the literature (Ref. 15). As shown in Fig. 1, a 650-nm-wavelength 19 × 19 dot-matrix structured laser pattern was projected onto the weld pool surface at 30 deg from horizontal. On the other side, the reflected laser light was collected by a screen placed on the path of the reflected laser pattern. A Point Grey GZL-CL-22C5M-C high-speed camera (camera 1 in Fig. 1) with a 650-nm center wavelength band-pass optical filter captured the images from the screen at a speed of 1000 fps. At each base current period, the high-speed camera captured three images of the weld pool surface to use as the raw data of the neural networks. In addition, a Point Grey FL3-FW-03S1C with no optical filter(camera 2 in Fig. 1) captured one image of the backside of the weld bead at the start of the base current period, saved in 8-bit black-and-white format. Figure 2A shows a typical reflected laser pattern image captured by camera 1 and used as input into our model. During the welding process, the weld pool surface was not even, which caused the reflected laser pattern to be irregular. As discussed, all the information regarding the backside weld penetration were contained in that image and used as the input data to the convolutional neural network. Figure 2B is a typical image captured by camera 2 and used to identify weld penetration state labels after

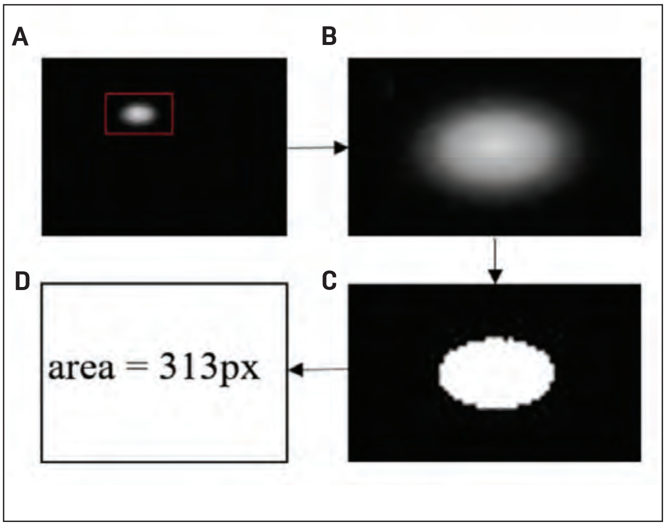

Fig. 4 — Weld joint penetration identification process: A — Raw image; B — ROI; C — binarized image; D — light area calculation.

some simple image processing, as discussed in detail in the next section. More than 300 welding experiments have been run for this application, and 3540 image pairs have been collected as our raw data set.

Weld Joint Penetration Labels Identification

As shown in Fig. 3, there are two kinds of weld joint penetration, complete joint penetration and incomplete joint penetration, depending on the geometry sizes of the weld pool and workpieces. The degree of welding penetration state is characterized as either the width b or the area Φ of the backside of the weld, which is zero for the case of nonpenetration in A and non-zero for the case of full penetration in B. Compared with using area, choosing width results in another problem: how to define the width for an irregular shape. A better approach is to measure the smallest and biggest measures of the pool and then take the average, but that requires an extra process. Based on this idea, the light area of the backside of the weld bead from camera 2 was used to identify the welding penetration state. The whole process is shown in Fig. 4. Initially, the region of interest (ROI) was selected around the weld bead to decrease calculation burden. A binary operation was performed with a threshold of 110 to filter out pixels that characterize unmelted base metal. The pixels kept can be considered as characterizations of the weld bead. Then, according to the accumulated number of pixels kept, weld penetration states were identified and assigned labels (Table 1). The primary goal is to discriminate between no penetration, incomplete joint penetration, and complete joint penetration of the weld; however, to add some additional differentiation, we used six different levels of penetration for these experiments. Throughout the experiments, all the lighting conditions and camera settings remained the same. The reason for the threshold being set to 110 was to eliminate the factors lighting condition, for example, that may affect the backside light area. Preliminary experiments were done to determine the best threshold setting.

Table 2 — Data Augmentation Summary

Label	Number of Raw Images	Number of Images after Augmentation
0	457	59,868
1	495	64,846
2	540	70,696
3	570	74,101
4	626	70,739
5	862	87,063

Data Augmentation

The original dataset of reflected laser patterns and weld penetration states included 3540 examples. This is insufficient to train CNNs, leading to overfitting as the number of parameters is often tens of millions or more. In Pinto et al. (Ref. 49), a simple V1-like model had been built, trained, and tested on this small dataset. However, when variations such as position changes or different sizes were added to the test set, the performance degraded dramatically. In this paper, a label-preserving data augmentation process was performed to increase the size of the dataset. The approach was similar to that in Ref. 24 where cropping original images into several patches was found to be an effective method for data augmentation (Ref. 50) and affine transformations, such as rotation and scaling for enlarging datasets.

Considering the fact that skilled welders are able to determine weld penetration states at different positions, distances, and orientations, the three geometric transformations of shifting, scaling, and rotation were used for transforming the raw input images. The data augmentation results are summarized in Table 2.

To make sure the testing results of the neural networks are accurate and will generalize, the training data set, validation set, and test set must be completely separate. To accomplish this, we randomly partitioned the data into 75% training, 12.5% validation, and 12.5% test sets, balancing the number of examples from each label category. This resulted in a training set, which contained 270,000 images; a validation set, which contained 45,000 images; and a test set, which contained 45,000 images being created.

III. Model Training

Architecture

Convolutional neural networks are used for many different computer vision tasks. For simple tasks, such as image classification, five to ten layers may be enough (Refs. 23, 24). However, if the task is complex, such as image segmentation or object detection, the neural network often contains more than ten layers. Examples include GoogLeNet (Ref. 1) with 22 layers and VGG-16 (Ref. 29) with 16 layers. Using deeper CNNs for simple tasks is not recommended because they require longer training time and increase the risk of overfitting. Details of the network architecture have to be designed to meet the requirements from each individual task. In our paper, a six-layer CNN architecture, includ-

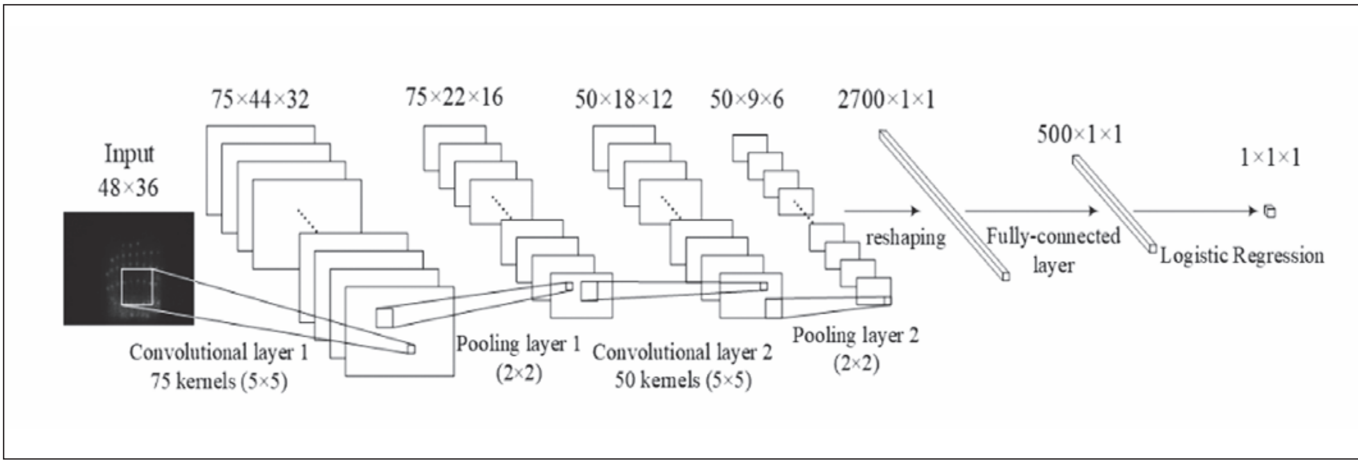

Fig. 5 — Architecture of proposed CNN.

Table 3 — Parameters Used in Proposed CNN

Layers	Number of Parameters
Convolutional–1	$(5 \times 5 + 1) \times 75 = 1950$
Pooling–1	$(1 + 1) \times 75 = 150$
Convolutional–2	$(75 \times 5 \times 5 + 1) \times 50 = 93{,}800$
Pooling–2	$(1 + 1) \times 50 = 100$
Fully connected	$2700 \times 500 + 500 = 1{,}350{,}500$
Softmax regression	$500 \times 6 + 6 = 3006$
Total	1,449,506

ing two convolutional layers, two max-pooling layers, one fully connected layer, and one softmax regression layer, had been selected based on preliminary experimentation using the validation set data. As shown in Fig. 5, 75 kernels with a size of 5 × 5 were used in the first convolutional layer. A 2 × 2 max-pooling layer followed the first convolutional layer. Adding a max-pooling layer enhanced the robustness of the position variance and significantly reduced the computational cost of the neural network. The second convolutional layer contained 50 kernels with a size of 5 × 5 followed by a 2 × 2 max pooling. All convolution operations were implemented without adding. Then, 50 × 9 × 6 data was reshaped to a column vector with a length of 2700 and followed with a fully connected layer of 500 neurons. Lastly, a softmax regression layer was used to calculate the predicted label ranging from zero to five.

Currently, many CNNs use the rectified linear unit (ReLU) function as an activation function. Compared with traditional activation functions, such as tanh and sigmoid, ReLU often converges faster (Ref. 24) and achieves better performance (Ref. 39, 51). Although tanh and ReLU achieved similar validation set performance in our experiments, we chose to use ReLU as the activation function for faster convergence and lower risk of saturation. The number of parameters used in this CNN is summarized in Table 3.

Training

In our experiments, all weights were initialized using a Gaussian distribution with a zero mean and 0.01 variance,

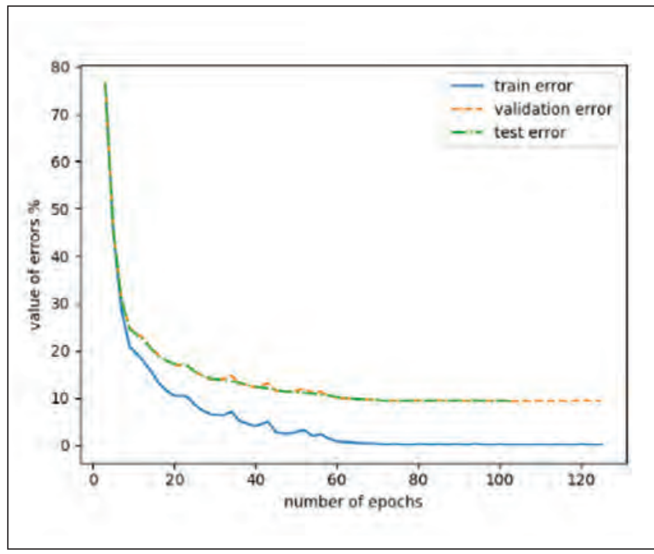

Fig. 6 — Errors in the training process.

and biases were set to zero. We used a modified Xavier initialization (Refs. 29, 40) rather than full Xavier initialization (Ref. 52) to help address convergence difficulties. The default learning rate created some initial saddle points, so the initialization was reduced further by 0.1. The result was a validation set error rate of 22.48%, which was higher than the Gaussian initialization with a 22.08% validation error rate on the same validation dataset.

The optimizer was a revised mini-batch gradient descent with a mini-batch size of 600. As a tradeoff of batch gradient descent and stochastic gradient descent, mini-batch gradient descent took a small size of training samples each time to calculate the negative gradient direction and adjusted parameters to minimize the cost function. Although the mini-batch gradient descent balanced the variance of convergence and computation efficiency, the speed of convergence was relatively slow. Thus, a momentum term was added to speed up the convergence speed (Ref. 53). Learning rate annealing was used to balance the training time and the training accuracy. The initial learning rate η_t was 0.01 in our experiments, decreasing by half if the validation error stopped decreasing for three epochs. Adaptive moment estimation (Adam) (Ref. 48) has become prevalent in recent CNNs. Combining the advantages of the RMSProp (Ref. 54) and the AdaGrad (Ref. 46) methods, this designed adaptive learning rates for each parameter. The convergence speed was faster than the revised mini-batch gradient descent, but the validation set performance was slightly worse than GD, so we did not use the Adam optimizer.

Batch normalization (BN)(Ref. 55) was used in our experiments before the activation function as a kind of dataprocessing, which can speed up the learning process (Refs. 23, 56). By forcing the output of the BN layer to be a designed distribution (Gaussian distribution in our experiments), the risk of activation function saturation was reduced. In addition, there was no need to add dropout — one way of controlling overfitting (Refs. 24, 57).

During the training process, the training set was used to adjust parameters to minimize the loss function as defined in Equation 5. Validation error was used to control the learning rate annealing and early stopping, as well as to compare different algorithms in the design stage. Test data were put aside during training and tuning. All the training had been run on a personal computer equipped with an EVGA GTX 1080 graphics processing unit (GPU). The complete training process used 171.43 min, with a final test set error of 9.29%. The details of the training process are shown in Fig. 6.

Testing

The prediction accuracy for a single image was 90.70%. In our paper, three images were captured for every base current period sharing the same label. Therefore, a voting mechanism was added based on combining results from the three images. This increased prediction accuracy to 97.57%. Further observation of the errors made by the system suggested that errors only occur when the weld joint penetration state is in the border between two adjacent labels.

Running the trained CNN on an AMD A6-3650 2.6 GHz takes more than 300 ms to get the predicted label. Running on a GPU is much faster, requiring only 1.2 ms with a typical GPU (Ref. 58). Currently, system limitations due to the presence of multiple data collection cards prevents installation of a GPU. In the future, the welding sensing and control system will be implemented with a GPU as well.

IV. Conclusion and Further Research

An innovative approach to identify the weld penetration state using CNN was presented in this paper. An advanced weld pool and weld penetration state sensing system had been designed and implemented to generate training data, and then additional geometric transformations have been used for data augmentation. A six-layer CNN had been implemented using the augmented dataset. The final test accuracy rate of the proposed CNN model was 90.70%, with accuracy improved to 97.57% by using a voting mechanism. Long term, the goal of this work is to support the implementation of this system to control weld joint penetration in an industrial production line setting.

References

1. Xiao, Y. H., and Ouden, G. D. 1990. A study of GTA weld pool oscillation. *Welding Journal* 69(8): 289-s to 293-s.

2. Xiao, Y. H., and Ouden, G. D. 1993. Weld pool oscillation during GTA welding of mild steel. *Welding Journal* 72(8): 428-s to 434-s.

3. Chen, W., and Chin, B. 1990. Monitoring joint penetration using infrared sensing techniques. *Welding Journal* 69(4): 181-s to 185-s.

4. Nagarajan, S., Banerjee, P., Chen, W., and Chin, B. A. 1992. Control of the welding process using infrared sensors. *IEEE Transactions on Robotics and Automation* 8(1): 86–93.

5. Nagarajan, S., Chen, W., and Chin, B. 1989. Infrared sensing for adaptive arc welding. *Welding Journal* 68(11): 462-s to 466-s.

6. Carlson, N., and Johnson, J. 1988. Ultrasonic sensing of weld pool penetration. *Welding Journal* 67(11): 239-s to 246-s.

7. Hardt, D., and Katz, J. 1984. Ultrasonic measurement of weld penetration. *Welding Journal* 63(9): 273-s to 281-s.

8. Mnich, C., Al-Bayat, F., Debrunner, C., Steele, J., and Vincent, T. 2004. In situ weld pool measurement using stereovision. *Japan-USA Symposium on Flexible Automation*, Denver, Colo.

9. Richardson, R., and Gutow, D. 1983. Coaxial arc weld pool viewing for process monitoring and control. *Welding Journal* 63(3): 43–50.

10. Zhao, C., Richardson, I., Kenjeres, S., Kleijn, C., and Saldi, Z. 2009. A stereo vision method for tracking particle flow on the weld pool surface. *Journal of Applied Physics* 105(12): 123104. DOI: 10.1063/1.3143789

11. Zhao, D., Yi, J., Chen, S., Wu, L., and Chen, Q. 2003. Extraction of three-dimensional parameters for weld pool surface in pulsed GTAW with wire filler. *Journal of Manufacturing Science and Engineering* 125(3): 493–503. DOI: 10.1115/1.1556400

12. Agapakis, J. E., and Bolstad, J. O. 1991. Vision sensing and processing system for monitoring and control of welding and other high-luminosity processes. *Optics, Illumination, and Image Sensing for Machine Vision V*, pp. 32–38. International Society for Optics and Photonics: Boston, Mass.

13. Kovacevic, R., and Zhang, Y. 1996. Sensing free surface of arc weld pool using specular reflection: Principle and analysis. *Proceedings of the Institution of Mechanical Engineers, Part B: Journal of Engineering Manufacture* 210(6): 553–564. DOI: 10.1243/PIME_PROC_1996_210_154_02

14. Zhang, Y., Song, H., and Saeed, G. 2006. Observation of a dynamic specular weld pool surface. *Measurement Science and Technology* 17(6): L9. DOI: 10.1088/0957-0233/17/6/L02

15. Song, H., and Zhang, Y. 2008. Measurement and analysis of three-dimensional specular gas tungsten arc weld pool surface. *Welding Journal* 87(4): 85-s to 95-s.

16. Ma, X., and Zhang, Y. 2011. Gas metal arc weld pool surface imaging: modeling and processing. *Welding Journal* 90(5): 85-s to 94-s.

17. Zhang, W., Wang, X., and Zhang, Y. 2013. Analytical real-time measurement of a three-dimensional weld pool surface. *Measurement Science and Technology* 24(11): 115011. DOI: 10.1088/0957-0233/24/11/115011

18. Zhang, W. J., Zhang, X., and Zhang, Y. M. 2015. Robust pattern recognition for measurement of three dimensional weld pool surface in GTAW. *Journal of Intelligent Manufacturing* 26(4): 659–676. DOI: 10.1007/s10845-013-0825-z

19. Zhang, W., Liu, Y., Wang, X., and Zhang, Y. 2012. Characterization of three-dimensional weld pool surface in GTAW. *Welding*

Journal 91(7): 195-s to 203-s.

20. Hubel, D. H., and Wiesel, T. N. 1968. Receptive fields and functional architecture of monkey striate cortex. *The Journal of Physiology* 195(1): 215–243. DOI: 10.1113/jphysiol.1968.sp008455

21. Fukushima, K., and Miyake, S. 1982. Neocognitron: A self-organizing neural network model for a mechanism of visual pattern recognition. *Competition and Cooperation in Neural Nets*, pp. 267-285.

22. LeCun, Y., et al. 1990. Handwritten digit recognition with a back-propagation network. *Advances in Neural Information Processing Systems,* pp. 396–404.

23. LeCun, Y., Bottou, L., Bengio, Y., and Haffner, P. 1998. Gradient-based learning applied to document recognition. *Proceedings of the IEEE* 86(11): 2278–2324. DOI: 10.1109/5.726791

24. Krizhevsky, A., Sutskever, I., and Hinton, G. E. 2012. Imagenet classification with deep convolutional neural networks. *Advances in Neural Information Processing Systems,* pp. 1097–1105.

25. Girshick, R., Donahue, J., Darrell, T., and Malik, J. 2014. Rich feature hierarchies for accurate object detection and semantic segmentation. *Proceedings of the IEEE Conference on Computer Vision and Pattern Recognition,* pp. 580–587.

26. Girshick, R. 2015. Fast r-cnn. *Proceedings of the IEEE International Conference on Computer Vision*, pp. 1440–1448.

27. Ren, S., He, K., Girshick, R., and Sun, J. 2015. Faster R-CNN: Towards real-time object detection with region proposal networks. *Advances in Neural Information Processing Systems*, pp. 91–99.

28. Zeiler, M. D., and Fergus, R. 2014. Visualizing and understanding convolutional networks. *European Conference.*

29. Simonyan, K., and Zisserman, A. 2014. Very deep convolutional networks for large-scale image recognition. arXiv preprint arXiv:1409.1556.

30. Goodfellow, I., et al. 2014. Generative adversarial nets. *Advances in Neural Information Processing Systems*, pp. 2672–2680.

31. Szegedy, C., et al. 2015. Going deeper with convolutions. *Proceedings of the IEEE Conference on Computer Vision and Pattern Recognition,* pp. 1–9.

32. He, K., Zhang, X., Ren, S. and Sun, J. 2016. Deep residual learning for image recognition. *Proceedings of the IEEE Conference on Computer Vision and Pattern Recognition,* pp. 770–778.

33. Abdel-Hamid, O., Mohamed, A.-R., Jiang, H., Deng, L., Penn, G., and Yu, D. 2014. Convolutional neural networks for speech recognition. *IEEE/ACM Transactions on Audio, Speech, and Language Processing* 22(10): 1533–1545. DOI: 10.1109/TASLP.2014.2339736

34. Sainath, T. N., et al. 2015. Deep convolutional neural networks for large-scale speech tasks. *Neural Networks* 64: 39–48. DOI: 10.1016/j.neunet.2014.08.005

35. Kim, Y. 2014. Convolutional neural networks for sentence classification. arXiv preprint arXiv:1408.5882.

36. Kalchbrenner, N., Grefenstette, E., and Blunsom, P. 2014. A convolutional neural network for modelling sentences. arXiv preprint arXiv:1404.2188.

37. Goodfellow, I., Bengio, Y., and Courville, A. 2016. *Deep Learning*. MIT Press.

38. Gu, J., et al. 2015. Recent advances in convolutional neural networks. arXiv preprint arXiv:1512.07108.

39. Maas, A. L., Hannun, A. Y., and Ng, A. Y. 2013. Rectifier nonlinearities improve neural network acoustic models. *Proceedings of the International Conference on Machine Learning* 30(1).

40. He, K., Zhang, X., Ren, S., and Sun, J. 2015. Delving deep into rectifiers: Surpassing human-level performance on imagenet classification. *Proceedings of the IEEE International Conference on Computer Vision*, pp. 1026–1034.

41. Boureau, Y.-L., and Cun, Y. L. 2008. Sparse feature learning for deep belief networks. *Advances in Neural Information Processing Systems*, pp. 1185–1192.

42. Hyvärinen, A., and Köster, U. 2007. Complex cell pooling and the statistics of natural images. *Network: Computation in Neural Systems* 18(2): 81–100.

43. Zeiler, M., and Fergus, R. 2013. Stochastic pooling for regularization of deep convolutional neural networks. *Proceedings of the International Conference on Learning Representation* (ICLR).

44. Bartlett, P. L., and Wegkamp, M. H. 2008. Classification with a reject option using a hinge loss. *Journal of Machine Learning Research* 9(8): 823–1840.

45. Qian, N., 1999. On the momentum term in gradient descent learning algorithms. *Neural Networks* 12(1): 145–151. DOI: 10.1016/S0893-6080(98)00116-6

46. Duchi, J., Hazan, E., and Singer, Y. 2011. Adaptive subgradient methods for online learning and stochastic optimization. *Journal of Machine Learning Research* 12(7): 2121–2159.

47. Zeiler, M. D. 2012. ADADELTA: An adaptive learning rate method. arXiv preprint arXiv:1212.5701.

48. Kingma, D., and Ba, J. 2014. Adam: A method for stochastic optimization. arXiv preprint arXiv:1412.6980.

49. Pinto, N., Cox, D. D., and DiCarlo, J. J. 2008. Why is real-world visual object recognition hard? *PLoS Computational Biology* 4(1): 27. DOI: 10.1371/journal.pcbi.0040027

50. Simard, P. Y., Steinkraus, D., and Platt, J. C. 2003. Best practices for convolutional neural networks applied to visual document analysis. *Proceedings of the Seventh International Conference on Document Analysis and Recognition*, p. 958: IEEE Computer Society.

51. Glorot, X., Bordes, A., and Bengio, Y. 2011. Deep sparse rectifier neural networks. *Proceedings of the Fourteenth International Conference on Artificial Intelligence and Statistics,* pp. 315–323.

52. Glorot, X., and Bengio, Y. 2010. Understanding the difficulty of training deep feedforward neural networks. *Proceedings of the Thirteenth International Conference on Artificial Intelligence and Statistics*, pp. 249–256.

53. Karpathy, A. 2016. Cs231n: Convolutional neural networks for visual recognition. *Neural Networks,* Vol. 1.

54. Tieleman, T., and Hinton, G. 2012. Lecture 6.5-rmsprop: Divide the gradient by a running average of its recent magnitude. *COURSERA: Neural Networks for Machine Learning* 4(2): 26–31.

55. Ioffe, S., and Szegedy, C. 2015. Batch normalization: Accelerating deep network training by reducing internal covariate shift. *International Conference on Machine Learning,* pp. 448–456.

56. Wiesler, S., and Ney, H. 2011. A convergence analysis of log-linear training. *Advances in Neural Information Processing Systems,* pp. 657–665.

57. Srivastava, N., Hinton, G., Krizhevsky, A., Sutskever, I., and Salakhutdinov, R. 2014. Dropout: A simple way to prevent neural networks from overfitting. *The Journal of Machine Learning Research* 15(1): 1929–1958.

58. Long, J., Shelhamer, E., and Darrell, T. 2015. Fully convolutional networks for semantic segmentation. *Proceedings of the IEEE Conference on Computer Vision and Pattern Recognition*, pp. 3431–3440.

CHAO LI, QIYUE WANG, WENHUA JIAO, MICHAEL JOHNSON, and YU MING ZHANG (yuming.zhang@uky.edu) are with the Department of Electrical and Computer Engineering, University of Kentucky, Lexington, Ky. LI, WANG, JIAO, and ZHANG are also with the Institute for Sustainable Manufacturing, University of Kentucky, Lexington, KY.

Effects of Filler Wire Intervention on Gas Tungsten Arc: Part I — Mechanism

A novel sensing method of detecting voltage signals between a filler wire and tungsten electrode/workpiece was proposed

BY S. ZOU, Z. WANG, S. HU, G. ZHAO, W. WANG, AND Y. CHEN

ABSTRACT

For gas tungsten arc welding (GTAW), the effects of filler wire on the GTA are worth being clarified, which will help deepen the understanding of arc characteristics and inspire new ideas for the real-time monitoring of weld quality. To this end, this work proposed a novel sensing method of detecting probe voltages (i.e., the voltage signals between a filler wire and tungsten electrode/workpiece). Based on this method, in this first part of the work, a tungsten probe was used to replace the filler wire and to interact with the arc in the specific experiments to elucidate the static and dynamic interaction mechanisms between the GTA and filler wire. The results showed that the filler wire intervention deflects the arc to various degrees and will change the voltage signals. As a metal conductor, the filler wire will increase the arc voltage by increasing the average electric field strength. However, its effects on the different areas of the arc are not always consistent, which makes the change trend of the probe voltages not always the same. Moreover, due to thermal inertia, the probe voltage does not strictly change synchronously with the arc voltage under the dynamic disturbance. This work lays a theoretical foundation for monitoring the stability of the GTAW process.

KEYWORDS

- Arc Characteristics • Arc Voltage • Arc Sensing
- Gas Tungsten Arc (GTA) • Filler Wire • Gas Tungsten Arc Welding (GTAW)

Introduction

Gas tungsten arc welding (GTAW) is one of the precision welding techniques for obtaining high-quality weldments. It can weld a variety of industrial structural metals and is widely used in aerospace, atomic energy, pressure vessels, and other industrial fields. Due to its wide application, the quality assurance of GTAW is particularly important. However, even with optimized welding parameters, it is still difficult to guarantee weld quality with automated GTAW in complex environments because of its uncertainty and time variation. This situation requires the development of on-line monitoring and control technologies for weld quality.

The geometry of the weld pool is closely related to the real-time welding state and largely determines the formation of welds after solidification. Therefore, the accurate extraction of weld pool geometry will help to understand and then monitor the dynamic welding process, and it will also contribute to providing useful feedback for the real-time control of weld quality. The extraction of weld pool geometry is often based on visual sensing techniques. Chen et al. used passive visual sensing to extract the distance between the tungsten electrode tip and its reversed reflection in the weld pool under suitable exposure conditions, to characterize the height of the weld pool surface (its concavity/convexity) (Ref. 1). Fan et al. developed a three-way passive visual sensing system to simultaneously detect the weld pool geometry from both sides of the workpiece (Ref. 2). Taking laser as an auxiliary light source, Zhang and Song et al. reconstructed the weld pool by virtue of the designed 3D visual sensing system (Refs. 3–5), and based on this system, Liu and Dong et al. have extracted the geometric parameters of the 3D weld pool for modeling of weld-quality control (Refs. 6, 7).

In addition to the weld pool geometry, the dynamic behaviors of the weld pool have also received much attention. During autogenous GTAW, the weld pool is excited to oscillate by pulse current. The frequency and amplitude of weld pool oscillation can be used to describe the weld penetration status because both of them will change as the volume of the weld pool changes. When the solid restraint at the bottom of the weld pool disappears, the weld pool will have a sudden subsidence, and its oscillation frequency and amplitude will be abruptly changed accordingly. This abrupt change can be used to characterize the critical complete joint penetration status. These dynamic behaviors of the weld pool can be monitored by the arc voltage (Refs. 8–11) or the evolution of the laser pattern reflected from the weld pool surface in the structured-laser visual sensing system (Refs. 12–14).

Arc sound is also a noteworthy information source that can reflect the weld pool status. It can be roughly considered that the arc sound signal in pulsed GTAW is determined by the arc sound source and the modulating arc sound channel. The sound source is generated from the arc energy change,

https://doi.org/10.29391/2020.99.023

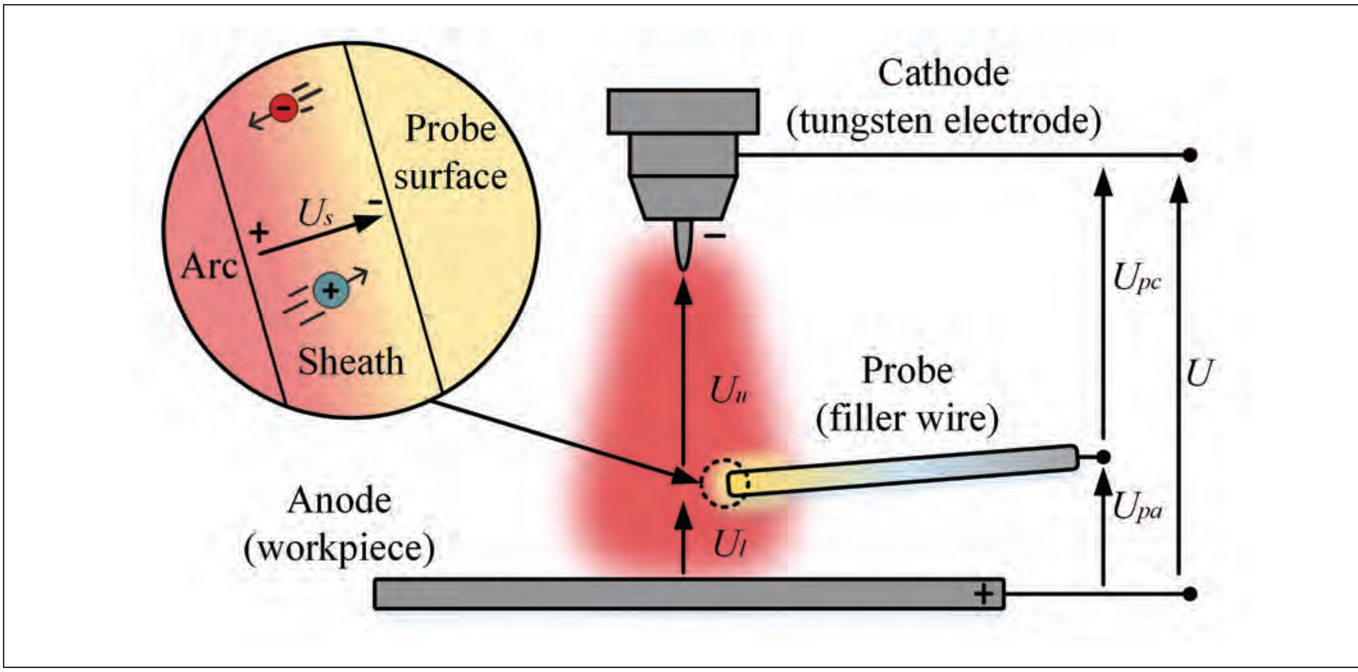

Fig. 1 — Schematic diagram of the sensing principle.

and the sound channel can be considered as a cavity covered by the shielding gas atmosphere (Refs. 15–17). According to Lv et al. (Refs. 16, 17), statistical characteristics of the arc sound in time domain can be used to distinguish different penetration statuses due to the difference in the arc energy, and the different penetration statuses will also result in different formant distribution of the sound channel because of the change in the sound channel state (e.g., an excessively penetrated weld pool will destroy the sound channel). Zhang et al. used the Fisher distance and principal component analysis to select the frequency components reflecting the weld penetration status in pulsed GTAW, then established a classification model and successfully distinguished the different weld penetration statuses (Ref. 18).

As mentioned above, so much valuable and potential information has been continuously mined, the relevant mechanisms have been deeply explained, and various sensing methods have been proposed to serve on-line monitoring and control of GTAW quality. However, the reported studies in the academic field have focused more on autogenous GTAW than GTAW with filler wire. Furthermore, researchers have devoted more attention to studies on weld pool status, often ignoring the effect of the liquid metal generated from the filler wire (if it is employed) on the process. Although the employment of the filler wire will expand the application of GTAW, it will also interfere with the GTA and impact the extraction of characteristic information about the weld pool (e.g., disturbing its regular oscillation frequency under pulse current), which is not conducive to the welding process stability and monitoring of the weld pool. Yudodibroto et al. studied the effects of filler wire on weld pool oscillation in GTAW and thought the oscillation frequency could still be measured to reflect the weld penetration status under the mode of uninterrupted metal transfer (Ref. 19), but the further study has not been reported yet; for instance, the interaction mechanisms between the filler wire and GTA are still unclear.

The purpose of this work is to clarify the effects of the filler wire intervention on the GTA. For this purpose, a novel sensing method of detecting the probe voltages (i.e., the voltage signals between the filler wire and tungsten electrode/workpiece) was proposed. Moreover, this work was split into two parts for elaboration. This first part aims at expounding the principal interaction mechanisms between the GTA and filler wire, and the second part will discuss the behaviors of liquid droplets. In the first part, to simplify the study, a tungsten probe was used to replace the filler wire and to interact with the arc through specific experiments. This work helped to enhance the understanding of electrical arc characteristics and laid the foundation for on-line monitoring and control of the GTAW quality when the filler wire was employed.

Sensing Methodology

In the autogenous GTAW process, electrical arc is established between the nonconsumable tungsten electrode tip and liquid weld pool surface. Weld pool behaviors will change arc length and thus change arc voltage (U, i.e., the voltage between the tungsten electrode and the workpiece). When the filler wire is introduced into the GTA, the feeding motion of the filler wire, the resulting metal transfer, and the pendant liquid droplets that oscillate at the end of the filler wire will affect the arc, and the filler wire itself as a suspended electrical conductor will also become an interference. The resultant interference signals will be coupled into the arc voltage, thereby obscuring the characteristic signals contained in the arc voltage that reflect the weld pool behaviors. It is difficult to distinguish their respective signal components and to clarify the interaction mechanisms between the filler wire and arc plasma with the arc voltage alone. Therefore, it may be possible to consider introducing additional sensing signals to help explain the relevant con-

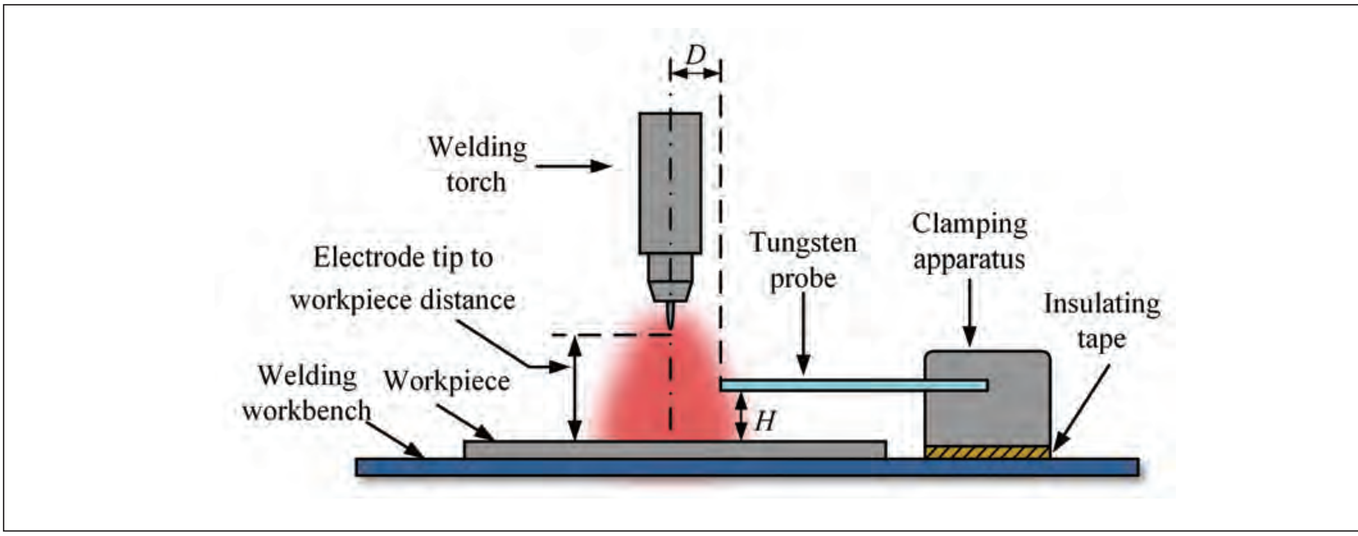

Fig. 2 — Experimental apparatus.

cerns.

Electrical arc is a self-sustaining discharge plasma whose electrical characteristics can be diagnosed by immersing metal probes (Ref. 20). Active (Ref. 21) or passive (Ref. 22) probe-sensing methods have also been used to monitor the keyhole process in plasma arc welding. Inspired by these, the filler wire can be regarded as a ready-made probe immersed in the arc atmosphere of GTAW, and probe voltages can be readily measured to provide more sensing information. Here, two probe voltages are detected, that is, the voltage between probe and tungsten electrode and the voltage between probe and workpiece, which are denoted as U_{pc} and U_{pa}, respectively. It can be roughly thought that these two probe voltages divide the arc voltage into upper and lower parts. In addition to the voltage drop of the upper or lower arc column region (denoted as U_u and U_l, respectively), these two probe voltages also contain the voltage drop of the cathode region (U_c) and the voltage drop of the anode region (U_a), respectively.

The number of positive and negative charges per unit volume at every moment is considered to be approximately equal in the GTA plasma, so the arc plasma is quasielectrically neutral. After the filler wire is introduced, electrons lighter than the positive ions will fly out of the arc plasma around the filler wire and flow to the surface of the filler wire at a faster rate, charging its surface to negative, relative to the arc plasma. As a result, a nonelectrically neutral transition layer, namely plasma sheath, will be formed between the arc plasma and the surface of the filler wire. Accordingly, the plasma sheath voltage is also implicit in the probe voltages. Although the sheath voltage (U_s) may be very small, it is the plasma sheath that connects the filler wire to the arc plasma. A simplified schematic of the above description is demonstrated in Fig. 1, and the approximate relationship of these voltage signals can be expressed by Equation 1:

$$\begin{aligned} U_{pa} &= U_a + U_l + U_s \\ U_{pc} &= U_c + U_u - U_s \\ U &= U_a + U_c + U_l + U_u = U_{pa} + U_{pc} \end{aligned} \tag{1}$$

When U is measured to reflect the overall electrical characteristics of GTA, U_{pc} or U_{pa} can be additionally used to reflect the local electrical characteristics of different regions of the GTA. Moreover, since the filler wire directly becomes a signal acquisition terminal, the probe voltages may be more suitable for characterizing the dynamic behaviors of the droplet at the end of the filler wire.

Experimental System and Design

Experimental System

The experimental system mainly consisted of the following three parts: welding system, high-speed camera system, and multichannel electrical signal acquisition system. The welding system was composed of a Fronius MagicWave 4000 GTAW power source (constant current mode), welding torch, and welding workbench. The Acuteye high-speed camera system equipped with optical dimmers and filters was used to provide auxiliary visual information about the arc shape. For the electrical signal acquisition system, electrical signals of interest were measured by Hall sensors and transmitted to a computer via a USB-4711A data acquisition card. The signal monitoring and recording was implemented by MATLAB® programming. The sampling frequency of electrical signals was 1024 Hz. The original images were captured at a frame rate of 1024 frames per second and their resolution was 256 × 256 pixels.

Experimental Design

The experimental materials were Q235 mild steel plates with a dimension of 300 × 60 × 4 mm as the base metal and pure argon of 99.99% with a flow rate of 10 L/min as the shielding gas. The diameter of the tungsten electrode was 2.4 mm and the length of the tungsten electrode protruding nozzle was 5 mm. Bead-on-plate welding was employed in the flat position.

Based on the proposed sensing method, three groups of

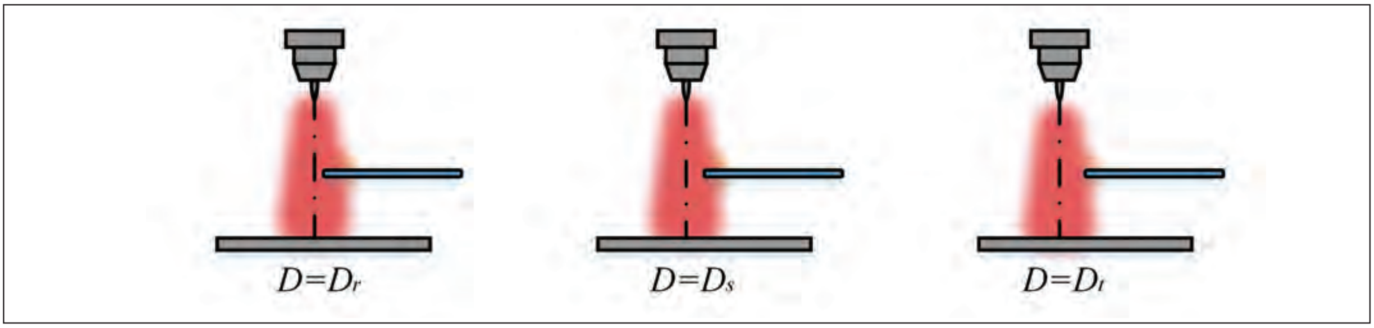

Fig. 3 — Diagram of relative position change ($0 < D_r < D_s < D_t$).

Table 1 — Experimental Parameters

Experiment	*I* (A)	*v* (cm/min)	ETWD* (mm)	*H* (mm)	*D* (mm)	Δ*T*(s)
#1	65	7	7	3, 2, 1	–	–
#2	65	7	6.5	2	0, 0.5	7, 6, 5, 4, 3, 2, 1, 0
#3	65	7	6	1.5	–	–

*Note: ETWD means electrode tip to workpiece distance.

experiments (#1, #2, and #3) have been designed and conducted. In all the experiments, a tungsten probe with a diameter of 2.4 mm was immersed into the arc atmosphere instead of the filler wire, and a relatively small welding current (I) was employed, which can ensure that the probe was not burnt as much as possible and the surface of the workpiece was slightly melted, thus avoiding the metal transfer and dynamic evolution behaviors of the weld pool. This way, the probe can simulate the filler wire to interfere with the arc plasma, thereby simplifying the objective of this study. Since the focus of this part of the work is only the inner interaction mechanisms between the GTA and filler wire, although this simulation is not equivalent to the actual filling process, it can also be considered that the effect of the filler wire as conductive metal on arc plasma follows similar mechanisms to that of the probe.

Figure 2 presents the schematic diagram of the experimental apparatus. As shown in Fig. 2, a tungsten probe was suspended parallel to the workpiece, and one end of this probe was fixed to the clamping apparatus. This clamping apparatus was placed on the welding workbench and isolated by nonconductive insulating tape. The axis of the welding torch was perpendicular to the workpiece surface. There are two positional parameters, D and H, in Fig. 2, where D is the horizontal distance between the probe tip and the symmetry axis of the electrode, and H is the height difference between the probe and the workpiece surface. When the horizontal relative position of the symmetry axis of the electrode and the probe tip is as shown in Fig. 2, D is positive, and when the vertical relative position of the workpiece surface to the probe tip is as shown in Fig. 2, H is positive.

The general experimental procedure was to keep the welding workbench stationary, suspend the probe at a height of H, and move the welding torch at a welding speed (v) in the horizontal direction to change D (v is too small to affect the arc shape). When the absolute value of D decreased, the direction of v was considered positive, indicating that the welding torch and the probe were approaching. The schematic relative position at different Ds can be seen in Fig. 3. During the experiments, arc voltage and probe voltage were collected, and the welding current was measured to ensure the voltage fluctuations were not caused by the current fluctuations. Experimental data was filtered by a simple moving average. Each average was calculated over a sliding window of 151 sample points, which was centered about the element in the current position.

The specific experimental designs and parameters are respectively shown in Fig. 4 and Table 1. Experiment #1 is mainly used to investigate the static effects of a probe on the GTA. As demonstrated in Fig. 4A, during Experiment #1, the welding torch moved horizontally several times to gradually go away from the probe tip until no probe voltage was detected. It moved 1 mm each time (e.g., $D_{a2} - D_{a1} = D_{a1} - D_{a0} = 1$ mm), and remained stationary for a while (10 s) after each movement. Experiment #1 had been conducted at different Hs, and in this way, the electrical signals can be obtained when the probe is in different spatial positions of the arc column.

Experiment #2 aimed to study the dynamic effects of an intermittent/continuous reciprocating probe on the GTA. The design of Experiment #2 is presented in Fig. 4B. The welding torch reciprocated equidistantly between position D = 0 mm and position $D = D_{b0}$ = 0.5 mm. Whenever the welding torch was horizontally displaced from its original position to the new position in the same reciprocating motion mode, it stayed at the new position for a period of time (ΔT) and then proceeded to the next step. Different ΔTs (e.g., $\Delta T_a > \Delta T_b$) have been set during Experiment #2. When ΔT was 0 s, the probe generated a continuous interference, and when ΔT was a non-zero value, the probe caused an intermittent interference.

Experiment #3 was about the dynamic effects of a continuously moving probe on the GTA at different positions. As shown in Fig. 4C, the welding torch reciprocated equidistantly several times between different horizontal positions to continuously generate dynamic interferences. The distance of

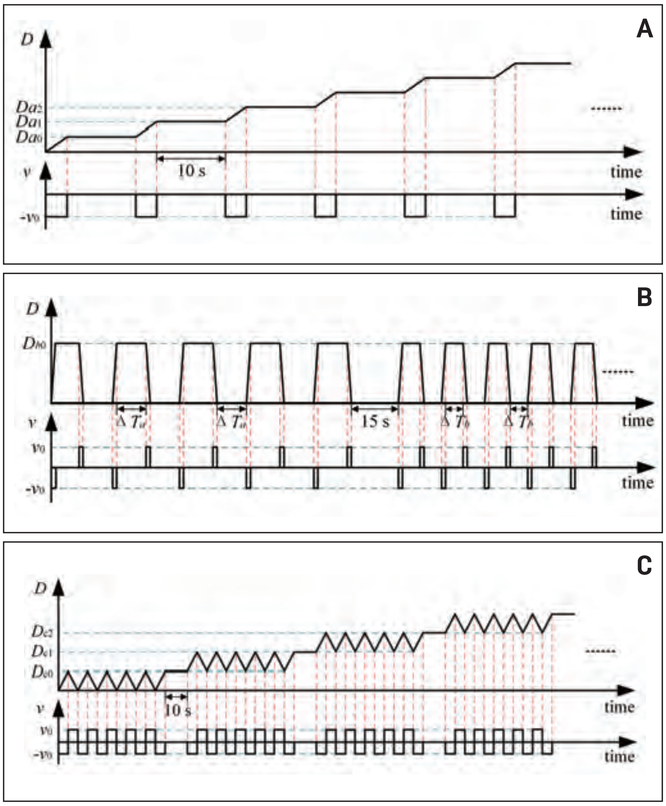

Fig. 4 — Experimental designs (v_0 = 7 mm/s). A — Experiment #1; B — Experiment #2; C — Experiment #3.

each movement was 1 mm, and at intervals, the welding torch moved to a farther distance from the probe for a new reciprocating motion (e.g., $D_{c2} - D_{c1} = D_{c1} - D_{c0} = 1$ mm).

Results and Discussion

Static Effects

Figure 5 displays the electrical signals measured in Experiment #1, where U_{pc} and U_{pa} were measured separately. In Fig. 5, D increases stepwise as time goes on. For ease of description, the process was roughly divided into phases A, B, and C, which respectively corresponded to the situation where the end of the probe was located in the original core area of the arc (the brightest area), the original noncore area of the arc, and the area outside the arc (no strict demarcation between the areas). The typical shapes of the core area of the arc can be seen in Fig. 6. Both the voltage signals and the arc shape were affected by the metal probe.

When the probe occupies the space area that originally belonged to the arc plasma, a plasma sheath will form near the probe surface and it will become a new partial edge area of the arc plasma. Accordingly, the overall arc shape will be changed. From phase A to B, U drops stepwise and each drop resulted from an increase in D, while the growth in D did not cause such a change in U during phase C. Therefore, the metal conductor caused an increase in the arc voltage after it had immersed into an area of the GTA.

This can be explained from two aspects. On one hand, after the probe is directly inserted into the arc column, the conductive cross section in the vicinity of the probe is forcibly reduced, which destroys the conductive path with the minimum energy consumption under the original conditions, thus tending to change the direction of electron flow. Although the arc column will resist this change to keep the original conductive path as much as possible, the conductive path following the minimal energy principle will still tend to have different degrees of deflection (tend to become longer) under new conditions. On the other hand, the probe intervention will alter the thermal field of the arc column. Since the probe that is cold relative to the arc plasma increases the arc heat loss, the arc column will automatically shrink to reduce the contact area with the external medium, thereby minimizing the heat loss. It will also contribute to the reduction in the conductive cross section of the arc plasma near the probe, which will increase the average current density and thus increase the average electric field strength. In this way, the intervention of the metal probe causes the arc voltage to rise.

The relationship between the static probe at different positions and the stable arc voltage can be obtained by calculating the mean value of U in the rectangular frames of Fig. 5A, C, and E, and the results are as shown in Fig. 7. With the increase in D, U declines more and more gently, and the increase in H contributes to the rise of U. This is because the ionization in the core area of the arc is more sufficient, so the interference of the metal probe will gradually weaken as it moves away from the core region of the arc. In addition, the cathode is an electron emission source. The closer the probe is to the cathode, the greater its influence on the GTA will be. Therefore, the arc voltage will increase as H rises.

It can be further found from Fig. 5 that whenever D is changed once, U can quickly level off after a small variation, while the changes in U, U_{pc}, and U_{pa} are not completely consistent with one another. During phase A, when U reaches a new stable level, U_{pc} and U_{pa} are still changing in opposite directions, and any of them has a greater variation than U. However, during phase B, the variation in U_{pc} and U_{pa} caused by the change in D becomes modest, and the trend of U_{pa} in phase B is opposite to that in phase A. Also, the transition period of U_{pc} and U_{pa} becomes very short or even inconspicuous. In the final phase C, although U is almost unaffected by the change in D, the change in D will once again cause U_{pc} and U_{pa} to change significantly.

As mentioned earlier, the arc voltage signal can reflect the overall electrical characteristics of the arc, and the probe voltage signal can reflect the electrical characteristics of the local area of the arc. Such diverse variations in U_{pc} and U_{pa} indicate that the influence of the metal probe on the electrical characteristics of different areas of the arc at different phases is not always consistent. During phase A, although the arc above the probe maintained its original shape as much as possible, the lower part of the arc severely deflected. The larger the H is, the more severe the deflection will be. This is because the electron flow needs to reform the shortest conductive path between the anode and cathode due to the physical barrier of the probe. As H rises, the electron flow from the cathode will encounter this barrier earlier and thus be deflected more. In addition, the decrease in temperature around the probe tends to suppress the thermal ionization around the probe. Nevertheless, the neutral particles above the probe can still be directly bombard-

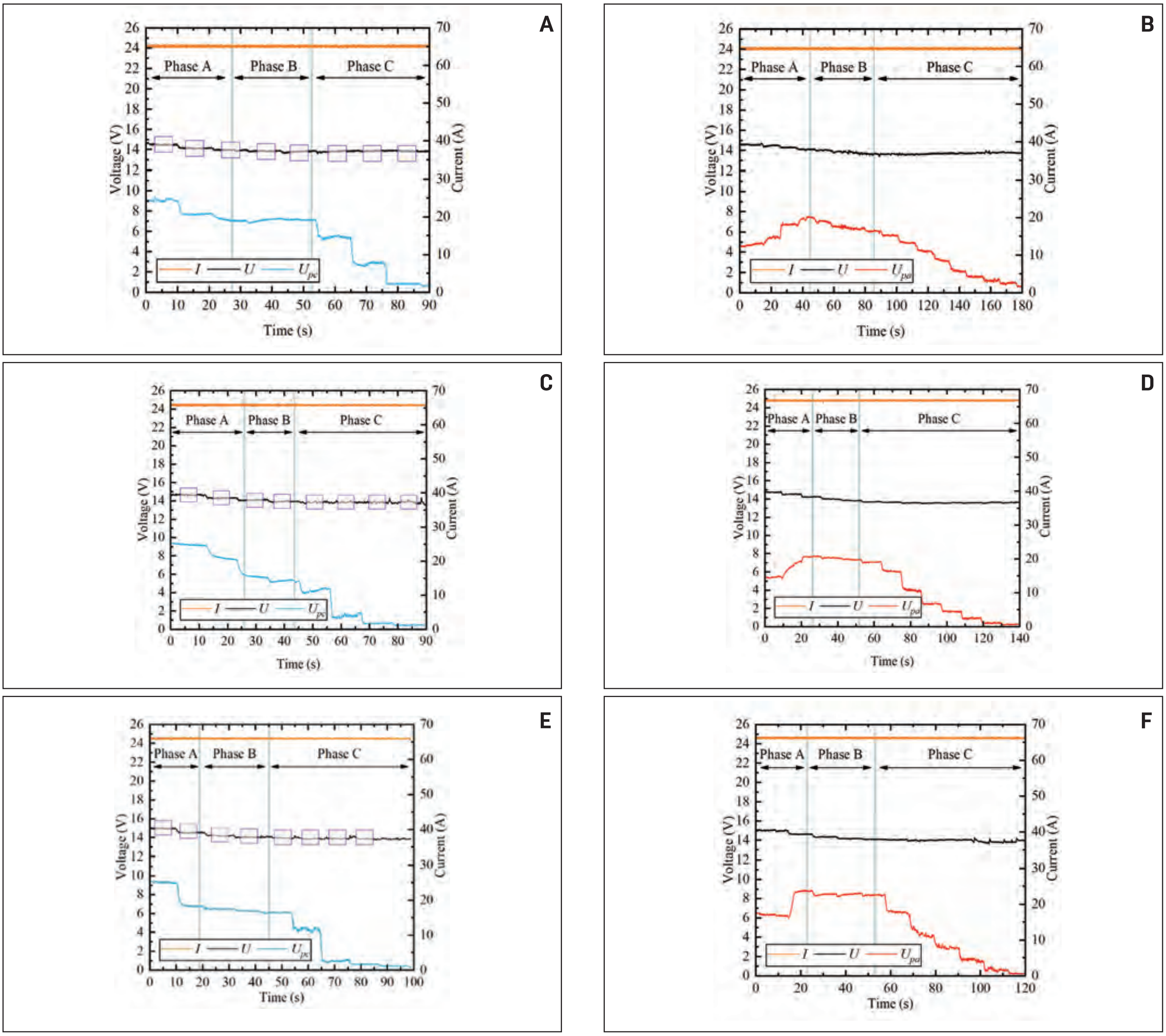

Fig. 5 — Electrical signals in Experiment #1. A — U_{pc} and U at H = 1 mm; B — U_{pa} and U at H = 1 mm; C — U_{pc} and U at H = 2 mm; D — U_{pa} and U at H = 2 mm; E — U_{pc} and U at H = 3 mm; F — U_{pa} and U at H = 3 mm.

ed by electrons from the cathode direction and thus be ionized. However, in the area below the probe, because of the physical block by the probe, it will be difficult for the neutral particles to be ionized by direct collision of electrons above the probe, and the originally charged ions will even be recombined due to insufficient energy. Therefore, during phase A, the decrease in *D* weakened the ionization of the lower part of the arc and then reduced the electric field, thus bringing U_{pa} down, which corresponded to a weaker heat production capacity, although the arc length below the probe seemed to be longer. Meanwhile, the heat production capacity of the upper part of the arc was enhanced to meet the increased overall heat production capacity of the arc column, so the ionization degree and electric field intensity of the upper part of the arc increased, and U_{pc} grew accordingly. In such a way, when the end of the probe is in the original core area of the arc, as *D* increases, the main conductive path of the arc is gradually restored, the arc deflection is reduced, and the gap in ionization between the upper and lower parts of the arc is narrowed, so U_{pa} rises and U_{pc} falls. In phase B, the end of the probe retreated to the original noncore area of the arc, and the main conductive path of the original core area was almost restored. The effects of the probe to the arc were weakened, and the probe no longer caused apparent arc deflection. The upper and lower parts of the arc presented as a whole, and the trend of U_{pa} and U_{pc} unified with that of *U*. During phase C, although the interference of the probe was not enough to change the arc voltage, the edge area of the arc still had a gradient distribution of unstable charges, so apparent changes in the probe voltages could still be detected.

Even if the physical medium forcibly intervenes in the core area of the arc, the arc can still self regulate in a short

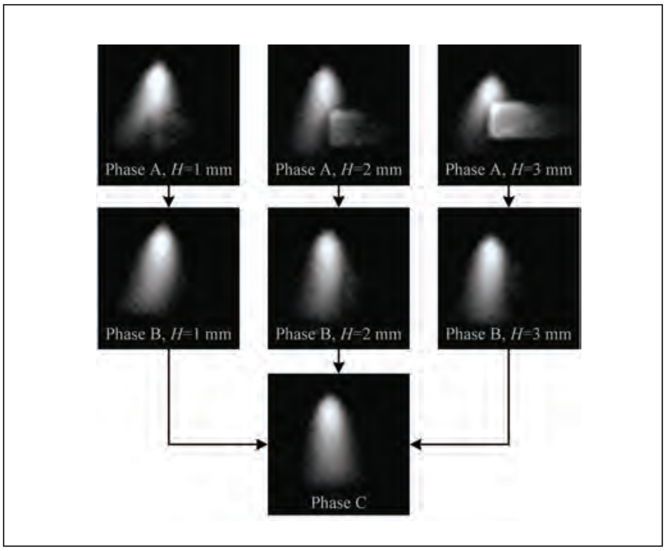

Fig. 6 — Typical shapes of the core area of the arc from phase A to C.

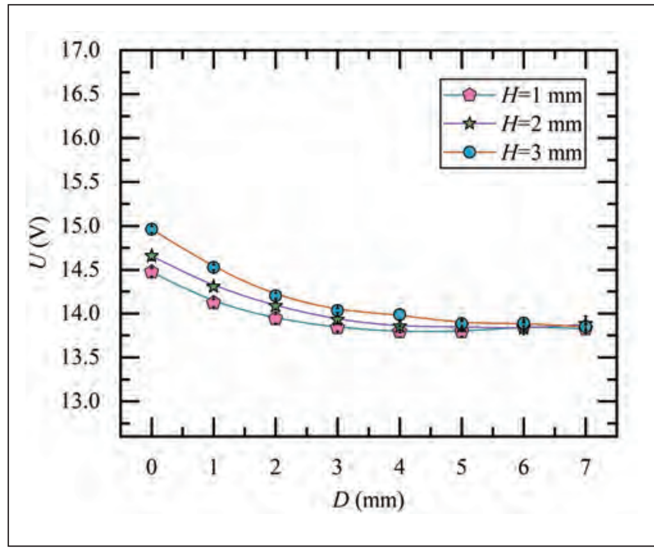

Fig. 7 — Arc voltage with the static probe immersed in different positions of the arc column.

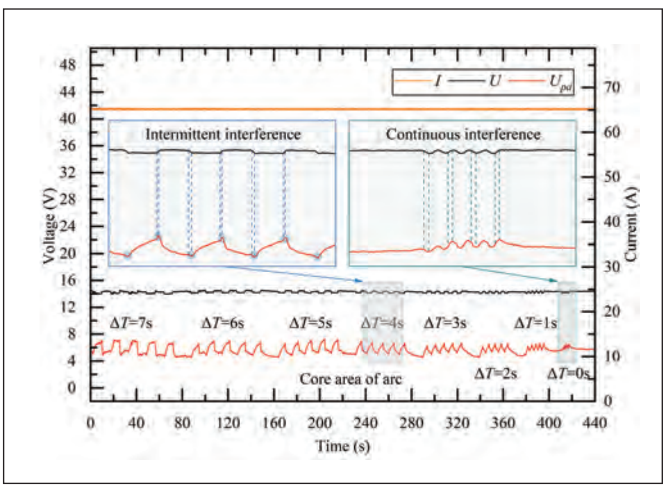

Fig. 8 — Electrical signals in Experiment #2.

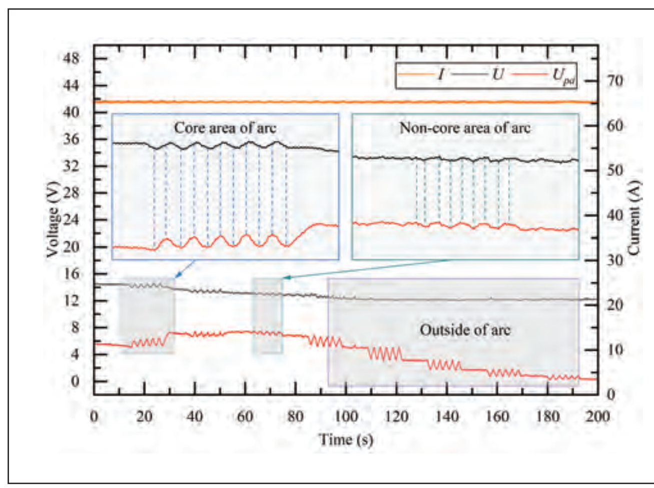

Fig. 9 — Electrical signals in Experiment #3.

time to present a new state of overall stable heat production with the lowest energy consumption. However, in the area near the anode, as the probe interference deepens, the arc stiffness is not as good as before, and it tends to be unstable. It is conceivable that as the interference increases, the unstable area starting from the anode side will gradually expand toward the cathode side. Eventually, the arc will extinguish because it will fail to maintain a stable self-sustained discharge process.

In the actual welding process, the interaction between the filler wire and arc should conform to the above mechanisms, which will also cause the similar interference to the arc (except for metal transfer). To minimize the interference of the filler wire, it may be recommended to keep the end of the filler wire melted in phase B. This is because, on the one hand, its interference on the core area of the arc is small; on the other hand, if the end of the filler wire is melted in phase C, although the arc shape is stable, the filler wire may be melted intermittently due to the lack of heat. In addition, according to Equation 1, only one of the probe voltages, along with the arc voltage, was sufficient to reflect the related effects, so the follow up will only focus on probe voltage U_{pa} to avoid repetition.

Dynamic Effects

In the actual welding process, the effects of the filler wire on the arc are more inclined to be dynamic effects. Figure 8 shows the electrical signals measured in Experiment #2, where the end of the probe occupied the original core area of the arc. Because the arc plasma possessed heat capacity, it can be observed that if ΔT was too short (less than the time constant), U_{pa} would not reach the stable level, and the fluctuation of U_{pa} caused by the variation in D would be more moderate with a decreasing ΔT.

During the intermittent interference period (e.g., when ΔT was 4 s), the local maximum of U_{pa} did not appear when U stayed at a lower level (when D was 0.5 mm), but approximately at a point when U was rising (when D was falling from 0.5 to 0 mm), or probably when U had just risen to the stable level (when D had just completed the drop from 0.5 to 0 mm). Similarly, the local minimum of U_{pa} in Fig. 8 generally occurs when U has just completed a drop, rather than when U keeps at a higher level. The above-mentioned changes are mainly due to the variation in D that can cause a sudden change in the conductive cross section, which can immediately change the current density and thus change electric field strength, while the arc itself has thermal inertia.

In the core area of the arc, the blocking by the probe tends to promote the ion recombination below the probe, while the ion recombination will lag behind the decrease in D due to the thermal inertia. Thus, below the probe, the decrease in the electric field strength caused by the ion recombination will lag behind the decrease in D. On the contrary, the decrease in D will lead to the sudden decrease in the conductive cross section, resulting in an immediate increase in electric field strength. Therefore, in the early stage of the decrease in D, U_{pa} will rise because of the immediate increase in electric field strength caused by the sudden decrease in the conductive cross section. If D has enough time to continue to decrease, the effect of ion recombination below the probe on the electric field strength will gradually emerge, thus reversing the growth in U_{pa}. Likewise, the gas ionization below the probe will also lag behind the increase in D, and U_{pa} will change in the opposite direction. Therefore, the rate of ion recombination and the rate of gas ionization will affect the moments at which the local maximum and local minimum of the U_{pa} occur, respectively. It can be observed that during the intermittent interference, the initial decline in U_{pa} is steeper than its initial rise, which shows that the rate of ion recombination is faster than that of gas ionization in the early period after D starts to vary. The same mechanism is also suitable for the continuous interference process. Thus, in Fig. 8, U_{pa} usually reaches the peak before D falls to 0 mm and falls to the bottom when D has just risen to 0.5 mm.

Figure 9 shows the electrical signals measured in Experiment #3 and that the dynamic probe continuously interfered with different areas of the arc column. It can also be seen that, in the core area of the arc, U_{pa} can reach the local minimum before U drops to the bottom. This is mainly because the change amount of D becomes 1 mm; it can rise to meet the moment that the decrease in U_{pa} is reversed by the increase in local electric field strength caused by the gas ionization of the lower part of the arc. Therefore, when the continuous interference occurs in the original core area of the arc, an impression is presented that U_{pa} does not strictly change synchronously with U, but often reaches peak or trough ahead of U. However, in the noncore area of the arc, the changes in U_{pa} and U seem to be more synchronous, and the dynamic relationship between them was more consistent with their static relationship because the effects of the probe on the arc were weakened. Additionally, the fluctuation of U_{pa} became significant again outside the arc, which indicated that there is a large ionization gradient, so that the movement of probe can be detected particularly clearly. Although the droplet behavior was not covered here, the mechanism of its dynamic interference should also follow the above description.

Conclusions

This part of the work mainly studied the mechanism of the effects of the filler wire as a metal conductor on GTA based on the proposed arc-sensing method of detecting probe voltages. The main conclusions drawn are as follows:

1) When the filler wire as a metal conductor is fed into the arc, the arc voltage (U) will rise due to the increase in the average electric field strength of the arc. The closer the filler wire is to the core area of the arc, the greater the U will be.

2) The probe voltages (U_{pa} and U_{pc}) can reflect the electrical characteristics of different local areas of the GTA. The effects of the filler wire as a metal conductor on the different areas of the arc at different phases are not always consistent. When the filler wire is immersed in the original core area of the arc, the arc will be deflected, U_{pa} will drop, and U_{pc} will grow. When the filler wire is immersed in the original noncore area of the arc, the upper and lower parts of the arc will act as a whole, and the trend of U_{pa} and U_{pc} will follow that of U.

3) When the filler wire as a metal conductor causes dynamic reciprocating interference to the arc, the probe voltage does not strictly change synchronously with the arc voltage, but sometimes reaches peak or trough ahead of the arc voltage due to the thermal inertia. Nevertheless, the dynamic effects on the arc can indeed be reflected in the probe voltage.

Acknowledgments

This study is supported by the National Natural Science Foundation of China (Grant No.: 51505326), Natural Science Foundation of Tianjin (Grant No.: 16JCQNJC04300), and the Regional Demonstration Project of Marine Economic Innovation and Development (Grant No.: BHSF2017-10).

References

1. Chen, Z. Y., Chen, J., and Feng, Z. L. 2017. Monitoring weld pool surface and penetration using reversed electrode images. *Welding Journal* 96(10): 367-s to 375-s.

2. Fan, C. J., Lv, F. L., and Chen, S. B. 2009. Visual sensing and penetration control in aluminum alloy pulsed GTA welding. *International Journal of Advanced Manufacturing Technology* 42(1–2): 126–137. DOI: 10.1007/s00170-008-1587-1

3. Song, H. S., and Zhang, Y. M. 2008. Measurement and analysis of three-dimensional specular gas tungsten arc weld pool surface. *Welding Journal* 87(4): 85-s to 95-s.

4. Zhang, W. J., Zhang, X., and Zhang, Y. M. 2013. Robust pattern recognition for measurement of three dimensional weld pool surface in GTAW. *Journal of Intelligent Manufacturing* 26(4): 659–676. DOI: 10.1007/s10845-013-0825-z

5. Zhang, W. J., Wang, X. W., and Zhang, Y. M. 2013. Analytical real-time measurement of a three-dimensional weld pool surface. *Measurement Science and Technology* 24(11): 115011. DOI: 10.1088/0957-0233/24/11/115011

6. Liu, Y. K., Zhang, Y. M., and Kvidahl, L. 2014. Skilled human welder intelligence modeling and control: Part 1 — Modeling. *Welding Journal* 93(2): 46-s to 52-s.

7. Dong, H., Cong, M., Zhang, Y. M., Liu, Y. K., and Chen, H. P. 2018. Modeling and real-time prediction for complex welding process based on weld pool. *The International Journal of Advanced Manufacturing Technology* 96(5-8): 2495–2508. DOI: 10.1007/s00170-018-1685-7

8. Cheng, Y. C., Xiao, J., Chen, S. J., and Zhang, Y. M. 2018. Intelligent penetration welding of thin-plate GTAW process based on arc voltage feedback. *Transactions of the China Welding Institution* 39(12): 1–4. DOI: 10.12073/j.hjxb.2018390287

9. Zhang, S. Q., Hu, S. S., and Wang, Z. J. 2016. Weld penetration sensing in pulsed gas tungsten arc welding based on arc voltage. *Journal of Materials Processing Technology* 229: 520–527. DOI: 10.1016/j.jmatprotec.2015.09.034

10. Renwick, R. J., Rarson, D. F., and Richardson, R. W. 1983. Experimental investigation of GTA weld pool oscillations. *Welding Journal* 62(2): 29-s to 35-s.

11. Xiao, Y. H., and Ouden, G. D. 1993. Weld pool oscillation during GTA welding of mild steel. *Welding Journal* 72(8): 428-s to 434-s.

12. Shi, Y., Li, C. K., Du, L. M., Gu, Y. F., and Zhu, M. 2016. Frequency characteristics of weld pool oscillation in pulsed gas tungsten arc welding. *Journal of Manufacturing Processes* 24: 145–151. DOI: 10.1016/j.jmapro.2016.08.010

13. Huang, J. K., Yang, M. H., Chen, J. S., Yang, F. Q., Zhang, Y. M., and Fan, D. 2018. The oscillation of stationary weld pool surface in the GTA welding. *Journal of Materials Processing Technology* 256: 57–68. DOI: 10.1016/j.jmatprotec.2018.01.018

14. Li, C. K., Shi, Y., Gu, Y. F., and Yuan, P. 2018. Monitoring weld pool oscillation using reflected laser pattern in gas tungsten arc welding. *Journal of Materials Processing Technology* 255: 876–885. DOI: 10.1016/j.jmatprotec.2018.01.037

15. Lv, N., and Chen, S. B. 2011. Investigation on acoustic signals for on-line monitoring of welding. *Robotic Welding, Intelligence and Automation, Lecture Notes in Electrical Engineering*, Springer, Berlin, Heidelberg, 88: 235–243.

16. Lv, N., Xu, Y. L., Zhong, J. Y., Chen, H. B., Wang, J. F., and Chen, S. B. 2013. Research on detection of welding penetration state during robotic GTAW process based on audible arc sound. *Industrial Robot* 40(5): 474–493.

17. Lv, N., Xu, Y. L., Fang, G., Zhao, H., and Chen, S. B. 2015. Mechanism analysis and feature extraction of arc sound channel for pulse GTAW welding dynamic process. *Robotic Welding, Intelligence and Automation, RWIA 2014, Advances in Intelligent Systems and Computing*, Springer International Publishing, Cham, 363: 249–261.

18. Zhang, Z. F., Wen, G. R., and Chen, S. B. 2018. Audible sound-based intelligent evaluation for aluminum alloy in robotic pulsed GTAW: Mechanism, feature selection and defect detection. *IEEE Transactions on Industrial Informatics* 14(7): 2973–2983. DOI: 10.1109/TII.2017.2775218

19. Yudodibroto, B. Y. B., Hermans, M. J. M., Hirata, Y., and den Ouden, G. 2004. Influence of filler wire addition on weld pool oscillation during gas tungsten arc welding. *Science and Technology of Welding and Joining* 9(2): 163–168. DOI: 10.1179/136217104225012274

20. Chen, S. J., Zhang, R. Y., Jiang, F., and Dong, S. W. 2018. Experimental study on electrical property of arc column in plasma arc welding. *Journal of Manufacturing Processes* 31: 823–832. DOI: 10.1016/j.jmapro.2017.12.028

21. Zhang, Y. M., Zhang, S. B., and Liu, Y. C. 2001. A plasma cloud charge sensor for pulse keyhole process control. *Measurement Science and Technology* 12(8): 1365–1370. DOI: 10.1088/0957-0233/12/8/352

22. Shan, P., Yi, X. L., Hu, S. S., and Luo, Z. 2003. Detection of plasma sheath voltage in plasma arc welding. *Transactions of the China Welding Institution* 24(2): 19–21.

SHUANGYANG ZOU, ZHIJIANG WANG (wangzj@tju.edu.cn), *SHENGSUN HU, GUANCHENG ZHAO, and WANDONG WANG are with the Tianjin Key Laboratory of Advanced Joining Technology, School of Materials Science and Engineering, Tianjin University, Tianjin, China. YOUQUAN CHEN is with the Department of Mechanical Engineering, College of Humanities & Information, Changchun University of Technology, Changchun, China.*


When the world is counting on you, you can count on us.
Being essential means the world is depending on you to keep moving forward, even when everything else is standing still. While the rest of the world is depending on you, you can depend on us.
LINCOLN ELECTRIC
AR20-17 | ©2020 Lincoln Global, Inc. All Rights Reserved.